

General Disclaimer

One or more of the Following Statements may affect this Document

- This document has been reproduced from the best copy furnished by the organizational source. It is being released in the interest of making available as much information as possible.
- This document may contain data, which exceeds the sheet parameters. It was furnished in this condition by the organizational source and is the best copy available.
- This document may contain tone-on-tone or color graphs, charts and/or pictures, which have been reproduced in black and white.
- This document is paginated as submitted by the original source.
- Portions of this document are not fully legible due to the historical nature of some of the material. However, it is the best reproduction available from the original submission.



ENERGY CONVERSION ALTERNATIVES STUDY
-ECAS-
GENERAL ELECTRIC PHASE I FINAL REPORT

VOLUME II, ADVANCED ENERGY CONVERSION SYSTEMS
Part 3, Direct Energy Conversion Cycles

by

J.C. Corman, R.B. Fleming, L.P. Harris, and R.V. Pohl

Corporate Research and Development
General Electric Company



Prepared for

NATIONAL AERONAUTICS AND SPACE ADMINISTRATION
ENERGY RESEARCH AND DEVELOPMENT ADMINISTRATION
NATIONAL SCIENCE FOUNDATION

NASA Lewis Research Center
Contract NAS 3-19406

(NASA-CF-134948-Vol-2-Pt-3) ENERGY
CONVERSION ALTERNATIVES STUDY (ECAS),
GENERAL ELECTRIC PHASE I. VOLUME 2:
ADVANCED ENERGY CONVERSION SYSTEMS. PART 3:
DIRECT ENERGY CONVERSION CYCLES (General

N76-23682

HC \$6.00

Unclas
25358
G3/44

1. Report No. NASA CR-134948 Volume II, Part 3		2. Government Accession No.		3. Recipient's Catalog No.	
4. Title and Subtitle ENERGY CONVERSION ALTERNATIVES STUDY (ECAS), GENERAL ELECTRIC PHASE I FINAL REPORT; VOLUME II, ADVANCED ENERGY CONVERSION SYSTEMS: PART 3, DIRECT ENERGY CONVERSION CYCLES				5. Report Date February 1976	
				6. Performing Organization Code	
7 Author(s) Sections 2.8 through 2.10. L.P. Harris Sections 2.11 and 2.12. R.B. Fleming Section 3. J.C. Corman Appendix A. R.V. Pohl				8. Performing Organization Report No. General Electric SRD-76-011	
				10. Work Unit No.	
9. Performing Organization Name and Address Corporate Research and Development General Electric Company Schenectady, New York 12301				11. Contract or Grant No. NAS 3-19406	
				13. Type of Report and Period Covered Contractor Report	
12. Sponsoring Agency Name and Address Energy Research and Development Administration National Aeronautics and Space Administration National Science Foundation Washington, DC				14. Sponsoring Agency Code	
15. Supplementary Notes Project Manager, G.J. Barna NASA Lewis Research Center Cleveland, Ohio 44135 G.R. Fox, Program Manager G.E. Corporate Research and Development Schenectady, New York 12301					
16. Abstract A parametric study was performed to assist in the development of a data base for the comparison of advanced energy conversion systems for utility applications using coal or coal-derived fuels. Estimates of power plant performance (efficiency), capital cost, cost of electricity, natural resource requirements, and environmental intrusion characteristics were made for ten advanced conversion systems. Over 300 parametric points were analyzed to estimate the potential of these systems. Emphasis of the study was on the energy conversion system in the context of a base loaded utility power plant. Although cases employing transported coal-derived fuels were included in the study, the fuel processing step of converting coal to clean fuels was not investigated except for cases where a low-Btu gasifier was integrated with the power plant. All power plant concepts were premised on meeting emission standards requirements. The investigative approach focused on achieving consistency and comparability in the analysis of the various conversion systems. Recognized advocate organizations were employed to analyze their respective cycles and to present their analyses for power plant integration by the GE systems evaluation team. Wherever possible, common subsystems and components for the various systems were treated on a uniform basis. A steam power plant (3500 psig, 1000 F, 1000 F) with a conventional coal-burning furnace-boiler was analyzed as a basis for comparison. Combined cycle gas/steam turbine system results indicated competitive efficiency and a lower cost of electricity compared to the reference steam plant. The Open-Cycle MHD system results indicated the potential for significantly higher efficiency than the reference steam plant but with a higher cost of electricity. The information contained in this report constitutes results from the first phase of a two phase effort. In Phase II, a limited number of concepts will be investigated in more detail through preparation of conceptual designs and an implementation assessment including preparation of R&D plans estimating the resources and time required to bring the systems to commercial fruition.					
17. Key Words (Suggested by Author(s)) Coal Energy Conversion Electrical Generation Utility Power Cost of Electricity			18. Distribution Statement Unclassified - unlimited		
19. Security Classif. (of this report) Unclassified		20. Security Classif. (of this page) Unclassified		21. No. of Pages 134	22. Price*

FOREWORD

The work described in this report is a part of the Energy Conversion Alternatives Study (ECAS)—a cooperative effort of the Energy Research and Development Administration, the National Science Foundation, and the National Aeronautics and Space Administration.

This General Electric contractor report for ECAS Phase I is contained in three volumes:

Volume I - Executive Summary

Volume II - Advanced Energy Conversion Systems

Part 1 - Open-Cycle Gas Turbines

Part 2 - Closed Turbine Cycles

Part 3 - Direct Energy Conversion Cycles

Volume III - Energy Conversion and Subsystems and Components

Part 1 - Bottoming Cycles and Materials of Construction

Part 2 - Primary Heat Input Systems and Heat Exchangers

Part 3 - Gasification, Process Fuels, and Balance of Plant

In addition to the principal authors listed, members of the technical staffs of the following subcontractor organizations developed information for the Phase I data base:

General Electric Company

Advanced Energy Programs/Space Systems Department

Direct Energy Conversion Programs

Electric Utility Systems Engineering Department

Gas Turbine Division

Large Steam Turbine-Generator Department

Medium Steam Turbine Department

Projects Engineering Operation/I&SE Engineering Operation

Space Sciences Laboratory

Actron, a Division of McDonnell Douglas Corporation

Argonne National Laboratory

Avco Everett Research Laboratory, Incorporated

Bechtel Corporation

Foster Wheeler Energy Corporation

Thermo Electron Corporation

This General Electric contractor report is one of a series of three reports discussing ECAS Phase I results. The other two reports are the following: Energy Conversion Alternatives Study (ECAS), Westinghouse Phase I Final Report (NASA CR-134941), and NASA Report (NASA TMX-71855).

TABLE OF CONTENTS

	<u>Page</u>
VOLUME I EXECUTIVE SUMMARY	
Summary.....	1
Introduction.....	3
Analytical Approach.....	7
Advanced Energy Conversion Systems.....	13
Summary of Results.....	43
VOLUME II ADVANCED ENERGY CONVERSION SYSTEMS	
Part 1 Open-Cycle Gas Turbines	
Summary.....	1
Introduction.....	3
1.0 Analytical Approach.....	7
2.0 Cycle Analyses, Results, and Discussion.....	21
2.1 Open-Cycle Gas Turbine.....	21
2.2 Open-Cycle Gas Turbine Combined Cycle—Air Cooled.....	44
2.3 Open-Cycle Gas Turbine Combined Cycle—Water Cooled.....	61
Appendix A Groundrules for Study.....	75
Appendix B Cost and Performance Evaluation Computer Program.....	81
Appendix C Operating and Maintenance Cost Estimates.....	87
Part 2 Closed Turbine Cycles	
Summary.....	1
Introduction.....	3
2.4 Closed-Cycle Gas Turbine.....	7
2.5 Supercritical CO ₂ Cycle.....	25
2.6 Advanced Steam Cycle.....	46
2.7 Liquid Metal Topping Cycle.....	74
Part 3 Direct Energy Conversion Cycles	
Summary.....	1
Introduction.....	3
2.8 Open-Cycle MHD.....	7
2.9 Closed-Cycle Inert Gas MHD.....	36

TABLE OF CONTENTS (Cont'd)

	<u>Page</u>
2.10 Closed-Cycle Liquid Metal MHD.....	63
2.11 Fuel Cells—Low Temperature.....	89
2.12 Fuel Cells—High Temperature.....	108
3.0 Summary of Results—Conversion Systems.....	117
Appendix A Power Conditioning Systems.....	127

VOLUME III ENERGY CONVERSION SUBSYSTEMS AND COMPONENTS

Part 1 Bottoming Cycles and Materials of Construction

Summary.....	1
Introduction.....	3
4.0 Bottoming Cycles.....	7
5.0 Materials of Construction.....	39

Part 2 Primary Heat Input Systems and Heat Exchangers

Summary.....	1
Introduction.....	3
6.0 Primary Heat Input Systems.....	7
7.0 Heat Exchangers.....	95
Appendix A Design Data and Equipment Outlines for Primary Heat Input Systems.....	101
Appendix B Equipment Performance Data for Primary Heat Input Systems.....	143
Appendix C Cost Data for Primary Heat Input Systems.....	181

Part 3 Gasification, Process Fuels, and Balance of Plant

Summary.....	1
Introduction.....	3
8.0 Gasification and Process Fuels.....	7
9.0 Balance of Plant.....	55
10.0 Summary of Results—Energy Conversion Subsystems and Components.....	121
Appendix A Coal Transportation Cost Estimates.....	129
Appendix B Balance-of-Plant Estimate Results for Parametric Point Variations.....	135

LIST OF ILLUSTRATIONS

Volume II, Part 3

<u>Figure</u>		<u>Page</u>
2.8-1	Open-Cycle MHD (Base Case 1).....	9
2.8-2	Indirectly Fired High-Temperature Air Preheater System.....	10
2.8-3	MHD—Gas Turbine Power Cycle.....	11
2.8-4	Seed Recovery Plant Block Diagram.....	13
2.8-5	MHD Channel Calculation Procedure.....	16
2.9-1	Closed-Cycle Inert MHD Topping Cycle.....	38
2.9-2	Heat Exchanger Cycling Sequence.....	42
2.9-3	Closed-Cycle Inert Gas MHD—Parallel Cycle.....	43
2.9-4	Closed-Cycle MHD Argon Purity Considerations.....	49
2.10-1	Closed-Cycle Liquid Metal MHD.....	65
2.10-2	47-MWe MHD Power Module with Nozzle-Separator- Diffuser.....	70
2.10-3	Schematic of Generator Assembly.....	74
2.11-1	Low-Temperature Fuel Cell (Base Case).....	90
2.11-2	Effect of Change in Catalyst Loading.....	97
2.11-3	Effect of Fuel Cell Life.....	98
2.12-1	High-Temperature Fuel Cell Base Case.....	109
3-1	Summary Comparison of Cycles (Efficiency).....	118
3-2	Summary Comparison of Cycles (Capital Cost).....	120
3-3	Summary Comparison of Cycles (Cost of Electricity).....	121
3-4	Screening Curves for Advanced Energy Conversion Cycles.....	123

LIST OF TABLES

<u>Table</u>		
2.8-1	Magnet for Base-Case MHD Generator Case 1— 2000 MWe Plant Size.....	18
2.8-2	Magnet Design Data for Base Case MHD Generator Case 24—SRC as Fuel.....	19
2.8-3	Air Preheater Cases 1, 2, and 3.....	21
2.8-4	Air Preheater Case 24—Base Case with SRC as Fuel.....	21
2.8-5	Estimated Costs for Construction and Operation of Seed Recovery Equipment.....	26
2.8-6	Parametric Variations for Task I Study (Open- Cycle MHD).....	27
2.8-7	Summary Sheet Open-Cycle MHD Base Case 1.....	28
2.8-8	Summary Sheet Open-Cycle MHD Base Case 24.....	29
2.8-9	Capital Cost Distributions for Open-Cycle MHD....	30
2.8-10	Power Output and Auxiliary Power Demand for Base Case and Parametric Variations: Open- Cycle MHD.....	33

LIST OF TABLES (Cont'd)

<u>Table</u>		<u>Page</u>
2.9-1	Refractory Storage Heat Exchangers for Closed-Cycle Inert Gas MHD Systems	47
2.9-2	MHD Generator Sizes for Cases 1 and 102	50
2.9-3	Size and Weight-MHD Generator-Diffuser & Fluid Inventory	52
2.9-4	Basis for Cost Estimates	54
2.9-5	Closed-Cycle Inert Gas MHD Parametric Variations for Task I Study	53
2.9-6	Summary Sheet Closed-Cycle Inert Gas MHD Base Case 1	55
2.9-7	Summary Sheet Closed-Cycle Inert Gas MHD Base Case 16	56
2.9-8	Capital Cost Distributions for Closed-Cycle Inert Gas MHD	57
2.9-9	Power Output and Auxiliary Power Demand for Base Case and Parametric Variations: Closed-Cycle Inert Gas MHD	60
2.10-1	Power Module Parameters	73
2.10-2	Raw Material and Fabrication Costs Used for Estimating Costs of Mixer/Generator/Separator Train	76
2.10-3	Power Module Weights	78
2.10-4	Power Module Costs	79
2.10-5	Parametric Variations for Task I Study Closed-Cycle Liquid Metal MHD	81
2.10-6	Summary of Results	82
2.10-7	Summary Sheet Liquid Metal MHD Base Case	83
2.10-8	Capital Cost Distributions for Closed-Cycle Liquid Metal MHD	84
2.10-9	Power Output and Auxiliary Power Demand for Base Case and Parametric Variations: Closed-Cycle Liquid Metal MHD	86
2.11-1	Capital Costs for Reformer System	94
2.11-2	Data for Fuel Cell Stack	95
2.11-3	Fuel Cell Cost Breakdown (Case 8, Solid Polymer Electrolyte [SPE] Cell with Oxygen)	100
2.11-4	Parametric Variations for Task I Study Fuel Cells—Low Temperature	101
2.11-5	Capital Cost Distributions for Low-Temperature Fuel Cell	103
2.11-6	Summary Sheet Fuel Cells—Low-Temperature Base Case	105
2.11-7	Power Output and Auxialiry Power Demand for Base Case and Parametric Variations: Fuel Cells—Low Temperature	106
2.12-1	Parametric Variations for Task I Study (Fuel Cells—High Temperature)	112
2.12-2	Capital Cost Distributions for High-Temperature Fuel Cells	113

LIST OF TABLES (Cont'd)

<u>Table</u>		<u>Page</u>
2.12-3	Summary Sheet Fuel Cells—High-Temperature Base Case	114
2.12-4	Power Output and Auxiliary Power Demand for Base Case and Parametric Variations: Fuel Cells—High-Temperature	115

Summary

ADVANCED ENERGY CONVERSION SYSTEMS

The objective of Phase I of the Energy Conversion Alternatives Study (ECAS) for coal or coal-derived fuels was to develop a technical-economic information base on the ten energy conversion systems specified for investigation. Over 300 parametric variations were studied in an attempt to identify system and cycle conditions which indicate the best potential of the energy conversion concept. This information base provided a foundation for selection of energy conversion systems for more in-depth investigation in the conceptual design portion of the ECAS study. The systems for continued study were specified by the ECAS Interagency Steering Committee.

The technical-economic results include efficiency, capital cost and cost of electricity. For reference purposes a steam cycle (3500 psi/1000 F/1000 F [2.41×10^7 N/m²/811 K/811 K]) with conventional coal burning furnace, stack gas cleanup and wet mechanical draft cooling towers was analyzed with the same analysis procedure employed for the advanced systems. This reference steam plant had an efficiency of approximately 37 percent. The open-cycle MHD system was the only plant to show efficiencies approaching 50 percent. A group of cycles—advanced steam, supercritical CO₂, liquid metal topping, and inert gas MHD—were estimated to have efficiencies in the 40 to 45 percent range.

The energy conversion systems with capital costs significantly lower than the reference steam plant were those with short construction times and simple construction, i.e., open-cycle gas turbines and low-temperature fuel cells. The more complex plants, i.e., open- and closed-cycle MHD and liquid metal topping, required longer construction time and were higher in capital cost.

Efficiency and capital cost are a part of the total technical-economic evaluation. The combination of these characteristics with the cost of fuel and operation and maintenance costs results in a cost of electricity for more complete comparisons. The only systems which were consistently lower than the reference steam plant's 30 mills/kWh at 65 percent capacity factor were the open-cycle gas turbine-combined cycle. MHD, supercritical CO₂, liquid metal top topping, and high-temperature fuel cells had a higher cost of electricity than the reference steam plant, as did many of the advanced steam cases because of their higher capital costs. The low capital cost plants—(low-temperature fuel cells and open cycle gas turbine, recuperative) utilized clean fuels and consequently had high fuel charges. These systems would be more economically applicable to peaking or mid-range duty.

Introduction

ADVANCED ENERGY CONVERSION SYSTEMS

Many advanced energy conversion techniques which can use coal or coal-derived fuels have been advocated for power generation applications. Conversion systems advocated have included open- and closed-cycle gas turbine systems (including combined gas turbine-steam turbine systems), supercritical CO₂ cycle, liquid metal Rankine topping cycles, magnetohydrodynamics (MHD), and fuel cells. Advances have also been proposed for the steam systems which now form the backbone of our electric power industry. These advances include the use of new furnace concepts and higher steam turbine inlet temperatures and pressures. Integration of a power conversion system with a coal processing plant producing a clean low-Btu gas for use in the power plant is still another approach advocated for energy conserving, economical production of electric power. Studies of all these energy conversion techniques have been performed in the past. However, new studies performed on a common basis and in light of new national goals and current conditions are required to permit an assessment of the relative merits of these techniques and potential benefits to the nation.

The purpose of this contract is to assist in the development of an information base necessary for an assessment of various advanced energy conversion systems and for definition of the research and development required to bring these systems to fruition. Estimates of the performance, economics, natural resource requirements and environmental intrusion characteristics of these systems are being made on as comparable and consistent a basis as possible leading to an assessment of the commercial acceptability of the conversion systems and the research and development required to bring the systems to commercial reality. This is being accomplished in the following tasks:

- | | | |
|----------|-------------------------------|--------------|
| Task I | Parametric Analysis (Phase I) | |
| Task II | Conceptual Designs | } (Phase II) |
| Task III | Implementation Assessment | |

This investigation is being conducted under the Energy Conversion Alternatives Study (ECAS) under the sponsorship of Energy Research and Development Administration (ERDA), National Science Foundation (NSF), and National Aeronautics and Space Administration (NASA). The control of the program is under the direction of an Interagency Steering Committee with participation of the supporting agencies. The NASA Lewis Research Center is responsible for project management of this study.

The information presented in this report describes the results produced in the Task I portion of this study. The emphasis

in this task was placed upon developing an information base upon which comparisons of Advanced Energy Conversion Techniques using coal or coal-derived fuels can be made. The Task I portion of the study was directed at a parametric variation of the ten advanced energy conversion systems under investigation. The wide-ranging parametric study was performed in order to provide data for selection by the Interagency Steering Committee of the systems and specific configurations most appropriate for Task II and III studies.

The Task II effort will involve a more detailed evaluation of seven advanced energy conversion systems and result in a conceptual design of the major components and power plant layout. The Task III effort will produce the research and development plans which would be necessary to bring each of the seven Task II systems to a state of commercial reality and then to assess their potential for commercial acceptability.

A prime objective of this study was to produce results which had a cycle-to-cycle consistency. In order to accomplish this objective and still ensure that each system was properly advocated, an organization which is or had been a proponent of the prime cycle was selected to advocate the energy conversion system and to analyze the performance and economics of the prime cycle portion of the energy conversion system, i.e., the parts of the system which were novel or unique to the system. The remaining subsystems, e.g., fuel processing, furnaces, bottoming cycles, balance of plant, were analyzed by technology specialist organizations which presently have responsibility for supplying these subsystems for utility applications. The final plant configuration and performance were produced by the General Electric Corporate Research and Development study team and this group performed the critical integration of the final plant concept. This methodology was used to provide a system-to-system consistency while maintaining the influence of a cycle advocate.

The ten energy conversion systems under investigation in this study are defined and analyzed in this volume of the report. These include:

1. Open-cycle Gas Turbine Recuperative
 - with clean and semi-clean fuels produced from coal
 - with and without organic bottoming cycles
2. Open-Cycle Gas Turbine
 - with air and water cooling of the gas turbine hot gas path
 - with clean and semi-clean fuels from coal and integrated low-Btu gasifiers

3. Closed-Cycle Gas Turbine
 - with helium working fluid
 - with a variety of direct coal and clean fuel furnaces
 - with and without organic and steam bottoming cycles
4. Supercritical CO₂ Cycle
 - with basic and recompression cycle variations
 - with a variety of direct coal and clean coal-derived fuel furnaces
5. Advanced Steam Cycle
 - with both throttle and/or reheat temperatures greater than present practice (1000 F [811 K])
 - with a variety of direct coal and clean coal-derived fuel furnaces
6. Liquid Metal Topping Cycle
 - with potassium and cesium as working fluids
 - with a variety of direct coal and clean fuel furnaces
7. Open-Cycle MHD
 - with direct coal and semi-clean fuel combustion
 - with standard steam and gas turbine bottoming
8. Closed-Cycle Inert Gas MHD
 - with parallel and topping configurations
 - with both direct coal and semi-clean fuel utilization
9. Closed-Cycle Liquid Metal MHD
 - with mixture of liquid sodium and helium as working fluids
 - with standard steam bottoming
 - with a variety of direct coal and clean fuel furnaces
10. Fuel Cells
 - both high and low temperature (less than 300 F [422 K])
 - with employment of clean process fuels for low temperature cells and low-Btu gasification at high temperature cells

The subsystems which complete the energy conversion system are discussed in Volume III of this report. The results as presented in the following sections include the total energy conversion system.

28 OPEN-CYCLE MHD

DESCRIPTION OF CYCLE

In open-cycle MHD power generation, fossil fuel is burned at high temperature (4500-5000 F [2756-3033 K]) and pressure (7-15 atm); the hot combustion gases then are "seeded" with small fractions (1 percent) of an alkali metal (potassium) introduced usually as a carbonate powder or solution; and the resulting gas mixture, which has an electrical conductivity of order 10 mho/m is then expanded through an MHD generator. In the generator, the conductive gas flow interacts with a high magnetic field (5-7 tesla) to generate voltages, as in any electrodynamic machine, perpendicular to the flow velocity and magnetic field. Electrodes at the sides of the generator channel provide electrical contact between the flow and an external load, thereby permitting d-c electric current flow and transfer of electric power to the inverters and then to the external a-c power system.

The gas flow leaves the generator channel, still at very high temperature (3600 F [2256 K]), when its electrical conductivity, which varies exponentially with temperature, has become too low for efficient MHD conversion. The remaining energy in the gas is then used in a series of oxidizer preheaters and (with steam bottoming) steam and water heaters as the gas flows through the power plant and cools toward stack temperature. Before the gas flow is released through the stack to the atmosphere, the alkali metal is reclaimed and recycled, and with it is removed any sulfur that was introduced with the fuel. The steam generated is used to drive conventional turbines which power air compressors and conventional a-c generators.

The design and cost estimation of the open-cycle MHD power systems has been a joint effort by Avco-Everett Research Laboratory, Foster Wheeler, Bechtel, and General Electric. The principal items designed and costed by personnel from each of these companies were as follows:

Avco-Everett

- combustor
- MHD nozzle/generator/diffuser
- superconducting magnet/Dewar
- refractory storage high temperature air preheater
- seed recovery and processing

Foster Wheeler

- coal handling auxiliaries
- radiant furnace
- steam superheater/reheater
- low-temperature air preheater
- economizer
- hot gas cleanup for air turbine (Case 22)

Bechtel

on-site labor and materials
cooling towers
balance of plant

General Electric

electrical inversion equipment
steam turbine/generator
steam turbine/compressor

In addition, General Electric has performed the system integration function.

Thirty different MHD power cycle cases have been analyzed in the Task I activity.* The cycle configuration considered for both base cases, Cases 1 and 24, and for all other cases except Case 22, is the binary MHD-Steam Power Cycle with direct combustion of the coal or solvent refined coal (SRC) fuel. The general configuration of this power cycle is illustrated in Figure 2.8-1, which gives pressures, temperatures and flow rates applicable for Case 1. Here the heat content of the MHD generator exhaust gases is utilized for power production in a bottoming steam plant and for preheating of the combustion air. The air preheater subsystem is divided into a regenerative type refractory heat exchanger operating at gas temperatures above 1400 F (1033 K) and a recuperative type metal tubular exchanger operating at lower gas temperatures. The high-temperature air heater receives heat from the main combustion gas flow after the flow leaves the radiant furnace. It is classified as directly fired and it is used in all MHD-Steam Power Cycle Configurations except Cases 9 and 10. Case 10 considers the alternate use of indirectly fired high-temperature regenerative type refractory heat exchangers as shown in Figure 2.8-2. This alternate of indirect firing of the high-temperature regenerative air preheater avoids problems related to MHD generator exhaust gas contamination by seed and ash. The fuel required for separate firing of the regenerator is produced from the more volatile matter in coal by rapid thermal devolatilization brought about by mixing part of the main coal fuel with a smaller fraction of the hot MHD generator exhaust gases as indicated in Figure 2.8-2.

The recuperative heat exchanger preheats the fuel oxidizer from the compressor outlet temperature to 1400 F (1033 K) in all cases except three. The three exceptions are:

1. Case 9 - This case involves oxygen enrichment with preheat of the oxygen enriched air to 1500 F (1089 K) in a recuperative heat exchanger only.

*The principal design parameters for these 30 cases are listed in Table 2.8-6.

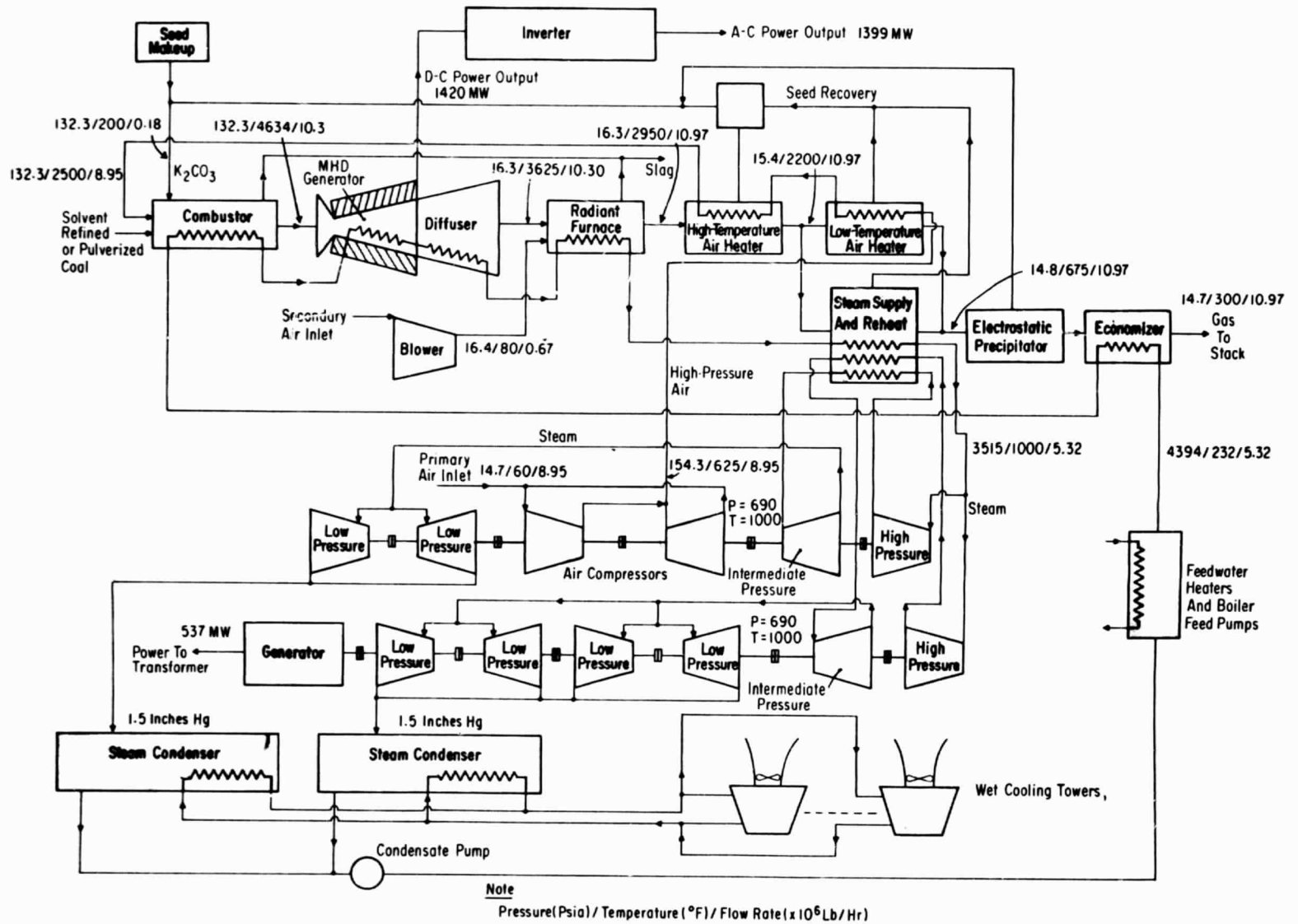
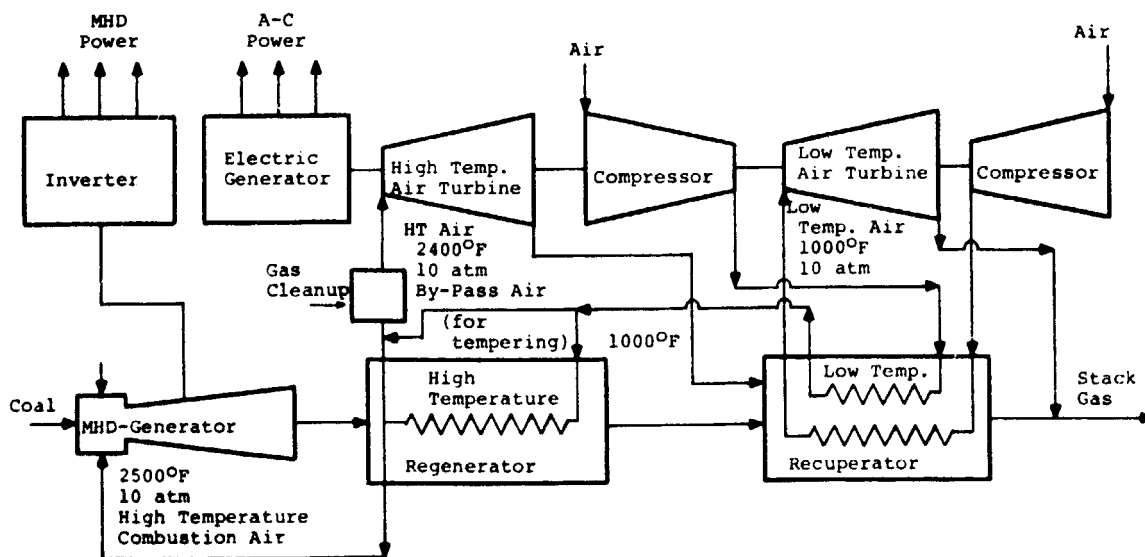


Figure 2.8-1 Open-Cycle MHD (Base Case 1)

One case, Case 22, considers a gas turbine bottoming plant instead of a steam bottoming plant. The cycle configuration for this Case is shown in Figure 2.8-3. The gas turbine bottoming plant consists of a high-temperature gas turbine and a lower-temperature gas turbine operating in series. Specific additional design data for this case is listed on Figure 2.8-3. An expensive and somewhat uncertain particulate removal process has been included near the inlet to the high-temperature turbine to reduce particles picked up in the refractory storage heat exchanger and ducts to the 30 ppm level required by gas turbine inlet specifications. A liquid cooling loop that probably would be required for control of wall temperatures in combustor, MHD generator, and diffuser has been neglected here in cost estimates. Performance calculations, however, have included the effects of heat losses from those components.

Direct combustion of the coal fuel in a single high-temperature MHD combustor has been considered for all cases. The MHD generator channel operates with ash laden combustion gases so that ash is continuously deposited and coats the channel walls.

The assumed degree of slag removal in the combustion process has been specified for each case. Additional slag removal also occurs from the MHD generator exhaust gas immediately upon exit



Heat Absorption From MHD Exhaust

	MHD Combustion Air	High Temperature Turbine Air	Low Temperature Turbine Air
High Temperature Regenerator MW	1120	1180	-
Low Temperature Recuperator MW	475	860	220
Total MW	1595	2740	220

Figure 2.8-3. MHD-Gas Turbine Power Cycle

from the MHD diffuser. The slag extracted here is assumed to be discarded. The solubility of seed in slag is limited and practically all of the seed remains in vapor form at these high exit gas temperatures.

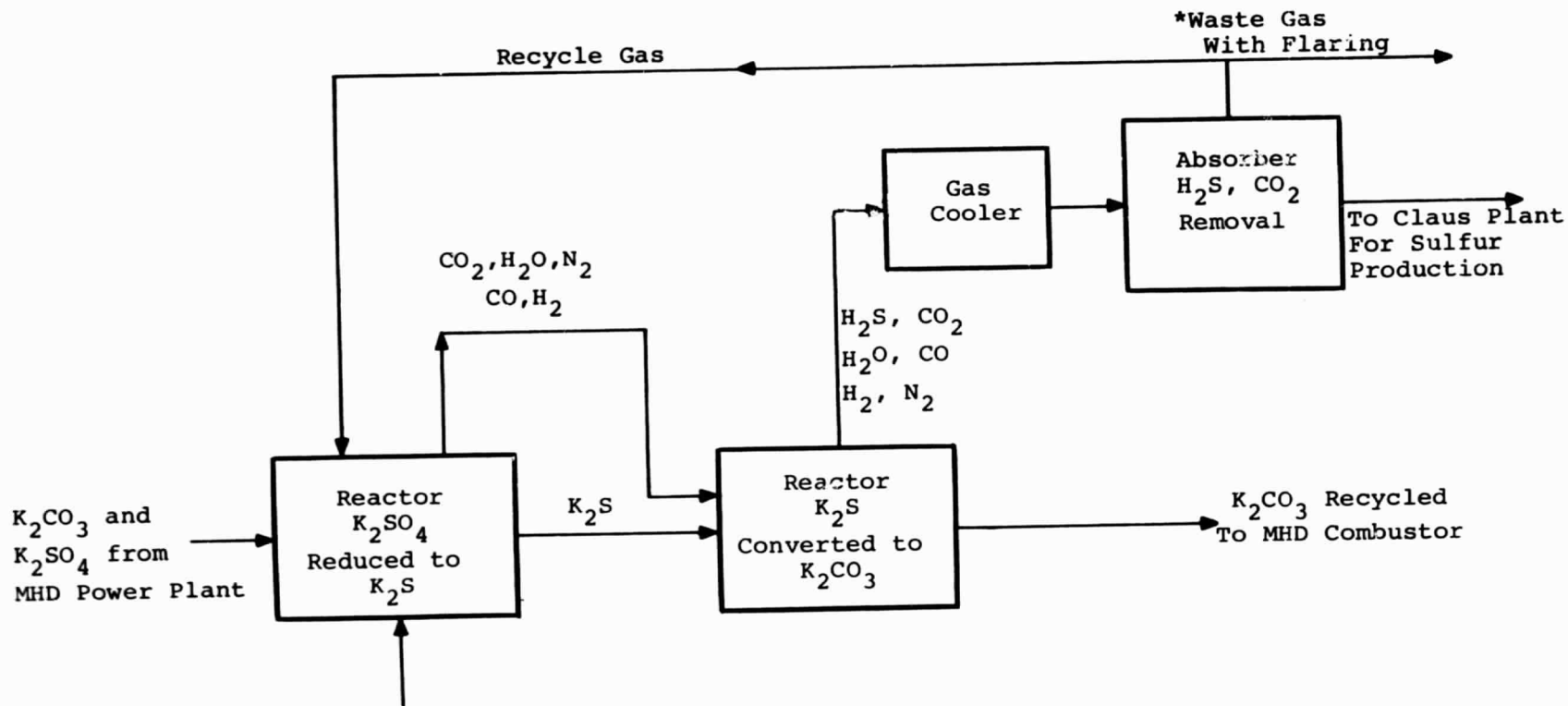
Fuel rich combustion in the high-temperature MHD burner with a fuel/air equivalence ratio of 1.07 has been assumed in all cases for the purpose of emission control of nitrogen oxides. Additional secondary air is added near the exit of the radiant furnace to bring the flow to fuel/air equivalence ratio of 1.0 for afterburning and complete oxidation of the fuel.

Seed recovery is combined with removal of sulfur oxides when this is necessary to satisfy sulfur emission control standards. Seed and remaining fly ash precipitated from the stack gas, and collected from the boiler and air heater in the bottoming plant, are processed as necessary and recycled. The processing of seed converts recovered potassium sulfate to potassium carbonate and produces elemental sulfur as a by-product. Because of uncertain market conditions, no economic credit is taken for the byproduct sulfur. This processing of recovered seed is schematically shown in Figure 2.8-4. The principle of the process is first to reduce recovered K_2SO_4 to K_2S . This reduction is accomplished by reacting K_2SO_4 with CO and H_2 provided by purchased low-Btu (LBtu) gas. The K_2S produced in the reduction process is further reacted with water vapor (H_2O) and carbon dioxide to form potassium carbonate (K_2CO_3) and hydrogen sulfide (H_2S). The hydrogen sulfide produced is fed to a Claus plant where elemental sulfur is produced as a byproduct.

The energy content of the LBtu reducing gas is significant for systems operating on high sulfur fuels. For systems fueled by Ill #6 coal (3.9 percent sulfur) the heating value of the reducing gas is approximately 5 percent of that of the coal flow.

The K_2CO_3 from the process is recycled to the MHD burner. The amount of fly-ash relative to recovered seed is so small that it can be directly recycled together with K_2CO_3 without incurring a serious build-up of ash.

The removal of sulfur from the combustion gas primarily as K_2SO_4 requires removal of 2.44 weight units of potassium for each weight unit of sulfur removed and thus imposes a lower limit on potassium seed flow for any given sulfur flow, a limit that can be governing when high sulfur coal is the fuel. For example, when Illinois #6 coal (3.9 percent sulfur) is burned, seed fractions less than approximately 1 percent K by weight in the combustion gases will not permit attainment of the EPA limits on SO_x emission unless the K_2SO_4 process is supplemented by some other sulfur removal process. For the Montana sub-bituminous (0.8 percent sulfur), North Dakota lignite (0.7 percent sulfur), and solvent refined coal liquid (0.8 percent sulfur) fuels, this effect does not provide practical limitations.



Reducing Gas ($CO + H_2$) Produced Directly From Coal on Site or Alternatively Delivered to Plant as Synthesis Gas.

*Without N_2 in Synthesis Gas all Gas Exiting from Absorber is Recycled

Figure 2.8-4. Seed Recovery Plant Block Diagram

ANALYTICAL PROCEDURES AND DESIGN ASSUMPTIONS

Working Fluid

Thermodynamic equilibrium calculations for the fuel-oxidizer and seed mixtures were conducted to establish the thermodynamic operating conditions of the working fluid for the MHD generator and the bottoming plant. For the MHD generator, the electrical properties of the working fluid are based upon thermal equilibrium conditions. The nitrogen oxide levels formed in the combustor are assumed to be frozen during rapid transit through the MHD nozzle-generator-diffuser, then brought to equilibrium again at temperatures near 2960 F (1900 K) during a 2-second dwell in the radiant furnace before final freezing caused by decreasing reaction rates in the cooling gas.

The parametric assumptions of fuel type and its heating value, oxidizer type, and its preheat temperature, seed material and its concentration, together with assumed combustion efficiency establish the initial gas stagnation conditions. In these calculations it has been assumed that the three different moist coals have been dried before burning by flue gases extracted from the bottoming plant. Illinois #6 bituminous coal has been assumed dried to 2 percent moisture content and Montana sub-bituminous and North Dakota lignite to 5 percent.

MHD Combustor

MHD combustor design has been based upon data and results from experimental work with MHD coal and oil combustors at Avco Everett Research Laboratory. The combustion reaction has been assumed to reach thermal equilibrium at combustor temperature. Combustor heat losses have been estimated at approximately 0.4 MW per square meter of combustor surface. For all coal fueled cases, a combustor residence time of 50 milliseconds has been selected in accordance with results from experimental work. The coal feed is pulverized coal designated as 70 percent through 200 mesh. The injection of the pulverized coal into the combustor is accomplished at flame holder type structures that create shear layers with recirculation zones for turbulent dispersion and rapid and homogeneous mixing of the injected coal with the preheated oxidizer.

The combustion chamber has a vertical arrangement with the generated combustion gases delivered to the MHD generator from the lower part of the burner. Seed is injected at the gas exit from the burner to avoid possible loss of seed in the slag extracted from the bottom of the burner.

The combustor design for burning of liquid solvent refined coal has been based on a combustor residence time of 15 milliseconds, which is in line with combustor residence times used in experimental MHD combustors using heavy fuel oils and fuel oil-pulverized coal mixtures.

MHD Generator

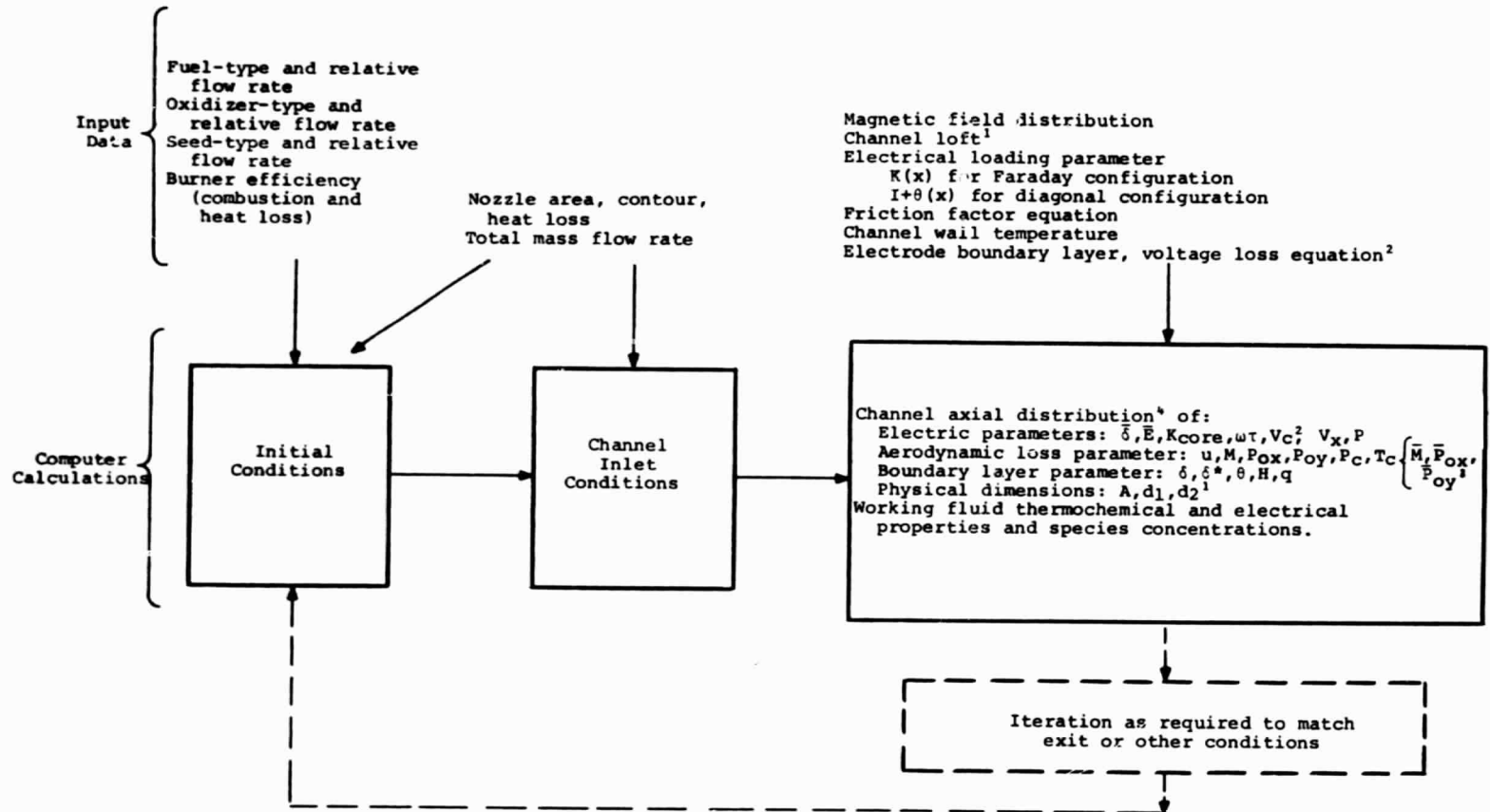
MHD Channel. The procedure for MHD channel calculations is outlined in the accompanying diagram (Figure 2.8-5). It is assumed that the flow is developing rather than fully developed. The flow is divided into an inviscid core occupying most of the channel area and a boundary layer confined to the immediate vicinity of the channel walls. Boundary-layer displacement thicknesses are calculated from momentum integral equations for both electrode and insulator walls, taking into consideration shape factor, compressibility and wall cooling effects.

The performance characteristics, in particular the Hall voltage and effective conductivity, are sensitive to nonuniformities in the flow. Nonuniformities in velocity, electrical conductivity, and Hall parameter in the vicinity of both the electrode and insulator walls are treated. Performance degradation due to finite segmentation and $\int_{\mathbf{x}} \times \mathbf{B}$ forces are also considered.

The plasma is assumed to be in chemical equilibrium at the local conditions, except in nitrogen oxide concentrations, at all points in the flow field. Since the plasma consists of combustion products, the electron density is assumed to be in Saha equilibrium at the translation temperature of the plasma. In the analysis, both the thermodynamic and the transport properties of the gas mixture are required. The thermodynamic equilibrium properties of the combustion products, considering up to fifty of the most important species, are calculated as a function of temperature and pressure. The electrical conductivity σ and the Hall parameter $\omega\tau$ are evaluated as a function of temperature and pressure using Frost's approximation with the effects of electron attachment to OH and other species included and accounting for magnetic field strength effects. The viscosity μ is evaluated using Wilke's mixture rule and the first approximation of the Chapman-Enskog expansion with Lennard-Jones' potentials for the individual species, except for H₂O where an experimental correlation is used.

In general, the calculations performed for each case illustrate that MHD generator specific power output, expansion efficiency and length are most strongly influenced by electrical loading parameter and air preheat temperature. It should be noted that inlet stagnation pressure which specifies the total isentropic enthalpy available for energy extraction is essentially a dependent variable which should be determined by the choice of electrical loading parameter, the preheat temperature, and other parameters. Because of this effect, the inlet pressure tends to vary among the cases studied more than most other design parameters.

The power output from the generator is almost unaffected by the variation in magnetic field between 5 and 7 tesla. The main reason for this is that the pressure ratio and thus available gas enthalpy for energy extraction is specified to be constant. The



- 1 The "Design" program calculates channel loft for a specified velocity distribution. The "Off" design program calculates velocity, etc. for a given channel loft.
- 2 Electrode and boundary layer voltage loss is specified by an equation based on experimental measurement as well as theoretical calculation.
- 3 Barred quantities are averages over the channel cross section.
- 4 Separate programs are used for the calculations of three-dimensional current distributions and end effects.

Figure 2.8-5. MHD Channel Calculation Procedure

reduction in field strength is compensated for by increased length without incurring serious heat and pressure losses for the relatively large generator capacity considered here. The power output could have increased with increased field strength if the ground rules under which the study was conducted had permitted an appropriate increase in pressure ratio. Due to programmatic limitations, few cases have been included in which major changes have been made in two parameters simultaneously.

The effect of seed variation on power output is also insignificant. This can be explained by the relative insensitivity of performance to length as indicated above, and by the relative insensitivity of conductivity to seed concentration in the range considered from 0.5 to 1.5 percent.

The diffuser performance is estimated assuming a 70 percent diffuser efficiency and a two-dimensional subsonic expansion, since data covering the high inlet blockage conditions characteristic of the MHD application are most complete for this type of diffuser. However, available evidence indicates that three-dimensional diffusers can be equally effective. A three-dimensional diffuser expansion would have the advantage of reducing the diffuser length by roughly a factor of two.

In a high-blockage situation, boundary-layer bleed and mechanical pumping to exhaust plenum pressure should be advantageous. However, no credit was taken for this possibility or for the beneficial effects of boundary layer cooling as the gas flows from the MHD duct into the relatively cold-walled diffuser.

MHD Magnet. The required magnetic field for the MHD generator is provided by a superconducting magnet. A saddle-shaped magnetic field coil has been selected and the axial magnetic field along the channel has been tailored to the MHD channel operating requirements. The actual magnetic field distribution and axial profile have been calculated and utilized in the MHD channel performance calculations. Magnet design data for the base Case 1 are listed in Table 2.8-1 and for base Case 24 in Table 2.8-2. The magnetic field profile rises sharply at the inlet end of the channel where it reaches its peak value. It then tapers off towards the channel exit where it drops off more rapidly. This decrease of the magnetic field from inlet to exit lowers the axial electrical field (Hall field) and Hall parameter within the MHD generator, which are important to generator design and operation. For Case 1 with an average magnetic field strength of 5 tesla, the axial electrical field within the channel is quite low and varies between 1.1 and 2.7 kV/m. For Case 24, with an average magnetic field strength of 6 tesla the axial electrical field varies between 1.2 and 4.0 kV/m, which still is within the range where experimental MHD channels have been successfully operated.

Table 2.8-1

MAGNET FOR BASE-CASE MHD GENERATOR
CASE 1-2000 MWE PLANT SIZE

Channel Specifications

Inlet	1.4297 m × 1.4297 m
Exit	3.653 m × 3.653 m
Active Length	25m
Field: Inlet	2.496 T
Bo max.	5.992 T
Exit	3.12 T
$VB^2 = \int_0^{25} AB^2 dl$	11,600 m ³ T ²

Magnet Design Data

Warm bore (circular)	Inlet	2.87 m
	Exit	6.50 m
Active length		25 m
Ampere turns		50.8 × 10 ⁶
Ampere meters		34.2 × 10 ⁸
Stored energy		15,200 megajoules
Current density, winding, average		2.0 × 10 ⁷ A/m ²
Dewar O.D.		
	Inlet end	9.3 m
	Exit end	13.6 m
Dewar length, overall		31 m
Conductor weight		900,000 kg
Main structure weight		1,900,000 kg
	(design stress 25,000 psi)	
Internal structure & miscellaneous weight		180,000 kg
Dewar weight		750,000 kg
	Total	<u>3,730,000 kg</u>

Table 2.8-2

MAGNET DESIGN DATA FOR BASE CASE MHD GENERATOR
CASE 24-SRC AS FUEL

Channel Specifications

Inlet	1.067 m sq.
Exit	3.499 m sq.
Active length	~20 m
Field: Inlet	3.21 T
Peak	7.72 T
Exit	2.40 T

Magnet Design Data

Warm bore (circular):	Inlet	2.60 m
	Exit	6.36 m
Active length		20 m
Field: Inlet		3.2
Peak		7.9
Exit		2.4
$VB^2 = \int_0^{20} AB^2 dl$		13,200 m ³ T ²
Ampere turns		76.4 × 10 ⁶
Current density, average		2.0 × 10 ⁷ A/m ²
Dewar O.D.		
Inlet end		9.8 m
Exit end		13.7 m
Dewar length		28 m
Conductor weight		1,036,000 kg
Main structure weight		2,100,000 kg
Intermediate structure & miscellaneous weight		200,000 kg
Dewar weight		<u>750,000 kg</u>
	Total	4,086,000 kg

High-Temperature Preheater

The high-temperature regenerative type air preheater subsystem design is based upon information and experimental results obtained in the development of such preheaters for MHD power system applications at Avco Everett Research Laboratory.

The thermal performance of the preheater has been calculated by computer techniques. This mathematical treatment is based upon two differential equations related to the flow of heat within the matrix and from the fluid to the matrix and vice versa. Preheater cycle time periods, materials, temperature gradients and temperature fluctuations within the refractory matrix, as well as the geometry, dimensions and height of the matrix have been selected, based upon experimental work along with detailed analysis of thermal stresses of refractory matrices and system requirements for high temperature regenerative preheaters.

For all cases except 9, which excludes a high-temperature preheater, a total of 6 preheater units has been assumed with 2 units on blow-down for heating of air, 3 units on reheat with hot combustion gases and one additional spare unit. The cycle time periods selected are four minutes on blow-down and six minutes on reheat.

The matrix for preheat temperatures of 2000 F (1367 K) and 2500 F (1644 K) consists of bricks with 1 1/2-in. hole diameter. One exception to this is Case 22 using a preheat temperature of 2500 F (1644 K) and gas turbine bottoming plant, in which case a hole diameter of 1 in. has been selected for the matrix bricks. The 1-in. hole diameter has also been employed for the higher preheat temperatures of 3100 F (1978 K) and 3600 F (2256 K) with direct firing of the preheaters. For the one case with indirect firing, Case 10 (with 3100 F preheat temperature), a smaller hole diameter of 1/4-in. has been selected for superior thermal performance. The fuel gas for indirect firing is produced by volatilization of a small part of the coal by mixing it with a small fraction of high temperature MHD combustion gases. In this way, rapid devolatilization of the volatile matter of coal is attained and a residence time of 100 milliseconds is adequate for volatilization to occur. The exit fuel gas temperature is 1880 F (1300 K) which is below the dew point for potassium seed. The remaining char, with ash and condensed seed from the volatilization process, is fed to the MHD burner where it is burned together with the main coal fuel feed.

Design data for the high temperature air preheater for the first base case, Case 1, and Cases 2 and 3, are listed in Table 2.8-3. Similar data for the second base case, Case 24, are listed in Table 2.8-4.

Table 2.8-3
AIR PREHEATER
CASES 1, 2, AND 3

	Case 1	Case 2	Case 3
Plant Size MWe	<u>2000</u>	<u>1200</u>	<u>600</u>
Air preheat temp (°F)	2500	2500	2500
Air pressure (atm)	10.5	10.5	10.5
Number of Heaters	6 [2 blowdown 3 reheat 1 spare	6 [2 blowdown 3 reheat 1 spare	6 [2 blowdown 3 reheat 1 spare
Heater bed dia. (ft)	30	24	17
Heater bed height (ft)	40	40	40
Heater total height (ft)	75	70	60
Heater bed weight (tons)	1400	900	450
Heater total weight (tons)	2400	1650	1000
Pressure drop			
Air side (atm)	0.01	0.01	0.01
Gas side (atm)	0.06	0.06	0.06

Table 2.8-4
AIR PREHEATER
CASE 24-BASE CASE WITH SRC AS FUEL

Air preheat temperature (°F)	3100
Air pressure (atm)	16
Number of Heaters	6 [2 blowdown 3 reheat 1 spare
Heater bed diameter (ft)	30
Heater bed height (ft)	40
Heater total height (ft)	75
Heater bed weight (tons)	1600
Heater total weight (tons)	2600
Pressure drop	
Air side (atm)	0.01
Gas side (atm)	0.10

COST BASIS

Combustor

The combustor and channel inlet expansion nozzle are cooled by boiler feedwater in all cases except for Case 22, which has a gas turbine bottoming plant. Cooling is contemplated in this latter case by utilizing a closed loop with an organic coolant (e.g., Dowtherm), together with an external heat exchanger. (In this case, the heat transferred to the coolant from the combustor is considered to be lost to the surroundings, whereas in the former case it is utilized for boiler feed water heating.)

Cooling of the combustion chamber and inlet nozzle permits the use of steel as the basic construction material. A metal tubular construction for the outer walls of the combustion chamber and nozzle is contemplated. The inner walls are lined with refractory which in time will be partly replaced by ash during operation.

MHD Channel Assembly

The MHD channel assembly includes the channel and diffuser. The channel walls consist of water (or Dowtherm) cooled inconel bars with refractory insulation in between, and a plastic backing structure reenforced with stainless steel ribs. The channel becomes lined with slag during operation. The diffuser walls are made of water-cooled steel tubes backed by insulation and structural steel.

Superconducting Magnet

Cost and weight estimates for magnets are based on the use of air-core saddle-coil magnets with windings of copper-stabilized NbTi superconductor maintained at liquid helium temperature by closed-loop refrigeration equipment. The typical magnet has a warm bore of circular cross section, increasing in diameter toward the low-field end to conform approximately to the increasing cross section of the MHD channel toward the exit (low-field) end. The windings themselves also diverge toward the exit end. The windings are enclosed in a close-fitting liquid helium container. Main structural members supporting the windings against gravity and magnetic forces are of aluminum alloy, operating at the same temperature as the coils. The structural members include shells enclosing the windings and carrying the major longitudinal magnetic forces together with ring girders or the equivalent clamped around the outside of the winding and shell assembly and carrying the radially-outward magnetic forces. The windings and structure are mounted in a vacuum jacket (Dewar) made of aluminum alloy. Multi-layer thermal insulation and intermediate temperature thermal shielding are provided to reduce heat transfer from the room-temperature jacket walls to the cold region.

All magnet designs incorporate full cryogenic stabilization with relatively low current densities (2 to 3×10^7 A/m²) and moderate structural stresses of 20,000 to 35,000 psi (15 to 25×10^6 kg/m²). To conserve superconductor, it is assumed that the windings are "graded," i.e., the amount of NbTi contained in the conductor in portions of the windings exposed to lower fields is reduced in inverse proportion to its current-carrying capacity, which increases with lowering field. For those magnets designed for the higher fields at the front end (above 6T), the end-turn configuration is spread out in order to reduce field concentration in the winding.

Costs of stabilized superconductor are based on recent vendor estimates for large cross-section, low-current density composite conductor (built-up type), adjusted in accordance with design magnetic field levels. Costs of aluminum alloy structure and vacuum jackets are likewise based on vendor estimates on large welded assemblies. Costs of magnet coil winding and assembly labor, accessory systems and installation are engineering estimates based on past Avco experience in MHD magnet work.*

High-Temperature Preheater

The design of the high-temperature preheater subsystem which forms the base for the cost analysis and determines the materials requirements is based upon data and information developed in Avco MHD preheater development work. This includes construction and operation of experimental preheaters, materials investigations, and design studies of large scale preheaters for commercial MHD power plant applications, as well as information gathered from other industrial and special applications of high-temperature regenerators.

A regenerative heat exchanger with a stationary refractory bed was selected because most data and information are available for this type of preheater design. Refractory type regenerators with stationary beds have also been used for several years within the steel and glass industry for preheating air to about 2500 F (1644 K) by waste heat recovery from high-temperature combustion gases containing some contamination of dust and alkalies. Dimensions of these large industrial regenerators are typically heights of 125-150 ft (38-46 m) and diameters of about 30 ft (9 m). High-temperature switch-over valves for cyclic operation of such regenerators are manufactured in sizes up to 6 ft (1.8 m) internal diameter.

Cost data have been obtained from refractory manufacturers, high-temperature valve manufacturers and steel fabricators in

*The estimates for the magnet system provided by Avco during Task I include some cost elements that should be included in Balance of Plant. The Avco estimates have been accepted as submitted, however, because it appears that actual double counting has not exceeded 15 percent of total installed magnet cost.

the preparation of cost estimates. Estimates for materials and costs comprise the total high-temperature preheater subsystem and include all regenerator units with their refractory matrix, refractory lining and insulation, steel vessels and structure. In addition for the one case, Case 10, with indirect firing, the analysis includes also the cost of the coal devolatilizer for production of the fuel gas required, as well as the auxiliary burner equipment for separate burning of this fuel.*

Present costs obtained for checker bricks of high purity magnesia and alumina are in the range of \$0.25 to \$0.35/lb (\$0.55 to \$0.77/kg) in bulk. These checkers with hole sizes (1 to 2 in. [2.5 to 5 cm]) similar to those used in directly fired regenerator matrix design have been used for industrial regenerators up to temperatures of 2600 F (1700 K). Cored bricks of high purity alumina have been used successfully in experimental MHD preheaters with clean combustion gases up to higher preheat temperature of 3100 F (2000 K), and also in wind-tunnel heaters at these high temperatures. According to rough estimates obtained from refractory manufacturers, costs in bulk of such cored bricks would be in the order of \$1.00/lb (\$2.20/kg) for high purity alumina or magnesia. The use of magnesia and alumina is limited to maximum preheat temperatures of about 3100 F (2000 K) because of their thermal properties. The selection of refractory materials is determined by several other factors in addition to thermal stability of the materials such as chemical stability, thermal fracture resistance and mechanical strength. For the very high preheat temperature of 3600 F (2256 K), zirconia material has been specified for the upper portion of the matrix operating at temperatures higher than 3000 F (1922 K). Bulk unit cost for this high temperature zirconia material has been estimated to \$3/lb (\$6.61/kg) from information gathered.

With the above data as basis, a cost of \$0.50/lb (\$1.10/kg) has been applied for refractory matrix material of magnesia or alumina for preheat temperatures of 2000 F (1367 K) and 2500 F (1644 K). For the higher preheat temperature of 3100 F (1977 K) the same unit cost (\$0.50/lb) has been applied to the part of the matrix designed to operate below 2500 F. For the portion of the matrix operating above this temperature, the use of more costly magnesia or alumina materials at a unit cost of \$1/lb (\$2.20/kg) has been assumed.

For the highest preheat temperature of 3600 F (2256 K), the matrix has been divided into three temperature zones with different materials and unit material costs. For the temperature zone below 2500 F (1644 K), magnesia or alumina material is assumed

*The estimates for the high-temperature air heater costs provided by Avco during Task I have been multiplied by the factor 0.61 to remove from those estimates cost elements that should be included in Balance of Plant. This factor was obtained from a breakdown of air heater costs provided by Avco during Task II efforts.

with a unit cost of \$0.50/lb (\$1.10/kg), for the middle temperature zone from 2500 F (1644 K) to 3000 F (1922 K), more costly magnesia or alumina materials are assumed with a unit cost of \$1/lb (\$2.20/kg), and for the higher temperature zone above 3000 F (1922 K), zirconia material is assumed with a unit cost of \$3/lb (\$6.61/kg).

The one case with indirectly fired regenerators utilizes a cored brick design with a relatively small 1/4-in. (0.64 cm) hole diameter which has a superior thermal performance compared to the brick designs with larger hole diameter of 1-in. (2.5 cm) and 1-1/2-in. (3.8 cm). For this specific case with cored bricks, the refractory material unit cost has been assumed to be \$1/lb (\$2.20/kg) for the complete matrix.

Other preheater types and concepts besides regenerators with stationary beds are under development or have been proposed. These include regenerators with moving refractory beds of the rotary and falling types, as well as more advanced and novel concepts involving coal ash as the intermediate heat transfer medium. Moving type bed systems would be more compact than fixed ones and hence could be less costly. The possible use of coal ash as the heat transfer media would obviously result in substantial savings of matrix costs.

Seed Recovery and Processing

The estimated costs associated with processing of seed using LBtu gas as the fuel source are listed in Table 2.8-5. Seed make-up costs related to the loss of seed in slag or otherwise are also included in this table.

RESULTS

The results of the Task I study cover a total of 30 systems outlined in Table 2.8-6. These systems were treated as a coal-fired base case, Case 1, with 22 parametric variations, and a semi-clean fuel fired base case, Case 24, with 6 parametric variations. Detailed results for the two base cases, Cases 1 and 24, are summarized in Tables 2.8-7 and 2.8-8. Table 2.8-9 gives the detailed cost distributions for all systems studied and Table 2.8-10 gives the distributions of output powers and auxiliary losses.

Although most of the parametric variations involve relatively small changes in the systems, a few such as Case 9 using oxygen enrichment of combustion air, Case 10 using separately fired high-temperature air heaters, and Case 22 using the air turbine bottoming system represent major departures. In addition to those major system changes, the parametric variations for the coal-fired systems include variations in nominal power output from 2000 MWe down to 600 MWe (Cases 1, 2, 3), the use of three different coals (Cases 1, 4, 5), variations in slag rejection during

Table 2.8-5

ESTIMATED COSTS FOR CONSTRUCTION AND OPERATION
OF SEED RECOVERY EQUIPMENT

<u>Power Plant:</u>								
Plant Fuel	Ill. #6	Montana	N.D.	SRC				
Plant Size (MW)	2000	1200	600	2000	2000	2000	2000	2000
Seed Concentration (% K)	1.0	1.0	1.0	0.5	1.5	1.0	1.0	1.0
<u>Processing Plant:</u>								
Direct Construction Cost (10 ⁶ \$)	8.0	6.0	4.0	5.0	8.0	2.0	2.5	1.0
*Fuel Cost (\$/hr)	1115	705	355	560	1115	121	174	37
Operation + Maintenance Cost (\$/hr)	60	38	19	38	60	30	30	20
Sulfur Produced (tons/hr)	20	12.6	6.4	10	20	2.2	3.1	0.6
<u>**Seed Make-up Cost:</u>								
For 80% or 90% Combustor Slag Removal (\$/hr)	62	38	19	31	93	65	67	54
For No Combustor Slag Removal (\$/hr)	186	114	57	93	279	195	201	54

*Based upon \$2.08/MBtu for synthesis gas as the fuel source.

**Based upon \$0.05/lb K₂O for potassium sulfide as seed make source.

REPRODUCIBILITY OF THE ORIGINAL PAGE IS POOR

Parameters	Common Elements: Direct Co								
	Case 1*	2	3	4	5	6	7	8**	9
Power Output (MWe)	1895	1180	599	1870	1867	1888	1888	1426	1991
Combustion									
Coal	Ill. #6	→		Mont	N. D.	Ill. #6			
Oxidizer	Air								Air/C
Combustor slag rejection (percent)	90					80	0	90	
Preheater									
Firing	Direct								
Oxidizer temperature (°F)	2500								1500
MHD Generator									
Type	Faraday								
Inlet pressure (atm)	9	8.9	8.7	7	6.5	9	→	7	10.2
Average magnetic field (T)	5								
Potassium seed (percent)	1.0								
Electrical load parameter	0.8								
Heat Exchangers									
Gas (Δp/p)	0.15								
Air (Δp/p)	0.10								
Steam Bottoming Cycle									
Turbine inlet temperature (°F)	1000/1000								
Turbine inlet pressure (psi)	3500								
Maximum feedwater temperature (°F)	232								
Air Bottoming Cycle									
Turbine inlet temperature (°F)	--	--	--	--	--	--	--	--	--
Pressure ratio	--	--	--	--	--	--	--	--	--
Heat Rejection (in. Hg)	WCT								
1.5	1.5								
Actual Powerplant Output (MWe)	1895	1180	599	1870	1867	1888	1888	1426	1991
Thermodynamic Efficiency (percent)	52.8	52.0	52.3	49.6	48.4	52.7	52.7	51.6	50.0
Powerplant Efficiency (percent)	49.2	48.5	48.7	47.9	46.5	49.1	49.1	47.2	46.9
Overall Energy Efficiency (percent)	48.3	47.6	47.8	47.8	46.3	48.1	48.1	46.1	46.1
Coal Consumption (lb/kWh)	0.65	0.67	0.66	0.80	1.07	0.66	0.66	0.69	0.69
Plant Capital Cost (\$ million)	2090	1239	715	2060	2107	2092	2091	2018	2016
Plant Capital Cost (\$/kWe)	1102	1049	1193	1101	1128	1108	1107	1415	1012
Cost of Electricity, Capacity Factor = 0.65									
Capital (mills/kWh)	34.9	33.2	37.7	34.8	35.7	35.0	35.0	44.7	32.0
Fuel (mills/kWh)	6.2	6.3	6.3	6.1	6.3	6.3	6.3	6.6	8.8
Maintenance and operating (mills/kWh)	2.8	2.9	3.2	2.9	2.9	2.8	2.8	3.6	2.3
Total (mills/kWh)	43.9	42.4	47.3	43.8	44.9	44.1	44.1	55.0	43.1
Sensitivity									
Capacity factor = 0.50 (total mills/kWh)	55.1	53.2	59.6	55.2	56.5	55.4	55.4	69.5	53.4
Capacity factor = 0.80 (total mills/kWh)	36.8	35.6	39.6	36.8	37.7	37.0	37.0	45.9	36.6
Capital Δ = 20 percent (Δ mills/kWh)	7.0	6.6	7.5	7.0	7.1	7.0	7.0	8.9	6.4
Fuel Δ = 20 percent (Δ mills/kWh)	1.2	1.3	1.3	1.2	1.3	1.3	1.3	1.3	1.3
Estimated Time for Construction (years)	7	6	6	7	7	7	7	7	7
Estimated Date of 1st Commercial Service (year)	1997	1997	1997	1997	1997	1997	1997	1997	1993

*Base case 1.

**Base case 1 configuration, reduced power output.

+ Base case 2.

DCT = Dry cooling tower

HT = High temperature

Ill. = Illinois

Mont = Montana

N. D. = North Dakota

WCT = Wet cooling tower

Table 2.8-7

SUMMARY SHEET
OPEN-CYCLE MHD BASE CASE 1

CYCLE PARAMETER	
Power Output (MWe)	1895
Combustion	
Coal	Illinois No. 6
Oxidizer	Air
Combustor slag rejection (percent)	90
Preheater	
Firing	Direct
Oxidizer temperature (°F)	2500
MHD Generator	
Type	Faraday
Inlet pressure (atm)	9
Average magnetic field (T)	5
Potassium seed (percent)	1.0
Electrical load parameter	0.8
Heat Exchangers	
Gas (Δp/p)	0.15
Air (Δp/p)	0.10
Steam Bottoming Cycle	
Turbine inlet temperature (°F)	1000/1000
Turbine inlet pressure (psi)	3500
Maximum feedwater temperature (°F)	232
Air Bottoming Cycle	
Turbine inlet temperature (°F)	--
Pressure ratio	--
Heat Rejection	Wet cooling tower

MAJOR COMPONENT CHARACTERISTICS

Major Component	Unit or Module		Units Required	total Cost (\$ x 10 ⁶)	\$/kW Output	
	Size (ft) (W x L (or D) x H)	Weight (lb) (x 10 ³)				
Combustor	9 dia x 27 long	0.051	5.00	1	5.00	2.64
Nozzle/generator/diffuser	Inlet area 22 ft ² Exit area 4100 ft ² } 250 long	2.92	7.90	1	7.90	4.17
Magnet and dewar	44 dia x 100 long	8.20	44.00	1	44.00	23.22
Radiant furnace	80 x 60 x 100	0.98	3.15	1	3.15	1.66
Superheater/reheater	80 x 38.7 x 70	9.50	22.72	1	22.72	11.99
Economizer	80 x 32.7 x 7.9	2.20	1.64	1	1.64	0.87
High-temperature air heater	34 dia x 75 high	4.85	2.07	6	12.4	6.54
Low-temperature air heater	80 x 36.5 x 29.6	3.30	12.26	1	12.26	6.47
Seed recovery system	--	--	0	1	8.00	4.22
Steam turbine-generator set	30 x 174 x 25	4.5	20.08	1	20.08	10.95
Inverters	--	--	86.60	1	86.60	45.70

PERFORMANCE AND COST	
Thermodynamic efficiency (percent)	52.8
Powerplant efficiency (percent)	49.2
Overall energy efficiency (percent)	48.3
Plant capital cost (\$ x 10 ⁶)	2090
Plant capital cost (\$/kWe)	1102
Cost of electricity (mills/kWh)	43.9

NATURAL RESOURCES	
Coal (lb/kWh)	0.65
Water (gal/kWh)	
Total	0.22
Cooling	0.22
Processing	0
Makeup	0
NO _x suppression	0
Stack gas cleanup	0
Land (acres/100 MWe)	3.71

ENVIRONMENTAL INTRUSION		
	Lb/10 ⁶ -Btu Input	Lb/kWh Output
SO ₂	1.2	0.8 x 10 ⁻²
NO _x	0.3	0.2 x 10 ⁻²
HC	0	0
CO	0	0
Particulates	0.1	0.08 x 10 ⁻²
		Btu/kWh
Heat to water		2468
Heat, total rejected		3652
		Lb/kWh
		Lb/Day
Wastes		
Furnace solids	0.0534	2.42 x 10 ⁶
Fly ash	0.006	0.27 x 10 ⁶

REPRODUCIBILITY OF THE ORIGINAL PAGE IS POOR

Table 2.8-9 (Page 1 of 3)

CAPITAL COST DISTRIBUTIONS FOR OPEN-CYCLE MHD

	CASE NO.	1	2	3	4	5	6	7	8	9	10
MAJOR COMPONENTS											
PRIME CYCLE											
MHD GEN-DIFFUSER	MMS	7.9	5.2	3.3	7.9	7.9	7.9	7.9	7.9	7.9	7.9
MAGNET	MMS	44.0	34.0	23.0	43.0	39.0	45.0	45.0	45.0	42.0	51.0
HIGH TEMP AIR PREHEATER	MMS	12.4	8.9	5.5	12.4	12.4	12.4	12.4	12.4	0.	14.7
LOW TEMP AIR PREHEATER	MMS	12.3	8.4	5.0	9.3	10.0	12.2	12.2	7.9	14.3	27.0
SEED RECOVERY SYSTEM	MMS	8.0	6.0	4.0	2.0	2.5	8.0	8.0	8.0	8.0	8.0
COMP WITH STEAM TURB DRIVE	MMS	13.4	11.7	10.5	12.9	12.8	13.4	13.4	11.9	11.4	13.0
BOTTOMING CYCLE											
SLAGGING BOILER	MMS	3.1	2.1	1.3	4.0	3.9	3.2	3.2	2.6	6.9	14.9
STEAM BOILER (SUPER-REHEAT -BOIL-ECON)	MMS	24.4	15.5	8.1	20.9	23.6	24.2	24.2	19.1	16.3	4.4
STEAM TURB-GEN	MMS	20.1	13.1	11.3	21.7	21.6	20.2	19.4	28.4	28.4	21.2
AIR TURB-COMB-GEN-CLEANUP	MMS	0.	0.	0.	0.	0.	0.	0.	0.	0.	0.
PRIMARY HEAT INPUT AND FUEL SYSTEM											
COMBUSTOR SYSTEM	MMS	29.2	18.7	9.6	31.2	42.5	29.2	29.2	23.0	30.7	28.8
SUB-TOTAL OF MAJOR COMPONENTS	MMS	174.7	123.6	81.6	165.2	176.0	175.7	174.9	166.1	165.9	190.9
BALANCE OF PLANT											
COOLING TOWER	MMS	8.2	5.0	2.8	8.2	8.2	8.2	8.2	8.2	8.2	8.2
DC TO AC INVERTERS	MMS	86.6	61.6	37.0	76.1	75.7	86.6	86.6	61.0	85.7	105.0
ALL OTHER	MMS	537.1	330.5	182.0	541.3	549.8	537.1	537.1	537.1	542.1	537.1
SITE LABOR	MMS	178.0	109.5	60.2	179.7	182.8	178.0	178.0	178.0	148.0	178.0
SUB-TOTAL OF BALANCE OF PLANT	MMS	809.9	506.6	282.0	805.2	816.5	809.9	809.9	784.3	784.0	828.3
CONTINGENCY	MMS	196.9	126.0	72.7	194.1	198.5	197.1	197.0	190.1	190.0	203.8
ESCALATION COSTS	MMS	395.7	216.3	124.8	390.0	398.9	396.1	395.8	382.0	381.7	409.6
INTEREST DURING CONSTRUCTION	MMS	513.1	266.4	153.7	505.6	517.2	513.6	513.2	495.2	494.9	531.1
TOTAL CAPITAL COST	MMS	2090.3	1238.9	714.7	2060.1	2107.1	2092.4	2090.7	2017.7	2016.5	2163.8
MAJOR COMPONENTS COST											
MAJOR COMPONENTS COST	\$/KWE	92.2	104.7	136.2	88.3	94.3	93.1	92.6	116.5	83.3	95.7
BALANCE OF PLANT	\$/KWE	427.3	429.3	471.0	430.7	437.3	428.9	428.9	550.1	393.7	415.4
CONTINGENCY	\$/KWE	103.9	106.8	121.4	103.8	106.3	104.4	104.3	133.3	95.4	102.2
ESCALATION COSTS	\$/KWE	208.8	183.2	208.4	208.6	213.6	209.8	209.6	267.9	191.7	265.4
INTEREST DURING CONSTRUCTION	\$/KWE	270.7	225.7	256.7	270.4	277.0	272.0	271.7	347.4	248.5	264.3
TOTAL CAPITAL COST	\$/KWE	1102.9	1049.8	1193.6	1101.8	1128.4	1108.0	1107.2	1415.2	1012.6	1085.1

Table 2.8-9 (Page 2 of 3)

CAPITAL COST DISTRIBUTIONS FOR OPEN-CYCLE MHD

	CASE NO.	11	12	13	14	15	16	17	18	19	20
MAJOR COMPONENTS											
PRIME CYCLE											
MHD GEN-DIFFUSER	MMS	7.9	7.9	7.9	7.9	7.9	7.9	7.9	7.9	7.9	7.9
MAGNET	MMS	48.0	61.0	46.0	58.0	31.0	22.0	23.0	24.0	44.0	52.0
HIGH TEMP AIR PREHEATER	MMS	16.0	16.0	12.4	12.4	12.4	12.4	12.4	12.4	12.4	12.4
LOW TEMP AIR PREHEATER	MMS	12.1	11.0	5.5	12.0	12.3	12.3	12.3	12.3	12.3	12.3
SEED RECOVERY SYSTEM	MMS	8.0	8.0	8.0	8.0	8.0	8.0	8.0	8.0	8.0	8.0
COMP WITH STEAM TURB DRIVE	MMS	18.9	19.6	12.4	13.3	13.4	13.4	13.4	13.4	13.4	13.4
BOTTOMING CYCLE											
SLAGGING BOILER	MMS	2.3	1.7	8.1	2.9	3.6	4.6	3.2	3.2	3.2	3.0
STEAM BOILER (SUPER-REHEAT -BOIL-ECON)	MMS	24.1	25.6	21.5	24.3	24.7	37.2	25.8	25.8	26.2	24.3
STEAM TURB-GEN	MMS	13.3	12.1	23.3	19.9	21.0	23.1	20.1	20.1	20.3	20.0
AIR TURB-COMB-GEN-CLEANUP	MMS	0.	0.	0.	0.	0.	0.	0.	0.	0.	0.
PRIMARY HEAT INPUT AND FUEL SYSTEM											
COMBUSTOR SYSTEM	MMS	30.1	30.2	29.2	29.4	29.2	29.2	29.2	29.2	29.2	29.2
SUB-TOTAL OF MAJOR COMPONENTS	MMS	180.6	193.1	174.3	188.0	163.4	170.1	155.3	156.3	176.8	182.5
BALANCE OF PLANT											
COOLING TOWER	MMS	8.2	8.2	8.2	8.2	8.2	8.2	8.2	8.2	8.2	8.2
DC TO AC INVERTERS	MMS	109.8	107.3	69.1	85.3	83.2	65.7	76.7	73.8	84.0	85.8
ALL OTHER	MMS	537.1	537.1	537.1	537.1	537.1	537.1	537.1	537.1	537.1	537.1
SITE LABOR	MMS	178.0	178.0	178.0	178.0	178.0	178.0	178.0	178.0	178.0	178.0
SUB-TOTAL OF BALANCE OF PLANT	MMS	833.1	830.6	792.4	808.6	806.5	789.0	800.0	797.1	807.3	809.1
CONTINGENCY	MMS	202.7	204.7	193.3	199.3	194.0	191.8	191.1	190.7	196.8	198.3
ESCALATION COSTS	MMS	407.4	411.4	388.5	400.5	389.8	385.4	383.9	383.1	395.5	398.5
INTEREST DURING CONSTRUCTION	MMS	528.2	533.4	503.7	519.3	505.4	499.7	497.8	496.8	512.8	516.7
TOTAL CAPITAL COST	MMS	2152.1	2173.3	2052.3	2115.7	2059.0	2036.0	2028.0	2024.0	2089.2	2105.1
MAJOR COMPONENTS COST											
BALANCE OF PLANT	\$/KWE	413.1	400.7	456.0	419.3	448.2	464.0	422.1	420.6	428.8	425.6
CONTINGENCY	\$/KWE	100.5	98.8	111.3	103.3	107.8	112.8	100.8	100.6	104.5	104.3
ESCALATION COSTS	\$/KWE	202.0	198.5	223.6	207.7	216.6	226.6	202.6	202.1	210.1	209.6
INTEREST DURING CONSTRUCTION	\$/KWE	261.9	257.3	289.9	269.2	280.9	293.9	262.6	262.1	272.4	271.8
TOTAL CAPITAL COST	\$/KWE	1067.1	1048.3	1181.1	1097.0	1144.3	1197.3	1070.0	1067.9	1109.8	1107.3

Table 2.8-9 (Page 3 of 3)

CAPITAL COST DISTRIBUTIONS FOR OPEN-CYCLE MHD

	CASE NO.	21	22	23	24	25	26	27	28	29	30
MAJOR COMPONENTS											
PRIME CYCLE											
MHD GEN-DIFFUSER	MMS	7.9	7.9	7.9	7.9	7.9	7.9	7.9	7.9	7.9	7.9
MAGNET	MMS	46.0	44.0	44.0	43.0	35.0	42.0	42.0	43.0	47.0	39.0
HIGH TEMP AIR PREHEATER	MMS	12.4	30.7	12.4	16.0	12.3	27.6	16.0	16.0	16.0	16.0
LOW TEMP AIR PREHEATER	MMS	12.3	40.0	12.3	10.7	10.3	6.4	10.6	10.6	10.6	10.6
SEED RECOVERY SYSTEM	MMS	8.0	8.0	8.0	1.0	1.0	1.0	1.0	1.0	1.0	1.0
COMP WITH STEAM TURB DRIVE	MMS	13.4	0.	13.4	18.8	13.0	13.4	16.4	16.4	16.4	16.4
BOTTOMING CYCLE											
SLAGGING BOILER	MMS	3.1	0.	3.1	2.4	3.5	0.	2.4	2.4	2.4	2.4
STEAM BOILER (SUPER-REHEAT -BOIL-ECON)	MMS	24.5	0.	24.4	21.0	19.1	13.8	21.0	21.0	21.0	21.1
STEAM TURB-GEN	MMS	20.1	0.	20.1	12.9	19.1	12.8	15.1	15.0	14.9	15.7
AIR TURB-COMB-GEN-CLEANUP	MMS	0.	121.1	0.	0.	0.	0.	0.	0.	0.	0.
PRIMARY HEAT INPUT AND FUEL SYSTEM											
COMBUSTOR SYSTEM	MMS	29.2	29.2	29.2	4.4	4.6	4.4	4.4	4.4	4.4	4.4
SUB-TOTAL OF MAJOR COMPONENTS	MMS	176.9	280.9	174.8	138.2	125.7	129.2	136.8	137.7	141.6	134.5
BALANCE OF PLANT											
COOLING TOWER	MMS	8.2	1.5	12.3	8.2	8.2	8.2	8.2	8.2	8.2	8.2
DC TO AC INVERTERS	MMS	83.7	86.6	86.6	97.4	71.0	114.6	100.6	91.3	97.3	97.8
ALL OTHER	MMS	537.1	538.2	552.2	476.6	476.6	476.6	476.6	476.6	476.6	476.6
SITE LABOR	MMS	178.0	178.0	188.5	158.5	158.5	158.5	158.5	158.5	158.5	158.5
SUB-TOTAL OF BALANCE OF PLANT	MMS	807.0	804.4	839.6	740.7	714.3	757.9	743.9	734.6	740.6	741.1
CONTINGENCY	MMS	196.8	217.1	202.9	175.8	168.0	177.4	176.1	174.5	176.4	175.1
ESCALATION COSTS	MMS	395.4	436.1	407.7	353.2	337.6	356.5	354.0	350.6	354.6	351.9
INTEREST DURING CONSTRUCTION	MMS	512.7	565.5	528.6	458.0	437.7	462.2	458.9	454.5	459.7	456.2
TOTAL CAPITAL COST	MMS	2088.8	2304.0	2153.5	1755.9	1783.3	1883.3	1869.8	1851.8	1872.9	1858.8
MAJOR COMPONENTS COST											
MAJOR COMPONENTS COST	\$/KWE	94.6	140.5	92.5	71.6	71.7	64.5	70.9	71.1	72.9	70.1
BALANCE OF PLANT	\$/KWE	431.6	402.5	444.5	383.4	407.2	378.1	385.3	379.3	381.3	386.2
CONTINGENCY	\$/KWE	105.2	108.6	107.4	91.0	95.8	88.5	91.2	90.1	90.8	91.3
ESCALATION COSTS	\$/KWE	211.5	218.2	215.8	182.9	192.4	177.8	183.3	181.0	182.5	183.4
INTEREST DURING CONSTRUCTION	\$/KWE	274.2	282.9	279.8	237.1	249.5	230.6	237.7	234.7	236.7	237.7
TOTAL CAPITAL COST	\$/KWE	1117.2	1152.8	1140.2	966.0	1016.6	939.4	968.4	956.2	964.2	968.7

Table 2.8-10

POWER OUTPUT AND AUXILIARY POWER DEMAND
FOR BASE CASE AND PARAMETRIC VARIATIONS:
OPEN-CYCLE MHD

	CASE NO.	1	2	3	4	5	6	7	8	9	10
PRIME CYCLE POWER OUTPUT	MW	1420.0	880.0	440.0	1290.0	1305.0	1420.0	1420.0	1000.0	1225.0	1500.0
BOTTOMING CYCLE POWER OUTPUT	MW	555.0	350.0	184.0	660.0	650.0	548.0	548.0	496.0	846.0	575.0
FURNACE POWER OUTPUT	MW	0.	0.	0.	0.	0.	0.	0.	0.	0.	0.
BALANCE OF PLANT AUX. POWER REQ'D.	MW	40.5	25.1	12.7	40.7	40.9	40.5	40.5	40.5	40.5	40.5
FURNACE AUX. POWER REQ'D.	MW	15.1	9.8	5.0	16.8	23.9	15.1	15.1	12.3	16.5	15.1
TRANSFORMER LOSSES	MW	9.9	6.2	3.1	9.8	9.8	9.8	9.8	7.5	10.4	10.4
INVERTER LOSSES	MW	14.2	8.8	4.4	12.9	13.1	14.2	14.2	10.0	12.3	15.0
NET STATION OUTPUT	MW	1895.3	1180.2	598.8	1869.8	1867.3	1888.4	1888.4	1425.7	1991.4	1994.0

	CASE NO.	11	12	13	14	15	16	17	18	19	20
PRIME CYCLE POWER OUTPUT	MW	1715.0	1850.0	1080.0	1470.0	1260.0	1095.0	1420.0	1420.0	1400.0	1430.0
BOTTOMING CYCLE POWER OUTPUT	MW	385.0	308.0	733.0	539.0	617.0	681.0	555.0	555.0	562.0	551.0
FURNACE POWER OUTPUT	MW	0.	0.	0.	0.	0.	0.	0.	0.	0.	0.
BALANCE OF PLANT AUX. POWER REQ'D.	MW	40.5	40.5	40.5	40.5	40.5	40.5	40.5	40.5	40.5	40.5
FURNACE AUX. POWER REQ'D.	MW	15.1	15.1	15.1	15.1	15.1	15.1	15.1	15.1	15.1	15.1
TRANSFORMER LOSSES	MW	10.5	10.8	9.1	10.0	9.4	8.9	9.9	9.9	9.8	9.9
INVERTER LOSSES	MW	17.7	18.5	10.8	14.7	12.6	11.0	14.2	14.2	14.0	14.3
NET STATION OUTPUT	MW	2016.7	2073.1	1737.5	1928.7	1799.4	1700.6	1895.3	1895.3	1882.6	1901.2

	CASE NO.	21	22	23	24	25	26	27	28	29	30
PRIME CYCLE POWER OUTPUT	MW	1395.0	1420.0	1420.0	1650.0	1290.0	1910.0	1650.0	1660.0	1670.0	1630.0
BOTTOMING CYCLE POWER OUTPUT	MW	554.0	652.0	554.0	354.0	532.0	170.0	353.0	349.0	345.0	361.0
FURNACE POWER OUTPUT	MW	0.	0.	0.	0.	0.	0.	0.	0.	0.	0.
BALANCE OF PLANT AUX. POWER REQ'D.	MW	40.5	33.7	46.1	41.2	41.2	41.2	41.2	41.2	41.2	41.2
FURNACE AUX. POWER REQ'D.	MW	15.1	15.1	15.1	4.6	4.6	4.6	4.6	4.6	4.6	4.6
TRANSFORMER LOSSES	MW	9.7	10.4	9.9	10.0	9.1	10.4	10.0	10.0	10.1	10.0
INVERTER LOSSES	MW	14.0	14.2	14.2	16.5	12.9	19.1	16.5	16.6	16.7	16.3
NET STATION OUTPUT	MW	1869.7	1998.6	1888.7	1931.7	1754.2	2004.7	1930.7	1936.6	1942.4	1918.9

combustion over 0-90 percent (Cases 1, 6, 7), reduction in combustion pressure to simulate an approximately 25 percent decrease in electrical load (Cases 1, 8), variations in air preheat temperature from 2000 F to 3100 F (1364 K to 1978 K) with corresponding changes in combustion pressure (Cases 1, 11, 13), variations of electrical load parameter over the range 0.6-0.85 (Cases 1, 14-16), variations in average magnetic flux density in the generator over 5-7 tesla (Cases 1, 17, 18), a "diagonal" generator connection (Case 19), variations in potassium seeding fraction over 0.5-1.5 percent (Cases 1, 20, 21), and heat rejection through dry cooling towers.

The variations studied among systems using the semi-clean fuel are generally similar, but less extensive. Because the lower ash content of this fuel should permit higher temperature operation of refractory storage heat exchangers, the maximum oxidizer preheat temperature studied here is 3600 F (2256 K).

DISCUSSION OF RESULTS

A review of the results tabulated in the lower part of Table 2.8-6 shows that for open-cycle MHD systems the estimated capital costs per kilowatt power capacity are relatively insensitive to all variations studied except the fuel. Estimated capital costs for coal fired systems are within 1110 ± 100 \$/kWe and those for systems using the semi-clean fuel are within 955 ± 16 \$/kWe. (An exception, Case 8, is only apparent because that system is operating below its capability.) These increments are well within the uncertainties that must be expected from estimates of advanced systems, and are too small to discern reliable trends. The major components cost typically is under 10 percent of the total capital costs. Balance-of-Plant costs typically are about 40 percent of the total costs. The remainder, about 50 percent, is composed of contingency, escalation, and interest. Thus even a 50 percent change in total equipment cost of the major components would cause only a 10 percent change in capital costs per kilowatt capacity.

The overall efficiencies for coal burning plants range from 43.4 to 52.8 percent. The variations in overall efficiencies are determined largely by changes in oxidizer preheat temperature (and combustion pressure) and the MHD generator efficiency, which is governed to a large extent by the electrical load parameter. Thus low electrical load parameter (Case 16) gives relatively poor efficiency, and high oxidizer preheat (Cases 11, 12) gives high efficiency. For the large unit sizes and high magnetic flux densities studied in Task I, changes in magnetic flux densities have little effect on overall efficiencies.

Since the calculations in Table 2.8-6 were completed, it was discovered that a failure to account properly in the overall energy balance for the energy required to dry the coal has resulted in significant errors in estimated efficiencies for Cases 4 and 5, using Montana sub-bituminous and North Dakota coals, respec-

tively. For Case 4 the overall energy efficiency should be reduced approximately one percentage point, and for Case 5 approximately two percentage points. The capital costs are correct as given.

The capital cost of electrical inversion equipment, approximately \$60/kilowatt of inverted power, is an important item among equipment costs. This charge could be reduced by as much as a factor of 2 by electrical redesign to reduce the number of independent electric circuits (presently 50), increase circuit voltages and decrease circuit currents.

The differences between plant and overall efficiencies for the coal burning systems are associated with the heat losses in generating from coal the LBtu gas used in seed reclamation. In calculating plant efficiency, the systems are charged for the higher heating value of the gas used. In calculating overall efficiencies, the systems are charged for the higher heating value of the coal from which that gas is made.

Estimates of total costs of electricity for almost all systems studied, both coal fueled plants and those burning semi-clean fuel, fell in the range 42 to 48 mills/kWh, about 50 percent above the corresponding estimates for steam systems. The single exception, Case 8, is for a system running well below its capacity and shows that operating procedures may have a large impact on overall costs.

The dominant factor in total cost of electricity for all the open-cycle MHD systems is the cost of invested capital. This conclusion holds even though substantial maintenance costs have been estimated for the major components (combustor, nozzle-generator-diffuser, radiant furnace, high temperature air heater) in contact with the highest temperatures of the gas flow.

RECOMMENDED CASE

Case 1, using coal fuel and air oxidizer, an exhaust fired high-temperature air heater providing 2500 F air preheat, and a magnetic flux density averaging 5 tesla in the MHD generator is the recommended starting point for Task II conceptual design. This type of system exhibits good technical performance and good prospects for possible future improvements. It also offers some fall-back positions such as the indirectly fired air heater or semi-clean fuel firing should technical problems prevent achievement of calculated performance for the system presently specified.

2.9 CLOSED-CYCLE INERT GAS MHD

DESCRIPTION OF CYCLE

The closed-cycle inert gas MHD system was conceived about fifteen years ago as a method through which the advantages of open-cycle MHD generation might be retained while its principal disadvantages, very high-temperature requirements and a very chemically active flow, could be ameliorated.

In the closed-cycle system, as the name indicates, the MHD generator working fluid is circulated in a closed loop. The heat input to this working fluid must then be through an input heat exchanger rather than through combustion. Because it need not be the result of combustion, there is more flexibility in the choice of the generator working fluid, and it usually is chosen to be helium or argon with cesium rather than potassium seeding.

The working fluid is, except for small molecular impurity levels, a mixture of atomic gases without rotational and vibrational modes that interact readily with thermal electrons. Therefore, it is possible in closed-cycle systems to maintain the conduction electrons in the flow at a higher temperature than the bulk gas and, since electron density tends to be governed by electron temperature rather than gas temperature, to gain substantially higher electron density and electrical conductivity than would exist at the same temperature in a combustion gas flow. This process occurs automatically when some of the generated open-circuit voltage is used internally in the generator.

Although the closed-cycle inert gas generators provide useful power conversion at lower peak temperatures (3000 F [1922 K]) than open-cycle MHD (4500 F [2756 K]) they still provide major technical challenges. The input heat exchanger remains a difficult development because it works up to the highest temperature of the cycle. In addition, the working fluid must be kept free of contaminants in order to take advantage of nonequilibrium effects. The electrical stability of the flow in the generator poses problems because the gas is subject to electric fields approaching breakdown conditions. Many of the materials problems, however, are simplified by the approximately 1500 F (833 K) reduction in working fluid temperatures from those of open-cycle MHD.

The design and cost estimation of the closed-cycle inert gas MHD systems has been a joint effort by General Electric, Foster Wheeler, and Bechtel. The principal items designed and costed by personnel from each of these companies were as follows:

General Electric refractory storage input heat exchangers
MHD nozzle/generator/diffuser
superconducting magnet/Dewar (except Case 102;
see below)

electrical inversion equipment
steam turbine/compressor
recuperative heat exchanger
argon precooler

Foster Wheeler

coal handling auxiliaries
steam generator
combustor system

} except Cases 101,
102; see below

Bechtel

site labor and materials
cooling towers
balance of plant

} except Case 101;
see below

In addition General Electric has performed the system integration function.

Twenty-four different closed-cycle inert gas MHD systems have been studied during Task I: a topping cycle base case plus 16 parametric variations and a parallel cycle base case plus 6 parametric variations.* The first base case, Case 1, illustrated in Figure 2.9-1, is a topping cycle fueled by an "over-the-fence" semi-clean fuel derived from coal, in this case a solvent refined coal liquid. Case 2 is a larger plant, 1200 MWe nominal rather than 600 MWe. In both these systems, and in all the others studied here, except a variation of Case 102, the fuel is burned in an atmospheric pressure furnace and the combustion gases ducted to the refractory storage heat exchangers that transfer the input energy to the argon flow used as working fluid for the MHD generator. Cases 4 through 6 utilize Intermediate-Btu gas fuels, also "over-the-fence" fuels, made from Illinois #6, Montana sub-bituminous and North Dakota Lignite coals, respectively. Cases 7 through 14 consider changes in peak temperatures and pressures, in magnetic flux densities in the MHD generators, and in the machine efficiency (turbine effectiveness) of the MHD nozzle/generator/diffuser combination. Case 15 is a system using dry cooling towers for heat rejection. Case 101 is a direct coal-fueled variation using a larger refractory storage heat exchanger with a checker matrix of 1 in. x 1 in. holes for gas flow. Case 102 is a larger, more efficient and less expensive direct coal fueled system. Both cases 101 and 102 require stack gas-cleanup equipment that is not needed for the other variations on the first base case.

Neither Case 101 nor 102 was among those originally selected for Task I analysis. Case 101 was added after the preliminary analyses had shown that the achievement of overall energy efficiencies exceeding 40 percent in closed-cycle inert gas MHD would require both direct coal firing and combustion gas pressure drops in the input heat exchangers below the large values originally selected. Case 101 has those features. Case

*The principal design parameters of all cases studied in Task I are listed in Table 2.9-5.

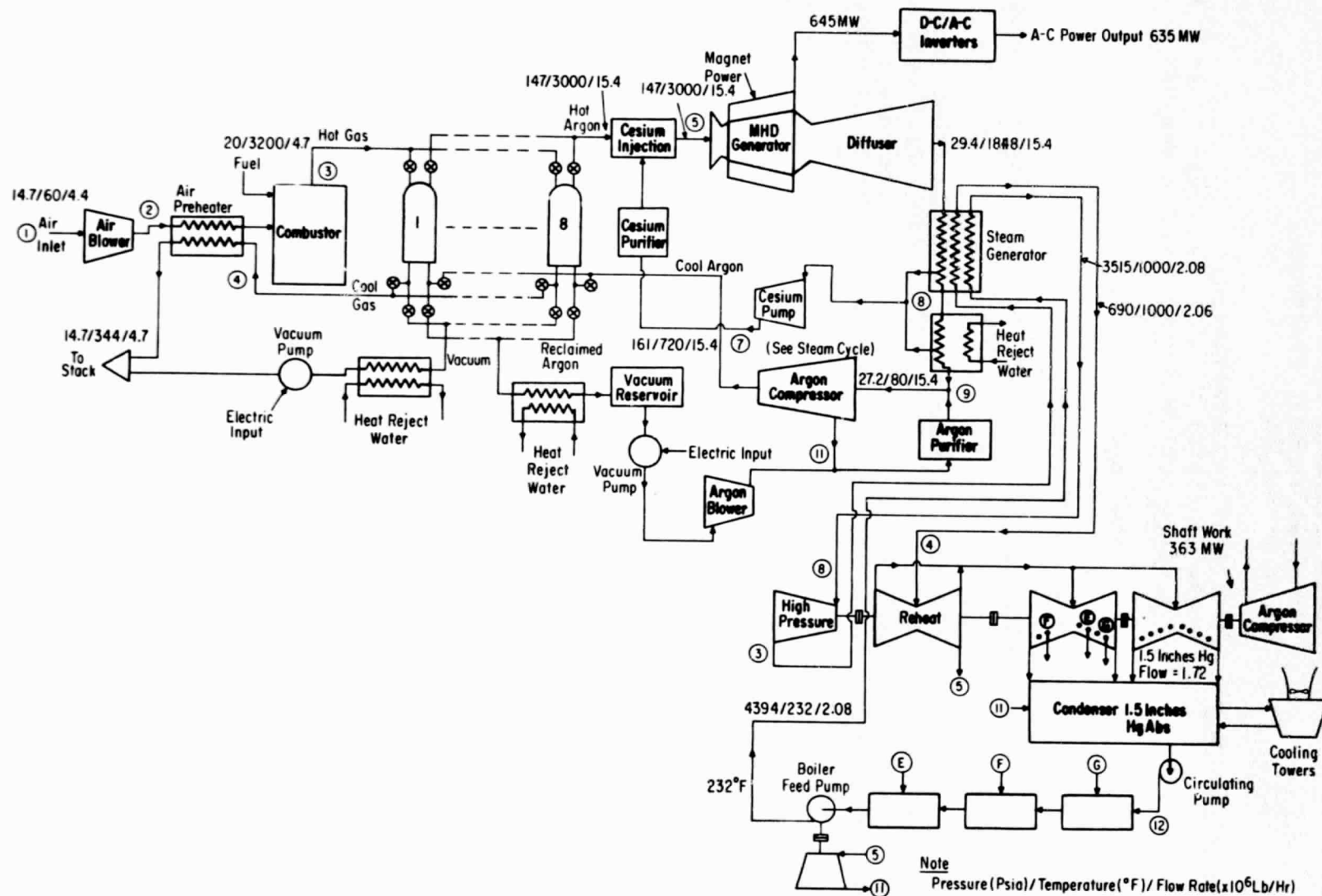


Figure 2.9-1. Closed-Cycle Inert MHD Topping Cycle

102 was added after completion of Task I in order to permit studies of the effects on overall system performance of improved MHD generator efficiency, increased generator inlet temperature, higher magnetic flux density, reduced pressure losses in the argon loop, and better steam cycle integration. This case features direct coal fueling (at atmospheric pressure), a "turbine effectiveness" of 0.78, and compact MHD generator and diffuser erected for vertical down-flow of the seeded argon working fluid through the generator. This arrangement permits a more compact layout for the entire system and reduced capital costs. Case 102 also uses a simplified steam cycle. In addition, a parametric variation of Case 102 has been studied in order to illustrate the effects of pressurized combustion and reduced sizes of MHD generators and diffusers on system capital costs. The cost achievements are the combustors, input heat exchangers, and combustion gas ducts.

Because of time pressures, the costing of on-site labor and materials, cooling towers, and balance of plant for Case 101 has not been done by Bechtel, but has been done at General Electric in the Systems and Plant Integration Team by combining with incremental adjustments portions of the Bechtel estimates for Cases 1 and 16. Similarly, the estimation of furnace performance and costs for Case 101 has not been done by Foster Wheeler, but has been done at General Electric by incremental adjustment of the Foster Wheeler estimate for Case 16.

For Case 102, furnace design, performance and costs have been estimated at General Electric by adjustment of Foster Wheeler estimates for Case 16. The superconducting magnet and Dewar for Case 102 have been designed and costed at Intermagnetics General Corporation.

In all other respects, and for all other cases, design and cost estimation has been done as indicated in the preceding table.

In these topping cycles, the MHD nozzle/generator/diffuser operates as an equivalent gas turbine-generator of a simple Brayton cycle. The MHD nozzle/generator/diffuser channel consists of a convergent-divergent accelerating nozzle, MHD generator, supersonic diffuser, transition section, and subsonic diffuser. For the base case, the generator inlet conditions are argon at 3000 F (1922 K) and 10 atm with 0.15 percent cesium injected upstream of the generator.

In any design, the generator exit conditions should be kept within the constraints of system design flexibility as well as efficiency. For example, it is desirable to have sufficient steam turbine shaft power to drive the compressors, and the pressure ratios across the MHD generators have been chosen sufficiently low to make that balance possible. With a "turbine effectiveness" of the nozzle/MHD generator/diffuser combination of 0.7 and a peak temperature of 3000 F (1922 K), as in Case 1, this constraint permits performance near the optimum, but with a

turbine effectiveness of 0.8 this constraint imposes a significant penalty, approximately one percentage point, on overall system efficiency.

The generator-diffuser exit gases serve to supply energy for the bottoming steam cycle. The specific steam bottoming cycle determines how much of the energy can be extracted from the MHD generator exit gases. To achieve a highly efficient steam plant, the feedwater must be heated by extracted steam in condensing feedwater heaters. Feedwater temperature of 510 F (539 K) produces approximately 45 percent steam cycle efficiency. The use of large amounts of thermal regeneration within the steam cycle and the consequent high final feedwater temperature, however, do not permit the MHD working fluid to be cooled to low temperature by the feedwater, but result in waste of heat from the seeded argon. A steam system employing a lower final feedwater temperature (232 F [384 K]) and a somewhat degraded steam cycle efficiency (\approx 40 percent) permits more energy to be transferred to the feedwater from the MHD exhaust and typically results in a more efficient total system. The most efficient system studied here, Case 102, uses a steam cycle with a final feedwater temperature of only 99 F (311 K) and no regenerative feedwater heating.

For the base case, Case 1, the argon transfers heat to the feedwater and steam to a gas temperature of 262 F (401 K). From 262 F (401 K) to 79 F (299 K), the gas is cooled in a pre-cooler rejecting heat to a wet cooling tower. Almost all of the 0.15 percent cesium seed will condense in the steam boiler-feedwater heater section. About 70 percent of the cesium condenses when the argon temperature is reduced from 600 F (589 K) to 450 F (506 K). Of the remaining cesium, an additional 95 percent is removed by reduction of the argon temperature from 450 F (506 K) to 262 F (401 K) resulting in a net residual cesium content of 20 ppm. The condensed cesium is collected into a reservoir, pumped, purified in a filter, and re-injected upstream of the MHD generator channel.

The pre-cooled argon is compressed and the high-pressure argon is fed back into the refractory storage heat exchanger. No intercooling stages are used for the base case MHD steam topping plant. The utilization of intercooling stages results in less effective utilization of waste heat and results in a reduction of overall efficiency.

The refractory storage heater array transfers the heat from the low-pressure combustion gases to the high pressure argon. In the design of the regenerative heat exchanger system, the following factors are significant:

1. Pressure drop in the combustion gas flow and the corresponding air compressor power.

2. Maximum ceramic temperature and combustion gas temperature determined from passage dimensions and height of exchanger. Both pressure drop and potential ash clogging of passages require that a minimum size passage be exceeded.
3. The heat exchanger matrix should be of sufficient heat capacity to minimize temperature fluctuations during the exchange cycles. As the matrix size is determined by heat transfer limitations, the heat capacity is more than adequate for the cycling utilized here.
4. Residual combustion gas impurities must be removed before the argon blowdown cycle.
5. The argon must be recovered before the heat exchanger matrix is reheated.

To meet all of these requirements and produce a continuous exchange of energy, multiple heat exchangers are required. A typical heat exchanger matrix that can be used for the base case MHD steam topping plant consists of eight heat exchangers plus a network of valves and ducting. No spare units have been included in these Task I designs.

The cycling of these heat exchangers is shown schematically in Figure 2.9-2. To minimize air compressor power, four heat exchangers are simultaneously heated by the combustion gases. Two heat exchangers are simultaneously cooled by the high-pressure argon. During the cycle one heat exchanger always has the residual exhaust gases being removed by a vacuum system and another heat exchanger has the residual argon being removed and returned to the compressor inlet after purification. Part of the main stream argon flow is diverted after the compressor entrance stage and recirculated through the argon purification loop back to the compressor inlet.

Heat is recovered from the high-temperature combustion gases which exit the refractory storage heat exchanger matrix to pre-heat the air leaving the air blower and entering the combustor.

The second base case, Case 16, is a system with the recuperative MHD Brayton cycle operating in parallel with a steam plant, as shown schematically in Figure 2.9-3. For this system, the only coupling between MHD cycle and steam cycle is the refractory storage heat exchanger in which the exhaust combustion gases from the reheat phase are utilized by the steam cycle boiler. As the overall efficiency of the parallel cycle is the weighted average of the MHD cycle and the steam cycle, there is a large incentive to maximize the efficiency of each cycle. This is less true for the MHD topping plant where reductions in the steam cycle efficiency resulted in a greater overall efficiency because of the close coupling between the MHD and steam cycles.

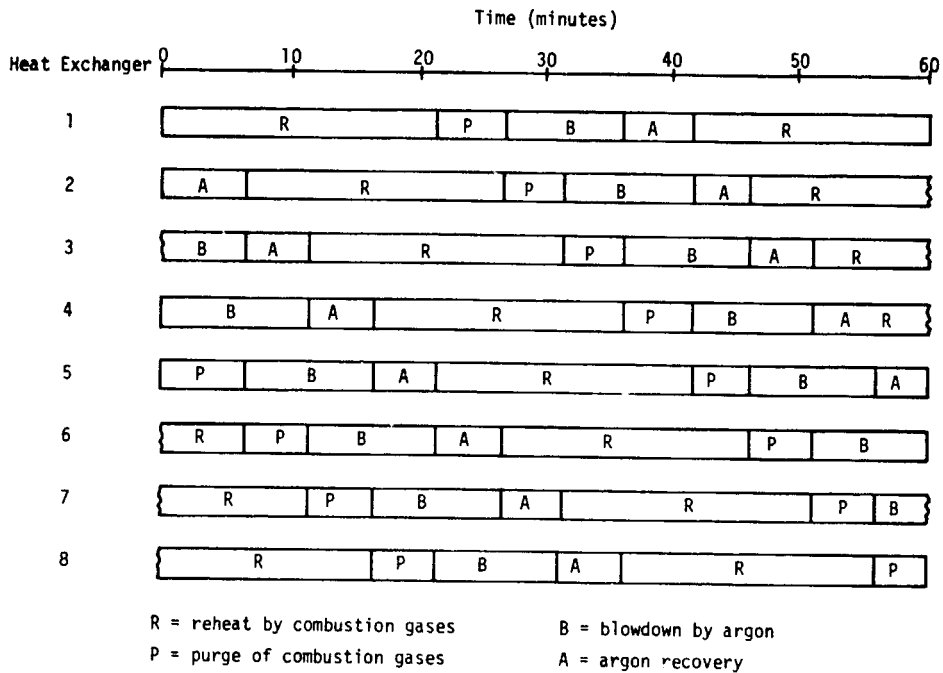


Figure 2.9-2. Heat Exchanger Cycling Sequence

To maximize the efficiency of the MHD cycle, two compressor intercooling stages are utilized. To reduce cost, the 85 percent effective recuperator utilizes six regenerative ceramic heat exchangers whose operation is similar to the heat exchangers transferring the energy from the combustion gases. To reduce pressure drop, four regenerators are simultaneously heated up by the low-pressure, high-temperature argon leaving the MHD generator-diffuser and two regenerators are simultaneously cooled by the high-pressure, low-temperature argon leaving the compressor.

The regenerative heat exchanger, in the base case, accepts the combustion gases from direct coal firing which exit the exchanger between 1900 F and 2000 F. The latter temperature is above the softening point of ash of some coals. The same number of heat exchangers and same cycling arrangement are utilized for the parallel cycle as for the MHD topping cycle. Because the bottom of the parallel cycle heat exchanger is at about 2000 F, the problem of support of the weight of the heat exchange matrix is more difficult than in the heat exchangers of Case 1.

The combustion gases exhausted from the refractory storage heat exchangers are cooled in the steam boiler to a temperature of 540 F (556 K), 30 F (17 K) above the final feedwater temperature. The exhaust gases then flow to the combustion air preheater, where they are cooled to stack temperature.

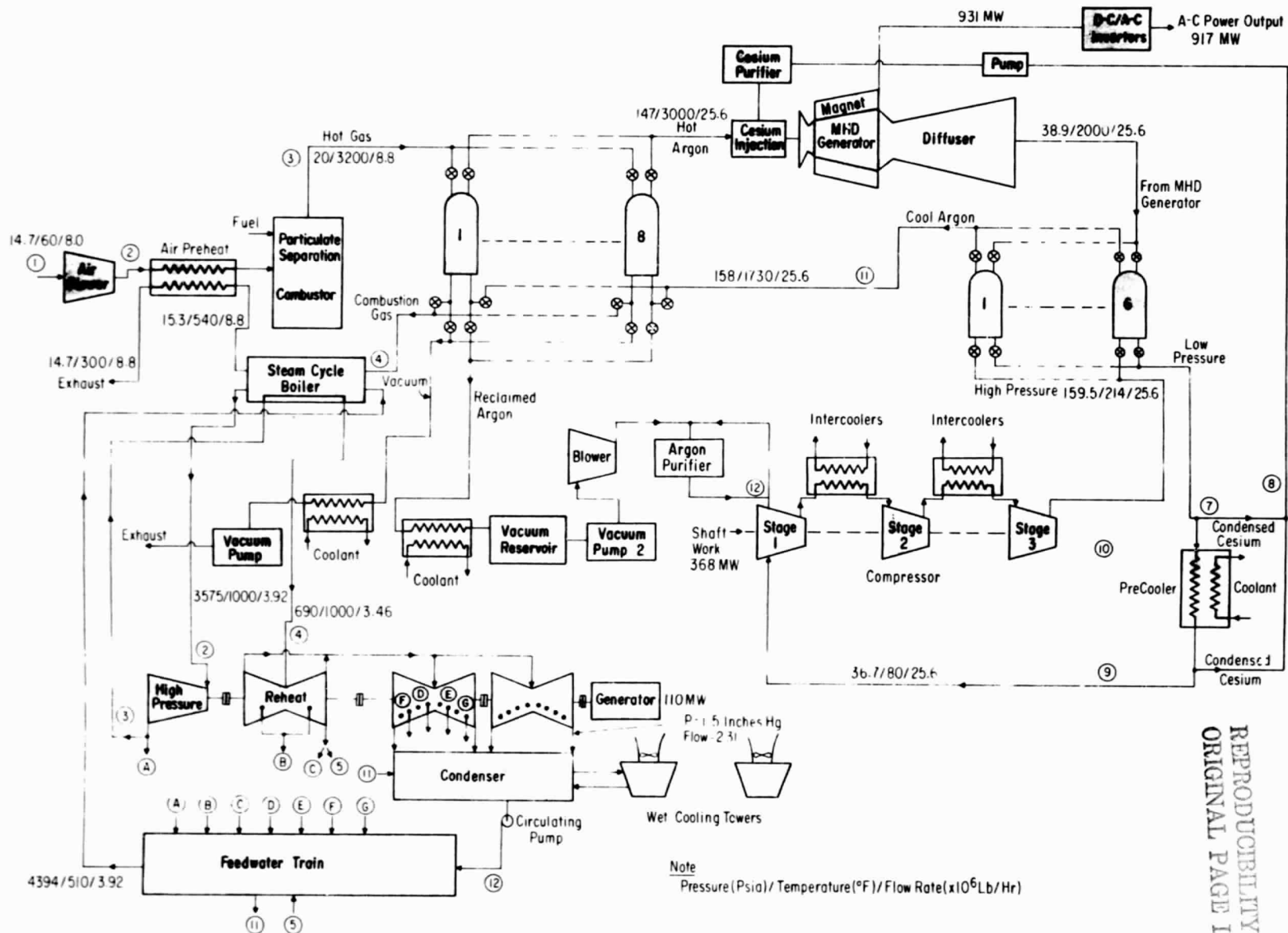


Figure 2.9-3. Closed-Cycle Inert Gas MHD-Parallel Cycle

REPRODUCIBILITY OF THE ORIGINAL PAGE IS POOR

Case 3 is a low power (100 MWe nominal) stand-alone MHD plant using recuperative heat exchangers rather than a steam bottoming cycle. Although it is listed here among the topping cycles, it actually bears greater similarity to the MHD section of the parallel cycles.

For both topping and parallel cycles, the principal variations involve changes in power levels (Cases 2, 3), in fuels (Cases 4-6, 17, and 18), peak temperatures (Cases 8-11) or MHD generator/diffuser outlet temperature (Case 19), MHD generator "turbine effectiveness coefficients" (Cases 12-14, 21) and magnet flux densities (Cases 7, 10, 20). Dry cooling towers also are included as alternate heat rejection apparatus (Cases 3, 15, 22). Case 101 provides a coal-fired topping cycle with low combustion gas pressure drop in the input heat exchangers. Case 102 provides a coal fired topping cycle with low combustion gas pressure drop, higher MHD generator "turbine effectiveness coefficient", a compact MHD generator/diffuser, and a simplified and less expensive steam cycle.

ANALYTICAL-PROCEDURE AND DESIGN ASSUMPTIONS

The cycle calculations consider the MHD system as a Brayton cycle with the combined equivalent turbine-generator efficiency represented by the MHD nozzle/generator/diffuser efficiency (turbine effectiveness). The range of generator-diffuser efficiencies is from 0.60 to 0.80 with the base case using a nominal value of 0.70.

In the cycle computations the following addition assumptions are made:

- Ratio of electrical output of transformer to steam turbine shaft output is 0.985
- Ratio of electrical output of transformer to MHD generator electrical output is 0.985
- Ducting, MHD generator and heat exchanger thermal losses are neglected.

The design pressure drops have been specified as design parameters for the principal heat exchangers. Additional allowances for pressure losses in ducting bring the total $\Delta p/p$ around the argon loop to values in the range of 0.15-0.20 except for cases 101 (0.12) and 102 (0.10). The principal characteristics of the refractory storage heat exchangers used to transfer heat from combustion gases to argon and for argon-argon recuperators are given in Table 2.9-1. All systems fueled by SRC or IBtu gas except Case 3, i.e., Cases 1, 2 and 4 through 15 use heat exchangers with 1/4-in. diameter gas passages. The systems fueled by coal directly, Cases 101, 102, 3, and 16 through 22, use 1 in. x 1 in. square gas passages in the input heat exchangers.

The argon-argon recuperators for Cases 3 and 16 through 22 also use 1 in. x 1 in. square passages.

The pressure ratios for the MHD nozzle/generator/diffuser train are limited to values that permit steam turbine drives for the argon compressors. Most of the topping cycles are so balanced that the argon compressor absorbs all the steam turbine power. The remaining topping cycles, Cases 8, 9, 13 and 14, have small turbine driven a-c generators that could be eliminated with little effect on overall system performance by selecting somewhat higher MHD pressure ratios.

The designs and performances of the combustor systems and the steam generators are described in Section 6. The argon compressors are axial flow machines and correspond in inlet volumetric flow to two of the larger gas turbine compressors that are now commercially available. The steam bottoming cycles used are conventional 3500/1000/1000 single reheat supercritical cycles with final feedwater temperatures of 99 F (311 K) for Case No. 102, 232 F (384 K) for all topping cycles except Case 102, and 510 F (539 K) for all parallel cycles, corresponding to cycle efficiencies (ratio of a-c electrical power out to the thermal power transferred to the steam) of approximately 0.388, 0.40 and 0.45, respectively. The actual heat rates for the turbine designs selected were calculated for each case. Because the efficiency of the a-c electrical generators is taken at 0.985, the ratios of turbine shaft power to steam thermal power are obtained by dividing the steam turbine efficiencies by 0.985. Those are the ratios of main interest for the balanced systems in which the steam turbines drive compressors only. In any case, a requirement for 1 MW of compressor shaft power causes a loss of only 0.985 MW of a-c electrical output at the generator terminals.

The designs of the inversion equipment are based on commercial experience with d-c links and are described in Appendix A.

The closed-cycle MHD gas heating system is similar to the preheat system used in steel blast furnaces. In the steel industry, ceramic heat exchangers have been used for over a century. Their heat source is the low-Btu gas exhaust of the blast furnace, which has a dust loading of 5 to as high as 50 grains per standard cubic foot of gas (7000 grains = 1 pound). Currently this dust level is reduced in a series of scrubbers to about 0.005 grains/ft³ prior to firing the stoves. Three or four stoves are cycled over 1 1/2-hour periods to produce hot air at about 2,000 F (1367 K). High hot air blast temperatures reduce the efficiency of the iron ore reduction in the blast furnace. Until about 1936, no gas cleanup was used and once a month a stove had to be cooled down and cleaned. This practice limited its life expectancy. During the next two decades, the dust loading was reduced to 0.2 grains/ft³ and the gas passage size in the stoves was reduced from 4 1/2 in. square to 2 in.

square. The stoves were cleaned every two years, the top few feet of the 100-ft high ceramic matrix was replaced, and the life expectancy of a stove was 15 to 20 years. Currently, the gas is cleaned to a 0.005 grain/ft³ dust level and the gas passages are 1 in. square (smaller sizes cause alignment problems).

The most severe operating conditions for a closed-cycle MHD heat exchanger would be in the direct coal fired application. If direct coal firing were used in the 600 MWe or 1200 MWe designs with 90 percent ash removed from the combustor, then the ash concentration in the combustion gases would be 0.3 grains/ft³. In the 600 MWe designs and the designs of cases 16 to 22, four heat exchangers are simultaneously heated up by the combustion gases. With the above ash loading, a heat exchanger with 1 in. square holes would be completely filled up with ash in 3000 hours, in the unlikely event that all the ash deposited in the heat exchanger. Systems using direct coal firing need periodic cleanup, which is assumed here to be done during scheduled shut-downs, approximately once a year.

The effect of variation of parameters on the regenerative heat exchanger design is illustrated in Table 2.9-1. It is assumed, based on experience in the steel industry, that a 1 in. by 1 in. checkerboard matrix is adequate for operation with the coal combustion gases for Cases 101, 102, and 16 through 22. If eight heat exchangers are cycled as shown in Figure 2.9-2, then a matrix 26 ft diameter by 70 ft high can transfer the heat to the argon for Case 1 with a maximum matrix temperature of about 3250 F (2061 K), permitting the use of alumina. If the passage dimensions were to be increased as for the 2 in. by 2 in. checkerboard matrix, the size, cost and maximum temperature would increase. In this case, the utilization of more expensive ceramics such as zirconia in the upper portion of the matrix would be required.

If the matrix passage dimensions are reduced, on the other hand, as for the case of 1/4-in. diameter holes, significant reductions in size and cost can occur. However, that requires relatively clean gas and a major extension from current steel industry practice.

The internal support of the heat exchanger matrix for the MHD closed-cycle topping cycles appears to offer no major problems. The combustion gas exit temperature is about 1000 F (811 K) and steels have good strength properties in this range. For the parallel cycle, support of the heat exchanger matrix is a problem as the combustion gas exit temperature is about 2000 F (1367 K) and there is a much more limited range of structural materials compatible with the combustion gases. The strengths of the superalloys are marginal at this temperature and among commercial alloys only 22H or Mo-Re appear useful.

Cases	Heat Exchanger Cycle	Nominal Heat Input	Ceramic Matrix Passage	Net High Temperature Gas
16-22, 101	8 Heat Exchangers 4 in Reheat (20 minutes) 1 in Purge (5 minutes) 2 in Blowdown (10 minutes) 1 in Argon recovery (5 minutes)	4.5×10^9 (Btu/hr)	1" x 1" 51% void	3253 1.135
--	Same as above	4.5×10^9 (Btu/hr)	2" x 2" 51% void	3434 1.1 a
1, 4-8, 12-15	Same as above	4.5×10^9 (Btu/hr)	1/4" Dia. holes 45% void	3200 1.3 a
9-11	Same as above	4.5×10^9 (Btu/hr)	1/4" Dia. holes 45% void	3800 1.36
3	Same as above	0.8×10^9 (Btu/hr)	1" x 1" 51% void	3253 1.11
--	6 Heat Exchangers 2 in Reheat (10 minutes) 1 in Purge (5 minutes) 2 in Blowdown (10 minutes) 1 in Argon recovery (5 minutes)	4.5×10^9 (Btu/hr)	2" x 2" 51% void	3460 1.33
2	11 Heat Exchangers 6 in Reheat (30 minutes) 1 in Purge (5 minutes) 3 in Blowdown (15 minutes) 1 in Argon recovery (5 minutes)	9×10^9 (Btu/hr)	1/4" Dia. holes 45% void	3200 1.3 a
--	Steel Industry Practice 4 Heat exchangers with external combustion chamber: 1 hr blast, 1/2 hr reheat	1.5×10^9 (Btu/hr)	1" x 1" Checker-board	>5000
102	14 Heat Exchangers 8 in Reheat (40 minutes) 1 in Purge (5 minutes) 4 in Blowdown (20 minutes) 1 in Argon recovery (5 minutes)	6.1×10^9 (Btu/hr)	1" x 1" 35% void	3400
16-22 (Recuperators)	6 Heat Exchangers 4 in Reheat (20 minutes) 2 in Blowdown (10 minutes)	4.8×10^9 (Btu/hr)	1" x 1" 51% void	2000 2.65
3 (Recuperators)	Same as above	0.7×10^9 (Btu/hr)	1" x 1" 51% void	1800

Table 2.9-1

FOLLOUT FRAME 2

HEAT EXCHANGERS FOR CLOSED-CYCLE GAS MHD SYSTEMS

Maximum Inlet Temperature	Maximum Ceramic Temperature	Matrix Dimensions	Overall Dimensions	Weight (lb) per Exchanger	Material Costs per Exchanger	Total Material Cost (\$10 ⁶)
3100 F atm	3100 F	26 ft Dia. 70 ft Height	30 ft Dia. 93 ft Height	5,013,000 lbs	\$4,432,000	35.5
3260 F atm	3260 F	26 ft Dia. 94 ft Height	30 ft Dia. 117 ft Height	6,580,000 lbs	\$5,856,000	46.9
3100 F atm	3100 F	24 ft Dia. 25 ft Height	28 ft Dia. 43 ft Height	2,268,000 lbs	\$2,008,000	16.1
3900 F atm	3900 F	24 ft Dia. 25 ft Height	28 ft Dia. 43 ft Height	2,930,000 lbs	\$7,567,000	60.5
3100 F atm	3100 F	146 ft Dia. 49 ft Height	16.5 ft Dia. 60 ft Height	631,000	\$ 541,000	4.33
3260 F atm	3260 F	26 ft Dia. 94 ft Height	30 ft Dia. 117 ft Height	6,580,000	\$5,856,000	35.2
3100 F atm	3100 F	24 ft Dia. 25 ft Height	28 ft Dia. 43 ft Height	2,268,000	\$2,008,000	22.1
2822 F	2822 F		28 1/2 ft Dia. 140 ft Height			
3200 F	3200 F	21 ft Dia. 60 ft Height	24 ft Dia. 90 ft Height	3,724,000	\$3,323,000	46.5
1830 F atm	1830 F	26 ft Dia. 61 ft Height	30 ft Dia. 84 ft Height	4,710,000	\$3,700,000	22.2
1700 F	1700 F	13 ft Dia. 71 ft Height	16 ft Dia. 86 ft Height	1,595,000	\$1,184,000	7.10

Another possible problem at high temperatures is self-support of the ceramic heat exchanger matrix. Multiple regenerative heat exchangers of maximum matrix heights of about two-thirds of that utilized in the steel industry (see Table 2.9-1) are considered for the MHD closed-cycle system. For the maximum argon temperatures of the base cases (3000 F [1992 K], the matrix support should present no problem with the maximum temperatures not much higher than that in the steel industry. For the higher temperature cases (3500 F [2200 K] and above), the problem of matrix creep stress limitations needs further evaluation.

The recuperators utilize a multiple regenerative heat exchanger reheat and blowdown cycle similar to the combustion gas heat exchangers. The use of metal recuperators is both too costly and too marginal in stress performance in event of transients resulting from removal of electrical load. However, the use of ceramic regenerative recuperators operating at a maximum temperature about 1000 F (556 K) less than the combustion gas regenerative heat exchangers should present few material problems of any significance.

The cesium inventory is assumed to be sufficient to be continually supplied to the MHD cycle for a period of 20 minutes without recycle. The total transit time of the argon within the MHD loop is less than one minute.

Both argon cleanup and cesium cleanup are needed. The purity considerations are illustrated in the schematic of Figure 2.9-4. The argon purification process can utilize charcoal bed purifier, cryogenic combustion product impurity removal or combinations of the charcoal and cryogenic purifiers. The cesium purification probably would be a combination of mechanical filtration and chemical reduction of carbonates, sulfates, hydroxides, oxides, and carbonyls formed by reactions between cesium and impurities in the argon as the argon flow is cooled during passage through the MHD generator and steam generator. An alternate possibility is the use of a small fraction of sodium in the cesium to getter impurities. Neither the argon cleanup system nor the cesium cleanup is well defined at this time. They are not expected, however, to have major impacts on either costs or technical feasibility.

The heat exchangers, valves, pumps and blowers required for pumping and argon reclamation from the input heat exchangers have been identified and costed as conventional equipment in the balance of plant. The corresponding power requirements are included in balance-of-plant auxiliary powers.

The MHD generator-diffuser size characteristics for Cases 1 and 102 are shown in Table 2.9-2. For all other cases, the generator-diffuser is scaled on the basis of fixed inlet flow rate per unit area from that for Case 1. In the design it is assumed

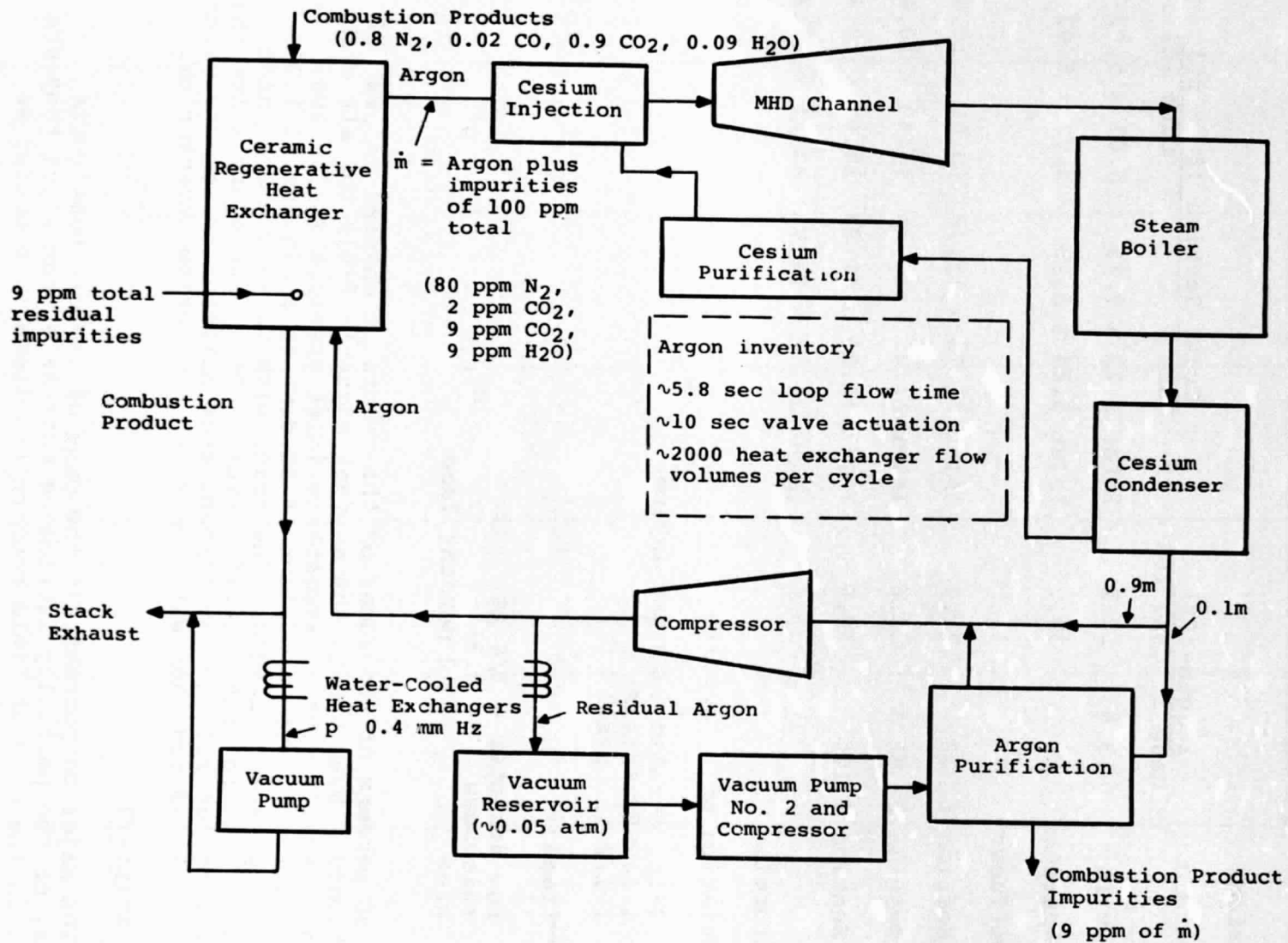


Figure 2.9-4. Closed-Cycle MHD Argon Purity Considerations

Table 2.9-2

MHD GENERATOR SIZES FOR CASES 1 AND 102

Dimensions

Component	<u>length-(ft)</u>		<u>Cross-Section (ft x ft)</u>	
	Case 1	Case 102	Case 1	Case 102
• Nozzle	13.5	10.1	Inlet 9.75 x 9.75	5.02 x 5.02
• Generator	50	33.5	Inlet 5.25 x 5.25	5.02 x 5.02
• Diffuser				
Section 1	22	21.7	Inlet 11.75 x 11.75	10.86 x 10.86
Section 2	52.5	32.6	Inlet 11.25 x 11.25	10.40 x 10.40
Section 3	105	10.9	Inlet 11.25 x 11.25	10.40 x 10.40
			Exit 21.75 x 21.75	22.21 x 22.21

Construction

Insulation and Structure

2-in. ceramic foam insulation
 1-in. fiberfrax
 1 1/2-in. steel

Electrodes

rod diameter = 1/4 in.
 thickness = 0.2 in.
 area = 50 percent face

that 50 percent of two faces of the generator channel consist of electrodes. Even though the average magnetic field for all cases except Case 102 with 10 atmosphere inlet pressure is 3T, the field will vary from a maximum of 5T down to a minimum of 1.25T over the generator length. The cases with 20 atmosphere inlet pressure require higher fields (average 6T). The overall lengths and weights of all the nozzle/generator/diffuser trains are given in Table 2.9-3 together with the argon and cesium inventories.

COST ANALYSIS

The major components, in the case of factory constructed items, or the partially fabricated materials from which they are made, in the case of field constructed items, are costed as

delivered to the construction site. Where possible, cost estimates are based on quotations or budgetary estimates made in accordance with commercial practice. The costs of field erection or construction, including both labor and construction materials, are included in balance-of-plant estimates of the architect/engineer.

Table 2.9-4 gives the figures used to estimate the costs of the parts delivered to the construction site for the refractory storage heat exchangers, MHD train, and superconducting magnet.

RESULTS

The principal design parameters and results of the performance calculations for all 24 cases studied here are included in Table 2.9-5. Tables 2.9-1, 2.9-2, 2.9-3, and 2.9-4 give size, weight and cost information on the MHD nozzle/generator/diffuser trains and the refractory storage heat exchangers. Tables 2.9-6 and 2.9-7 summarize for the two base cases studied, the semi-clean fuel fired topping cycle—Case 1, and the direct coal fired parallel cycle—Case 16, the performance and cost, characteristics of major components, consumption of natural resources and environmental intrusion. Table 2.9-8 gives calculated cost distributions for all cycles studied. Table 2.9-9 lists power outputs and auxiliary power demands for all systems studied in Task I.

DISCUSSION OF RESULTS

A review of the results tabulated in the lower part of Table 2.9-5 shows that the calculated total cost of electricity runs near 60-65 mills/kWh for the SRC fueled topping cycles and near 70-75 mills/kWh for the coal fueled parallel cycles, approximately 2 to 2.5 times electricity costs from advanced steam cycles. For the SRC fueled topping cycles, capital costs are in the range 1350 ± 60 \$/kWe except for the cases 9 through 11 using higher generator inlet temperatures and more expensive input heat exchangers, which have capital costs of 1516-1535 \$/kWe. Capital costs for the coal fueled parallel cycles are still higher, mainly because of increased balance of plant.

The SRC fueled low power recuperative MHD system, Case 3, has electricity costs and capital costs of 80 mills/kW-hr and 1825 \$/kWe. The coal fired topping cycle, Case 101, has electricity costs and capital costs of 62 mills/kWh and 1551 \$/kWe. The other coal-fired topping system, Case 102, with its higher efficiency and more compact plant, has electricity costs of 46 mills/kWh and 1109 \$/kWe. In all cases capital costs are the dominant factor in costs of electricity. Typically, contingency escalation and interest provide about 50% of total capital costs, the balance of plant provides 35-40 percent, and the major components 10-15 percent.

Table 2.9-3

SIZE AND WEIGHT-MHD GENERATOR-DIFFUSER & FLUID INVENTORY

Case (No.)	Overall Length (ft)	Maximum Width (ft)	Total Weight (Million lb)	Argon Inventory (SCF)	Cesium Inventory* (lb)
1,4,5,6,101	243	21.75 (square)	1.4	750,000	8,000
2	341	30.75	2.8	1,000,000	16,000
3	131	12.8	0.82	250,000	2,500
7	165	16.4	.95	750,000	8,000
8	273	24.5	1.77	750,000	10,000
9	216	19.4	1.1	750,000	5,000
10	125	13	0.5	750,000	6,000
11	192	17.2	.875	750,000	5,000
12	273	24.4	1.8	750,000	10,000
13	218	19.5	1.13	750,000	7,000
14	235	21	1.3	750,000	7,500
15	243	21.75	1.4	750,000	8,000
16,17,18	313	28	2.33	750,000	9,500
19	320	28.6	2.43	750,000	10,000
20	222	19.8	1.2	750,000	9,500
21	308	27.4	2.3	750,000	9,500
22	313	28	2.33	750,000	9,500
102	108	22.2	1.36	1,000,000	10,000

*20-minute flow

FOLDOUT FRAME

CLOSED-C
PARAMETRIC VAR

Parameters	Common Parameters: Top						
	Case 1	101	102	2	3	4	5
<u>Power Output (MWe)</u>	583	600	930	1168	88	586	5
<u>Combustion</u>							
Coal and conversion process	Ill. #6 SRC	Ill. #6 Direct	Ill. #6 Direct	Ill. #6 SRC	→	Ill. #6 IBtu	Mont
Oxidizer	Air						
Combustion slag rejection (percent)	0	80	90	0			
<u>MHD Generator</u>							
Inlet pressure (atm)	10						
Inlet temperature (°F)	3000	→	3121	3000			
Outlet temperature (°F)	1840	→	1771	1840			
Turbine effectiveness	0.7	→	0.78	0.7			
Type	Faraday						
Average magnetic field (T)	3	→	4.5	3			
Cesium seed (percent)	0.15						
Inert gas	A						
<u>Heat Exchangers</u>							
<u>Input</u>							
Combustion gas (Δp/p)	0.30	0.11	0.09	0.30	0.11	0.30	
Argon (Δp/p)	0.05	→	0.004	0.03			
Steam generator/precooler							
Argon (Δp/p)	0.085	→	0.05	0.085			
Regenerator/precooler (Δp/p)	--	--	--	--	0.08	--	
Regenerator effectiveness (percent)	--	--	--	--	0.85	--	
<u>Argon Compressor Efficiency (percent)</u>							
88							
<u>Steam Bottoming Cycle</u>							
Turbine inlet temperature (°F)	1000/1000	→			--	1000/1000	
Turbine inlet pressure (psi)	3500	→			--	3500	
Maximum feedwater temperature (°F)	232	→	88	232	--	232	
<u>Heat Rejection (in. Hg)</u>							
WCT	1.5	→			DCT	WCT	1.5
<u>Actual Powerplant Output (MWe)</u>	583	600	930	1168	88	586	5
<u>Thermodynamic Efficiency (percent)</u>	50.1	49.8	55.9	50.2	42.4	50.1	50
<u>Powerplant Efficiency (percent)</u>	41.5	41.8	46.0	41.6	35.6	37.8	37
<u>Overall Energy Efficiency (percent)</u>	32.4	41.8	46.0	32.5	27.8	26.4	26
<u>Coal Consumption (lb/kWh)</u>	0.98	0.76	0.69	0.97	1.14	1.20	1.1
<u>Plant Capital Cost (\$ million)</u>	787	931	1033	1641	162	767	7
<u>Plant Capital Cost (\$/kWe)</u>	1349	1551	1109	1404	1825	1307	13
<u>Cost of Electricity, Capacity Factor = 0.65</u>							
Capital (mills/kWh)	42.7	49.0	35.1	44.4	57.7	41.3	41
Fuel (mills/kWh)	14.8	6.9	6.3	14.8	17.2	18.1	18
Maintenance and operating (mills/kWh)	3.2	5.6	4.2	2.8	5.6	4.3	4
Total (mills/kWh)	60.7	61.6	45.6	62.0	80.5	63.7	63
<u>Sensitivity</u>							
Capacity factor = 0.50 (total mills/kWh)	74.5	78.0	57.4	76.1	99.5	77.4	77
Capacity factor = 0.80 (total mills/kWh)	52.1	51.4	38.2	53.1	68.7	55.1	55
Capital Δ = 20 percent (Δ mills/kWh)	8.5	9.8	7.0	8.9	11.5	8.3	8
Fuel Δ = 20 percent (Δ mills/kWh)	3.0	1.4	1.3	3.0	3.4	3.6	3
<u>Estimated Time for Construction (years)</u>	6	7	6	7	4	6	6
<u>Estimated Date of 1st Commercial Service (year)</u>	2000	2000	2000	2005	2000	2000	20

REPRODUCIBILITY OF THE ORIGINAL PAGE IS POOR

* Base case 1. DCT = Dry cooling tower N. D. = North Dakota
 ** Base case 2. IBtu = Intermediate Btu SRC = Solvent refined coal
 Ill. = Illinois Mont = Montana WCT = Wet cooling tower

Table 2.9-4

BASIS FOR COST ESTIMATES

- Regenerative Heat Exchanger/Recuperator
 - Materials
 - Alumina (80% theoretical density) \$ 1.20/lb
 - Steel 0.42/lb
 - Insulation 0.90/lb
 - Zirconia 5.00/lb
 - Mo-Re 1 3.00/lb
 - Incoloy 800H 2.63/lb
 - Super 22-H 4.75/lb
 - Factory Fabrication 1.0 Steel Cost

- MHD Generator-Diffuser
 - Materials
 - Insulation \$ 0.90/lb
 - Steel 0.42/lb
 - Tantalum/Tungsten 60.00/lb
 - Factory Fabrication 1.0 Steel Cost

- Inventory
 - Argon \$ 5.75/100 SCF
 - Cesium 50.00/lb

- Magnet
 - Materials
 - Aluminum \$ 1.00/lb
 - Steel 2.00/lb
 - Superconductor 3.42/lb
 - Factory Fabrication 1.0 (Steel and Aluminum Cost)

Table 2.9-7

SUMMARY SHEET
CLOSED-CYCLE INERT GAS MHD BASE CASE 16

CYCLE PARAMETER	
Power Output (MWe)	934
Combustion	
Coal and conversion process	Illinois No. 6 Direct
Oxidizer	Air
Combustion slag rejection (percent)	90
MHD Generator	
Inlet pressure (atm)	10
Inlet temperature (°F)	3000
Outlet temperature (°F)	2000
Turbine effectiveness	0.7
Type	Faraday
Average magnetic field (T)	3
Cesium seed (percent)	0.15
Inert gas	Argon
Heat Exchangers	
Input	
Combustion gas (Δp/psi)	0.3
Argon (Δp/psi)	0.05
Steam generator/precooler	
Argon (Δp/psi)	0.085
Regenerator/precooler (Δp/psi)	0.08
Regenerator effectiveness (percent)	0.85
Argon Compressor Efficiency (percent)	
	88
Steam Bottoming Cycle	
Turbine inlet temperature (°F)	1000/1000
Turbine inlet pressure (psi)	3500
Maximum feedwater temperature (°F)	510
Heat Rejection	
	Wet cooling tower

PERFORMANCE AND COST	
Thermodynamic efficiency (percent)	46.0
Powerplant efficiency (percent)	37.1
Overall energy efficiency (percent)	37.1
Plant capital cost (\$ x 10 ⁶)	1726
Plant capital cost (\$/kWe)	1849
Cost of electricity (mills/kWh)	71.7

NATURAL RESOURCES	
Coal (lb/kWh)	0.85
Water (gal/kWh)	
Total	0.20
Cooling	0.20
Processing	0
Makeup	0
NO _x suppression	0
Stack gas cleanup	0
Land (acres/100 MWe)	6.10

ENVIRONMENTAL INTRUSION		
	Lb/10 ⁶ -Btu Input	Lb/kWh Output
SO ₂	1.2	1.1 x 10 ⁻²
NO _x	0.7	0.64 x 10 ⁻²
HC	0	0
CO	0	0
Particulates	0.1	0.09 x 10 ⁻²
		Btu/kWh
Heat to water		2096
Heat, total rejected		5787
	Lb/kWh	Lb/Day
Wastes		
Furnace solids	0.074	1.6 x 10 ⁶
Fine dust from cyclones	0.82 x 10 ⁻²	0.18 x 10 ⁶
Fly ash		

MAJOR COMPONENT CHARACTERISTICS

Major Component	Unit or Module			Units Required	Total Cost (\$ x 10 ⁶)	\$/kW Output
	Size (ft) (W x L for DI x H)	Weight (lb) (x 10 ³)	Cost (\$ x 10 ⁶)			
Furnace	80 dia x 130 high	2.51	13.1	2	26.3	28.2
Primary heat exchanger	30 dia x 90 high	5.01	4.4	8	35.2	37.7
MHD nozzle/generator/diffuser	Inlet area 156 ft ² Exit area 784 ft ² } 313 long	2.34	4.4	1	4.4	4.7
Magnet and dewar	33 dia x 88 long	3.00	25.5	1	25.50	27.3
Argon/argon recuperator	30 dia x 88 high	0.86	3.70	6	22.2	23.8
Flue gas/steam boiler	40 x 115 x 30	4.70	14.00	1	14.00	15.0
Steam turbine-generator set	30 x 150 x 25	2.70	4.70	1	4.7	5.0
Inverters	--	--	72.6	1	72.6	77.7

Table 2.9-8 (Page 1 of 3)

CAPITAL COST DISTRIBUTIONS FOR CLOSED-CYCLE INERT GAS MHD

	CASE NO.	1	2	3	4	5	6	7	8	9	10
MAJOR COMPONENTS											
PRIME CYCLE											
MHD GEN-DIFFUSER	MMS	2.7	5.3	1.6	2.7	2.7	2.7	1.3	3.4	2.1	1.0
MAGNET	MMS	17.7	32.0	3.0	17.7	17.7	17.7	15.8	19.5	16.0	12.8
HIGH TEMP RECUPERATOR (REGEN)	MMS	0.	0.	7.2	0.	0.	0.	0.	0.	0.	0.
RECUPERATOR	MMS	0.	0.	0.	0.	0.	0.	0.	0.	0.	0.
PRECOOLER	MMS	3.6	7.2	1.8	3.6	3.6	3.6	2.4	3.6	3.0	3.2
COMP WITH STEAM TURB DRIVE	MMS	18.1	27.6	3.1	18.1	18.1	18.1	18.1	13.8	16.7	14.9
SEED SYSTEM	MMS	0.	0.	0.	0.	0.	0.	0.	0.	0.	0.
BOTTOMING CYCLE											
STEAM BOILER	MMS	8.9	17.8	0.	8.4	8.6	8.6	8.9	12.1	11.7	6.1
STEAM TURB-GEN	MMS	0.	0.	0.	0.	0.	0.	0.	4.4	0.8	0.
PRIMARY HEAT INPUT AND FUEL SYSTEM											
COMBUSTOR SYSTEM	MMS	23.6	46.5	10.8	18.7	18.8	18.9	23.6	21.4	25.2	18.4
HEAT INPUT EXCH (REGENERATIVE)	MMS	16.0	22.0	4.3	16.0	16.0	16.0	16.0	16.0	60.8	60.8
SUB-TOTAL OF MAJOR COMPONENTS	MMS	90.6	158.4	31.8	85.2	85.5	85.6	86.1	72.2	136.3	117.2
BALANCE OF PLANT											
COOLING TOWER	MMS	4.0	8.0	1.2	4.0	4.0	4.0	4.0	4.0	4.0	4.0
STACK-GAS CLEAN-UP EQUIP.	MMS	0.	0.	0.	0.	0.	0.	0.	0.	0.	0.
DC TO AC INVERTERS	MMS	51.6	98.1	12.1	51.6	51.6	51.6	51.6	43.4	49.6	30.9
ALL OTHER	MMS	195.8	391.7	39.0	191.4	191.4	191.4	195.8	195.8	195.8	195.8
SITE LABOR	MMS	58.5	117.0	11.7	57.9	57.9	57.9	58.5	58.5	58.5	58.5
SUB-TOTAL OF BALANCE OF PLANT	MMS	309.9	614.8	64.0	304.9	304.9	304.9	309.9	301.7	307.9	289.2
CONTINGENCY	MMS	80.1	154.6	19.2	78.0	78.1	78.1	79.2	79.2	88.8	81.3
ESCALATION COSTS	MMS	137.4	310.7	22.3	133.9	134.0	134.0	135.9	135.9	152.4	139.5
INTEREST DURING CONSTRUCTION	MMS	169.3	402.9	24.2	164.9	165.0	165.1	167.4	167.4	187.8	171.8
TOTAL CAPITAL COST	MMS	787.4	1641.4	161.6	767.0	767.5	767.7	778.5	778.4	873.3	799.0
MAJOR COMPONENTS COST											
MAJOR COMPONENTS COST	\$/KWE	155.3	135.6	359.6	145.3	145.7	145.7	147.9	168.3	236.7	225.2
BALANCE OF PLANT	\$/KWE	531.4	526.2	725.4	520.0	519.6	519.2	532.3	539.0	534.8	555.7
CONTINGENCY	\$/KWE	137.3	132.4	216.6	133.1	133.0	133.0	136.0	141.5	154.3	156.2
ESCALATION COSTS	\$/KWE	235.6	266.0	252.2	228.3	228.3	228.2	233.4	242.7	264.8	268.0
INTEREST DURING CONSTRUCTION	\$/KWE	290.3	344.8	274.0	281.2	281.2	281.1	287.5	299.0	326.1	330.1
TOTAL CAPITAL COST	\$/KWE	1350.0	1404.9	1825.8	1307.9	1307.8	1307.2	1337.1	1390.4	1516.7	1535.2

REPRODUCIBILITY OF THE
ORIGINAL PAGE IS POOR

Table 2.9-8 (Page 2 of 3)

CAPITAL COST DISTRIBUTIONS FOR CLOSED-CYCLE INERT GAS MHD

	CASE NO.	11	12	13	14	15	16	17	18	19	20
MAJOR COMPONENTS											
PRIME CYCLE											
MHD GEN-DIFFUSER	MMS	1.7	3.5	2.2	2.5	2.7	4.4	4.4	4.4	4.6	2.5
MAGNET	MMS	12.4	21.0	15.0	16.5	17.7	25.5	25.5	25.5	26.3	24.8
HIGH TEMP RECUPERATOR (REGEN)	MMS	0.	0.	0.	0.	0.	22.2	22.2	22.2	22.2	22.2
RECUPERATOR	MMS	0.	0.	0.	0.	0.	0.	0.	0.	0.	0.
PRECOOLER	MMS	3.6	7.5	2.8	3.0	3.6	11.6	11.6	11.6	9.6	8.4
COMP WITH STEAM TURB DRIVE	MMS	12.8	21.1	14.6	16.6	18.2	15.7	15.8	15.7	9.4	15.8
SEED SYSTEM	MMS	0.	0.	0.	0.	0.	0.	0.	0.	0.	0.
BOTTOMING CYCLE											
STEAM BOILER	MMS	4.4	12.0	7.8	8.3	8.7	14.0	14.4	14.8	15.3	14.0
STEAM TURB-GEN	MMS	0.	0.	2.5	0.7	0.	4.7	5.4	6.0	12.1	4.6
PRIMARY HEAT INPUT AND FUEL SYSTEM											
COMBUSTOR SYSTEM	MMS	16.2	41.5	20.9	21.4	24.2	26.3	28.8	32.2	29.5	26.3
HEAT INPT EXCH (REGENERATIVE)	MMS	60.8	16.0	16.0	16.0	16.0	35.2	35.2	35.2	35.2	35.2
SUB-TOTAL OF MAJOR COMPONENTS	MMS	111.9	122.6	81.8	85.0	91.1	159.6	163.3	167.6	164.2	153.8
BALANCE OF PLANT											
COOLING TOWER	MMS	4.0	4.0	4.0	4.0	4.2	8.0	8.0	8.0	8.0	8.0
STACK-GAS CLEAN-UP EQUIP.	MMS	0.	0.	0.	0.	0.	53.5	53.5	53.5	53.5	53.5
DC TO AC INVERTERS	MMS	23.9	59.1	47.7	50.2	52.1	72.6	72.6	72.6	53.6	72.6
ALL OTHER	MMS	195.8	195.8	195.8	195.8	197.2	383.6	384.7	387.2	383.6	383.6
SITE LABOR	MMS	58.5	58.5	58.5	58.5	59.4	135.9	136.5	137.3	135.9	135.9
SUB-TOTAL OF BALANCE OF PLANT	MMS	282.2	317.4	306.0	308.5	312.9	653.6	655.3	658.6	634.6	653.6
CONTINGENCY	MMS	78.8	88.0	77.6	78.7	80.8	162.6	163.7	165.2	159.8	161.5
ESCALATION COSTS	MMS	135.2	151.0	133.1	135.0	138.6	326.8	329.0	332.0	321.0	324.5
INTEREST DURING CONSTRUCTION	MMS	166.6	186.0	163.9	166.4	170.8	423.7	426.5	430.5	416.2	420.7
TOTAL CAPITAL COST	MMS	774.8	865.0	762.4	773.6	794.2	1726.4	1737.8	1754.0	1695.8	1714.1
MAJOR COMPONENTS COST											
	\$/KWE	220.3	182.9	140.6	147.0	156.5	171.0	172.2	174.6	183.6	165.3
BALANCE OF PLANT											
	\$/KWE	555.6	473.5	526.2	533.4	537.5	700.1	691.1	686.3	709.7	702.3
CONTINGENCY											
	\$/KWE	155.2	131.3	133.6	136.1	138.8	174.2	172.7	172.2	178.7	173.5
ESCALATION COSTS											
	\$/KWE	266.2	225.2	228.8	233.5	238.1	350.1	346.9	346.0	359.0	348.7
INTEREST DURING CONSTRUCTION											
	\$/KWE	328.0	277.5	281.9	287.6	293.3	453.9	449.8	448.6	465.5	452.1
TOTAL CAPITAL COST	\$/KWE	1525.2	1290.3	1310.9	1337.6	1364.2	1849.2	1832.7	1827.7	1896.6	1841.9

Table 2.9-8 (Page 3 of 3)

CAPITAL COST DISTRIBUTIONS FOR CLOSED-CYCLE INERT GAS MHD

	CASE NO.	21	22	101	102
MAJOR COMPONENTS					
PRIME CYCLE					
MHD GEN-DIFFUSER	MMS	4.2	4.4	2.7	2.6
MAGNET	MMS	24.3	25.5	17.7	25.9
HIGH TEMP RECUPERATOR (REGEN)	MMS	22.2	22.2	0.	0.
RECUPERATOR	MMS	0.	0.	0.	0.
PRECOOLER	MMS	9.2	11.6	3.6	4.4
COMP WITH STEAM TURB DRIVE	MMS	13.3	16.4	18.1	20.0
SEED SYSTEM	MMS	0.	0.	0.	0.
BOTTOMING CYCLE					
STEAM BOILER	MMS	13.4	14.1	8.9	13.6
STEAM TURB-GEN	MMS	6.9	4.1	0.	0.
PRIMARY HEAT INPUT AND FUEL SYSTEM					
COMBUSTOR SYSTEM	MMS	25.7	26.3	11.2	19.4
HEAT INPUT EXCH (REGENERATIVE)	MMS	35.2	35.2	35.2	46.2
SUB-TOTAL OF MAJOR COMPONENTS	MMS	154.4	159.8	97.4	132.1
BALANCE OF PLANT					
COOLING TOWER	MMS	8.0	10.4	4.0	5.3
STACK-GAS CLEAN-UP EQUIP.	MMS	53.5	53.5	26.2	54.2
DC TO AC INVERTERS	MMS	69.4	73.0	51.6	59.1
ALL OTHER	MMS	383.6	386.1	191.3	204.5
SITE LABOR	MMS	135.9	137.7	68.0	70.1
SUB-TOTAL OF BALANCE OF PLANT	MMS	650.4	660.7	341.1	393.2
CONTINGENCY	MMS	161.0	164.1	87.7	105.1
ESCALATION COSTS	MMS	323.4	329.7	176.2	180.3
INTEREST DURING CONSTRUCTION	MMS	419.3	427.5	228.5	222.1
TOTAL CAPITAL COST	MMS	1708.5	1741.8	931.0	1032.7
MAJOR COMPONENTS COST					
MAJOR COMPONENTS COST	S/KWE	164.2	173.1	162.3	142.0
BALANCE OF PLANT	S/KWE	691.6	715.5	568.5	422.6
CONTINGENCY	S/KWE	171.1	177.7	146.2	112.9
ESCALATION COSTS	S/KWE	343.9	357.1	293.7	193.7
INTEREST DURING CONSTRUCTION	S/KWE	445.9	463.0	380.8	238.7
TOTAL CAPITAL COST	S/KWE	1816.7	1886.3	1551.6	1109.9

Table 2.9-9

POWER OUTPUT AND AUXILIARY POWER DEMAND
FOR BASE CASE AND PARAMETRIC VARIATIONS:
CLOSED-CYCLE INERT GAS MHD

	CASE NO.	1	2	3	4	5	6	7	8	9	10
PRIME CYCLE POWER OUTPUT	MW	648.8	1299.3	100.7	648.8	648.8	648.8	648.8	531.0	621.1	570.7
BOTTOMING CYCLE POWER OUTPUT	MW	0.	0.	0.	0.	0.	0.	0.	103.0	14.2	0.
FURNACE POWER OUTPUT	MW	0.	0.	0.	0.	0.	0.	0.	0.	0.	0.
BALANCE OF PLANT AUX. POWER REQ'D.	MW	20.5	39.0	2.5	20.0	20.0	20.0	20.5	20.5	20.5	20.5
FURNACE AUX. POWER REQ'D.	MW	35.3	72.5	8.2	32.7	32.2	31.8	36.3	45.2	29.6	21.2
TRANSFORMER LOSSES	MW	3.2	6.5	0.5	3.2	3.2	3.2	3.2	3.2	3.2	2.9
INVERTER LOSSES	MW	6.5	13.0	1.0	6.5	6.5	6.5	6.5	5.3	6.2	5.7
NET STATION OUTPUT	MW	583.3	1168.3	88.5	586.4	586.9	587.3	582.3	559.8	575.8	520.4

	CASE NO.	11	12	13	14	15	16	17	18	19	20
PRIME CYCLE POWER OUTPUT	MW	553.6	753.2	597.4	628.0	654.5	931.0	931.0	931.0	678.1	931.0
BOTTOMING CYCLE POWER OUTPUT	MW	0.	0.	44.7	13.2	0.	110.0	127.0	140.0	321.0	107.0
FURNACE POWER OUTPUT	MW	0.	0.	0.	0.	0.	0.	0.	0.	0.	0.
BALANCE OF PLANT AUX. POWER REQ'D.	MW	20.5	20.5	20.5	20.5	27.0	40.7	40.8	40.7	40.7	40.7
FURNACE AUX. POWER REQ'D.	MW	16.8	51.0	30.7	32.8	35.5	52.2	54.4	56.0	52.5	52.2
TRANSFORMER LOSSES	MW	2.8	3.8	3.3	3.2	3.3	5.2	5.3	5.4	5.0	5.2
INVERTER LOSSES	MW	5.5	7.5	6.0	6.3	6.5	9.3	9.3	9.3	6.8	9.3
NET STATION OUTPUT	MW	508.0	670.4	581.6	578.4	582.2	933.6	948.2	959.6	894.1	930.6

	CASE NO.	21	22	101	102
PRIME CYCLE POWER OUTPUT	MW	890.2	935.8	644.7	1016.0
BOTTOMING CYCLE POWER OUTPUT	MW	155.0	95.0	0.	0.
FURNACE POWER OUTPUT	MW	0.	0.	0.	0.
BALANCE OF PLANT AUX. POWER REQ'D.	MW	40.7	40.7	20.0	45.9
FURNACE AUX. POWER REQ'D.	MW	49.9	52.2	15.0	24.4
TRANSFORMER LOSSES	MW	5.2	5.2	3.2	5.1
INVERTER LOSSES	MW	8.9	9.4	6.4	10.2
NET STATION OUTPUT	MW	940.5	923.4	600.0	930.5

REPRODUCTION OF THE
ORIGINAL PAGE IS POOR

The thermodynamic and power plant efficiencies of the SRC fueled topping plants are higher than those of the coal fueled parallel cycles, but the energy lost in the production of the semi-clean fuel overbalances that advantage. Thus the overall efficiencies of the SRC fueled topping cycles are in the range 26 to 36 percent, while those for the coal fueled parallel cycle are in the range 35 to 39 percent. The SRC fueled low power recuperative cycle, Case 3, has a low overall efficiency of about 28 percent. Only the coal fired topping cycles, Case 101 at about 42 percent and Case 102 at 46 percent, have overall efficiency above 40 percent.

Among the parameters varied, the turbine effectiveness (Cases 1, 12, 13, 16, 21, and 102) produced the greatest effects on efficiency. Increase in the peak argon temperature also tended to increase system efficiency. The design pressure drop for combustion gases passing through the refractory storage input heat exchanger is an important parameter affecting both efficiency, through changes in required furnace auxiliary power, and capital cost, through changes in heat exchanger size and cost.

Pressurization of the combustion system provides significant gains. Estimates made for a modification of Case 102 in which the combustion system is pressurized to 4 atmospheres by a balanced gas turbine/air compressor set operating with turbine inlet temperature of 546 F (559 K) indicate savings of approximately 6 percent in total capital cost relative to the corresponding system with atmospheric combustion. These savings result primarily from use of fewer refractory storage heat exchangers (10 instead of 14) and smaller combustion gas ducts; there is little net change in equipment costs for the furnace system. In addition, gains in overall system efficiency totaling approximately 3 percent (1.4 percentage points) result from a 1 percent improvement in furnace efficiency (lower stack temperature) and a net saving of nearly 18 MWe in auxiliary power (fans). Thus furnace pressurization to 4 atmospheres for Case 102 should result in a system providing 948 MWe at a capital cost of \$1015/kWe and an overall efficiency of 47.4 percent.

The relatively high compression power requirements of the argon working fluid are a disadvantage of this system. The argon compressors for the 600 MWe (nominal) systems studied here differ very little in power requirements from the air compressors for the 2000 MWe (nominal) open-cycle MHD systems. At the higher values of MHD "turbine effectiveness," the closed-cycle inert gas MHD topping systems must operate significantly below optimum pressure ratios in the argon loop to get sufficient steam power to drive the argon compressor. This problem can be alleviated by higher peak argon temperatures and by lower final feedwater temperatures in the steam bottoming cycle, both of which have been used in Case 102, and possibly by some argon compressor intercooling. A less attractive alternative is the provision of some auxiliary electric motor drive for the argon compressor.

It seems clear in retrospect that this first attempt at total system design did not begin with the system configurations most likely to be successful. The parallel cycle and the low power MHD recuperative cycle appear not to be attractive. The MHD topping cycles can have attractive overall energy efficiencies, but not when fueled with the semi-clean fuel because of the 0.78 fuel conversion efficiency factor for producing this fuel from coal. The system providing the best possibility for attractive overall efficiencies and cost of electricity is the coal fueled topping cycle. Success with this system probably will require MHD "turbine effectiveness" exceeding 0.70 and careful integration of both the steam cycle and the furnace with the topping cycle. Further, the working fluid gas must be kept "pure" to take advantage of the nonequilibrium effects. The design of the MHD equipment also must permit an economical plant layout and reduced balance-of-plant costs.

RECOMMENDED CASE

Case 102, the coal-fueled MHD topping cycle is the recommended starting point for future system study. This system provides the highest efficiency, lowest capital cost, and lowest total cost of electricity among the closed-cycle inert gas MHD systems analyzed here. Further study of this system should include consideration of pressurized combustion, which provides significant gains in lowered capital costs and increased efficiency.

2.10 CLOSED-CYCLE LIQUID METAL MHD

DESCRIPTION OF CYCLE

The closed-cycle liquid metal MHD system is similar to the closed-cycle inert gas system in its recirculation of the generator working fluid and in requiring a heat exchanger which operates at peak cycle temperature. However, it differs greatly in getting electrical conduction in the working fluid by means of a liquid metal flow, which provides an electrical conductivity that is essentially independent of the fluid temperature.

Of the many ways tried thus far to use the high conductivity of liquid metals in MHD power generation, the one that works best appears also to be the simplest. The liquid metal is pressurized and heated to peak cycle temperature (1300 F [978 K]) in an input heat exchanger. It then flows to the entrance of the MHD generator where pressurized (and possibly also heated) gas (helium) is injected as a uniform dispersion of bubbles occupying over half the volume of the flow.

The bubbles and liquid flow together as a two-phase mixture through the generator and its magnetic field. The liquid provides the necessary electric conductivity and, because it has much greater heat capacity than the bubbles, maintains the gas temperature nearly uniform as the bubbles expand through the generator. The bubbles provide the compressibility needed to convert heat to energy of directed motion in an expansion engine. After leaving the MHD generator, the gas and bubbles are separated, the liquid is recycled directly to the input heat exchanger, and the energy in the gas is transferred to the bottoming cycle prior to recompression and return to the generator entrance.

The closed-cycle liquid metal MHD generators have provided the lowest temperature MHD generators and the most efficient machines demonstrated to date. Materials problems are less difficult here than in the inert gas systems. These favorable features are offset by inconveniently low output voltages, by cycle efficiency problems associated with losses from the large recirculating power in the circulating liquid metal flow and with pinch-point problems in the steam generator transferring heat to the bottoming cycle, and by cost problems associated with circulation and processing of the four working fluids used (combustion gases, helium, liquid metal, and steam).

The design and estimation of the closed-cycle liquid metal MHD systems has been a joint effort of Argonne National Laboratory (the system advocate), Foster Wheeler Energy Corporation, Bechtel Corporation, and the General Electric Company. The principal items designed and costed by personnel from each of these companies are as follows:

- Argonne National Laboratory
MHD mixer/generator/separator
Superconducting magnet/dewar
- Foster Wheeler Corporation
Coal handling auxiliaries
Atmospheric fluidized bed furnace
Air preheater
Steam boiler
Hot gas cleanup for gas turbines (Case 10) } except Case 101;
see text below
- Bechtel Corporation
Site labor and materials } except Case 101;
Cooling towers } see text below
Balance of plant }
- General Electric Company
Electrical inversion equipment
Steam turbine/helium compressor
Combustion gas and helium turbines
Helium recuperators
Helium precoolers
Coal gasification equipment
Liquid metal pumps

In addition, General Electric has performed the system integration function.

Eighteen different MHD power cycles have been analyzed in the Task I Study.* The power level for the base case, Case 1, illustrated in the schematic of Figure 2.10-1, is set at a nominal 600 MWe. Unlike the other types of MHD systems, these liquid metal systems are best suited for relatively low magnetic flux densities and low power outputs, and the 600 MW (nominal) systems studied here have 13 or 14 generators operating mechanically in parallel but electrically in series, each usually producing approximately 50 MWe at 30-35 volts. The magnetic flux densities are in the range 1 to 2 tesla. Most of these systems use atmospheric fluidized bed (AFB) furnaces for heat input and sulfur emission control, and the 600 MW (nominal) systems use three AFB tower modules.

Case 2 is similar to Case 1 except that its lower power level (300 MWe nominal) requires only 7 MHD power modules instead of 13 and it produces d-c electric power at a lower voltage, 210V instead of 390V. Case 3, a 1200 MWe nominal system, uses 14 somewhat larger MHD power modules, each producing 87.5 MWe at 35V. The magnetic flux density is slightly lower, 0.97 tesla rather than

*The principal design parameters of these eighteen systems are included in Table 2.10-5.

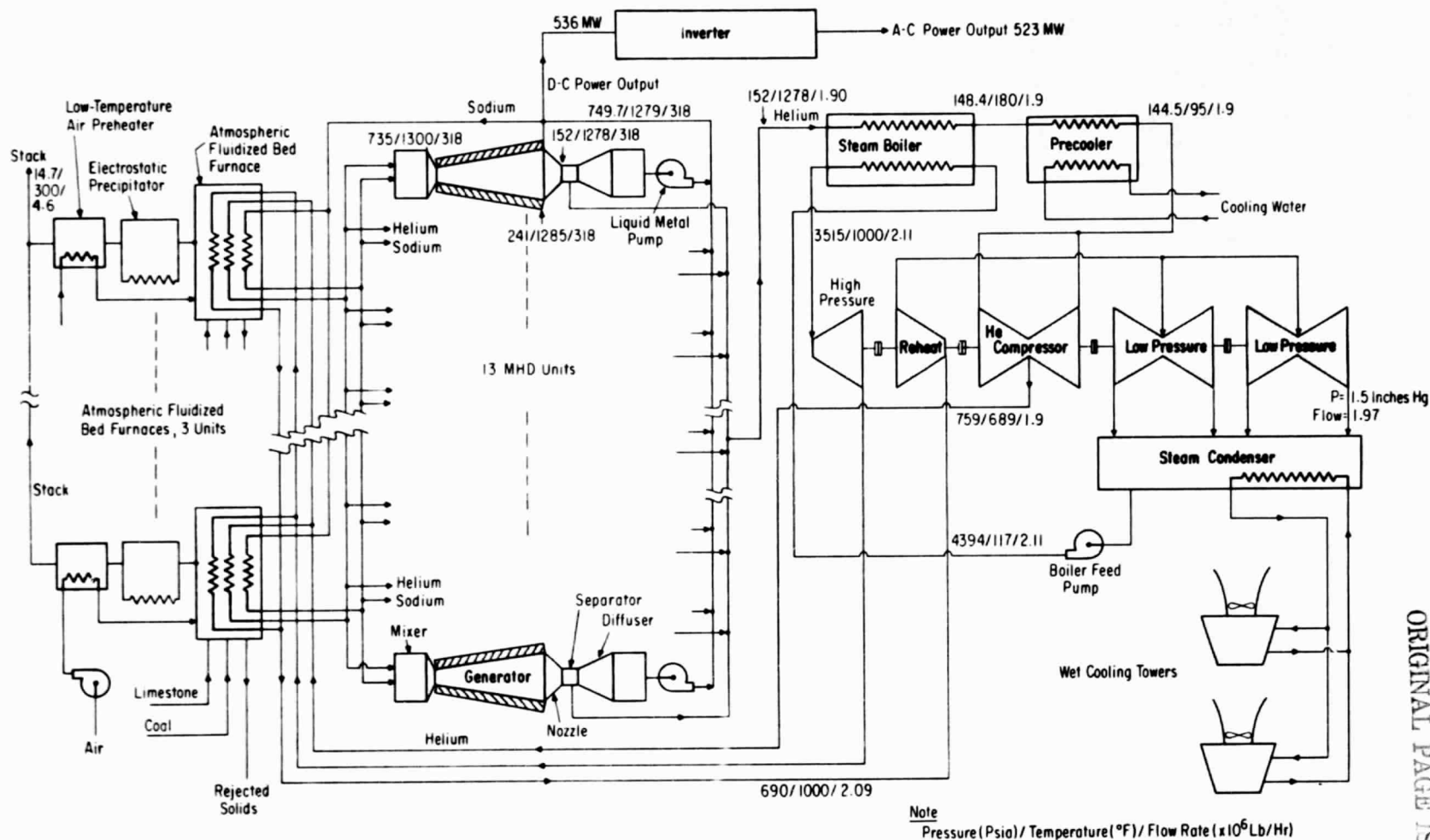


Figure 2.10-1. Closed-Cycle Liquid Metal MHD

REPRODUCIBILITY OF THE ORIGINAL PAGE IS POOR

1.13 tesla, for this case. Cases 4 and 5 are similar to Case 1 except that the fuels burned in the AFB furnaces are Montana sub-bituminous and North Dakota Lignite, respectively.

Cases 6, 7, and 8 are similar to Case 1 except that the fuels used are low-Btu gases made from Illinois #6, Montana sub-bituminous and North Dakota lignite coals, respectively. These gases are burned in pressurized furnaces at 10 atmospheres pressure. Because the pressurizing gas turbines and steam turbine generator used in these cases produce substantially more power than is required to operate the integrated gasifiers and furnaces, each of these cases gains substantial power, more than the output of the MHD generator, from the furnace turbine generator.

Case 9 is similar to Case 1 except that the fuel is high-Btu gas burned in a pressurized furnace. The furnace turbine generator for this case provides only about 10 percent of the total power output.

Case 10 is similar to Case 1 except that the furnace is of pressurized fluidized bed (PFB) type burning Illinois #6 coal. The furnace turbines produce about 24 percent of the power output for this case.

Cases 11 and 12 differ from Case 1 mainly in their higher peak temperatures, 1400 F (1033 K) and 1500 F (1089 K) instead of 1300 F (978 K), and in the use of lithium instead of sodium as the liquid metal. Sodium carryover past the separator to the steam generator becomes a significant problem at temperatures above 1300 F (978 K) because of the relatively high vapor pressure of sodium at such temperatures.

Case 13 differs from the base case primarily in use of a higher peak pressure at generator inlet, 100 atmospheres (10.1 MN/m²) rather than 50, and a slightly lower pressure ratio across the MHD generator.

Cases 14 and 15 explore the effects of changes in electric load parameter and thus of changes in "effective turbine efficiency" of the MHD mixer/generator/separator chain.

Case 16 is similar to Case 1 except that dry cooling towers are used rather than wet towers for system heat rejection.

Case 17 is a variation in system configuration that uses a recuperative heat exchanger and helium turbine in place of the boiler and steam turbine bottoming cycle. The AFB furnaces also are simplified in this variation because of elimination of the steam reheat.

Case 101 is a variation in which a larger pressure drop is used in the separator together with lower estimates of separator losses to gain a system of higher efficiency and lower cost that does not require the expensive mechanical pumps for liquid metal

recirculation used in the base case. This case was not one of the original points selected for analysis. It was added in the course of performing Task I following evaluation of preliminary results for the other points. Because of pressures on time, the costing of on-site labor and materials, cooling towers, and balance of plant for Case 101 has not been done by Bechtel, but has been done at General Electric by the Systems and Plant Integration Team by making incremental adjustments to Bechtel estimates for Case 1. Similarly, estimation of the costs of the AFB furnaces for Case 101 has not been done by Foster Wheeler, but has been done at General Electric by incremental adjustment of the Foster Wheeler estimate for Case 1. Among the closed-cycle liquid metal MHD systems, only Case 101 was handled in this manner.

ANALYTICAL PROCEDURE AND DESIGN ASSUMPTIONS

The scheme of the systems programming was to model at an adequate but simple level to facilitate efficient computer usage and thus enable thorough parametric studies. Consequently, two levels of analysis were used:

- a. The MHD generator model
- b. The integrated systems model

In the integrated systems model the MHD generator was modeled by defining an isentropic efficiency. Using the isentropic efficiency in conjunction with the model for the ideal device, the duct (MHD generator) performance was determined including the power output and the thermodynamic state points of the fluid mixture. The isentropic efficiency and the duct configuration corresponding to that efficiency at the operating conditions in question were determined through the use of the MHD generator model. Discussions of the generator model and the integrated systems model follow.

MHD Generator

The equations and model used to analyze the two-phase liquid-metal MHD (LMMHD) generator have been described previously. (See, for example, ref. 1.) The major points are summarized below. The following basic assumptions are used in the solution:

1. The walls of the fluid channel parallel to the current flow are perfect insulators. (In practice a thin coating of electrically-conducting metal may be required to protect the insulator, but the coating thickness is negligible compared with the liquid-metal thickness. The coating may be included in the model.)
2. The fluid channel walls perpendicular to the current flow (electrodes) are perfect electrical conductors (compared with the fluid).

3. The velocity of the liquid phase along the generator axis is constant.
4. The effect of slip between the liquid and gas phases is ignored, or the liquid and gas have the same (constant) velocity. It is felt that by proper design, including high velocities and possibly the use of surfactive agents, the slip can be made relatively small. (Slip may be included.)
5. The magnetic flux density is constant between the generator electrodes and zero outside of the electrodes (i.e., no field overhang).
6. There is no variation of the fluid or flow properties perpendicular to the axis of the generator (i.e., the flow is quasi-one-dimensional).
7. The distance between the electrodes is constant.
8. The electrical conductivity of the two-phase fluid is given by a least-squares-fit of a fourth-order polynomial in powers of the void fraction to experimental data.
9. There is no contact resistance between the electrodes and the working fluid.
10. Heat transfer to the surroundings is negligible.

The conservation equations of mass, momentum, and energy; the perfect gas equation of state; and the slip equation (if slip was included) were solved simultaneously in finite-difference form. Values of the terminal voltage, load factor (ratio of terminal voltage to generated voltage), aspect ratio (ratio of generator length to electrode spacing), and inlet and exit void fractions were preselected; and from these the magnetic field strengths and channel dimensions calculated. The finite-difference calculations were continued downstream of the generator entrance for small increments of pressure drop until the generator void fraction reached the desired exit value, at which point the calculation was terminated. End losses were accounted for by an empirical relation, assuming that 90 percent of the normal dissipation can be eliminated by vaning or tailoring of the magnetic fields. Finally, an adjustment in the generator exit temperature was made to account for the dissipation in the fluid due to the end losses.

The ability to reduce the end losses by 90 percent from those calculated with no vanes or field extension is a key point. Previous results for pure liquid flows have demonstrated that a nonoptimized field extension reduced the end losses by 72 percent, vanes alone by up to 83 percent, and an improved combination of vanes and the existing field extension by 88 percent. A

generator has not been tested with an optimum field extension profile, but it is expected that a 90 percent reduction is attainable without the use of insulating vanes.

The choices of aspect ratio and load factor in the generator are adjusted to yield an efficiency of around 80 percent at reasonable generator dimensions. Increasing the aspect ratio above the nominal 7.5 selected increases the efficiency and the generator length, the latter more quickly than the former. Increasing the load factor above the 0.93 selected decreases the generator efficiency and length. The efficiency as a function of load factor goes through a peak around 0.93 because as the load factor is increased the ohmic losses internal to the generator and the power density decrease while the end loss remains about constant.

Integrated Systems Model

The integrated systems model for the LMMHD-Steam Cycle is considered as six major subsystems or components. These are:

- Mixer
- MHD generator (duct)
- Nozzle-separator-diffuser
- Steam bottoming cycle and interface
- Compressor
- Fluidized bed and associated interfacing heat exchangers

The analysis of the last three has been conventional. The modeling of the mixer, MHD generator, and separator assembly, illustrated in Figure 2.10-2, is described here. All of the components have been analyzed assuming a steady-state, lumped (no space-dependent variation) model.

Mixer. For the mixer the following assumptions were made:

1. The mixture at the exit of the mixer is homogeneous and at the mixed mean temperature of the fluids.
2. Make-up liquid metal is added in the mixer in the amount carried over in the gas stream at the separator exit.

MHD Generator. The following assumptions were made in analyzing the LMMHD generator:

1. The flow is steady.
2. The generator is described by a lumped control volume (i.e., spatial dependence of the thermodynamic variables is neglected).

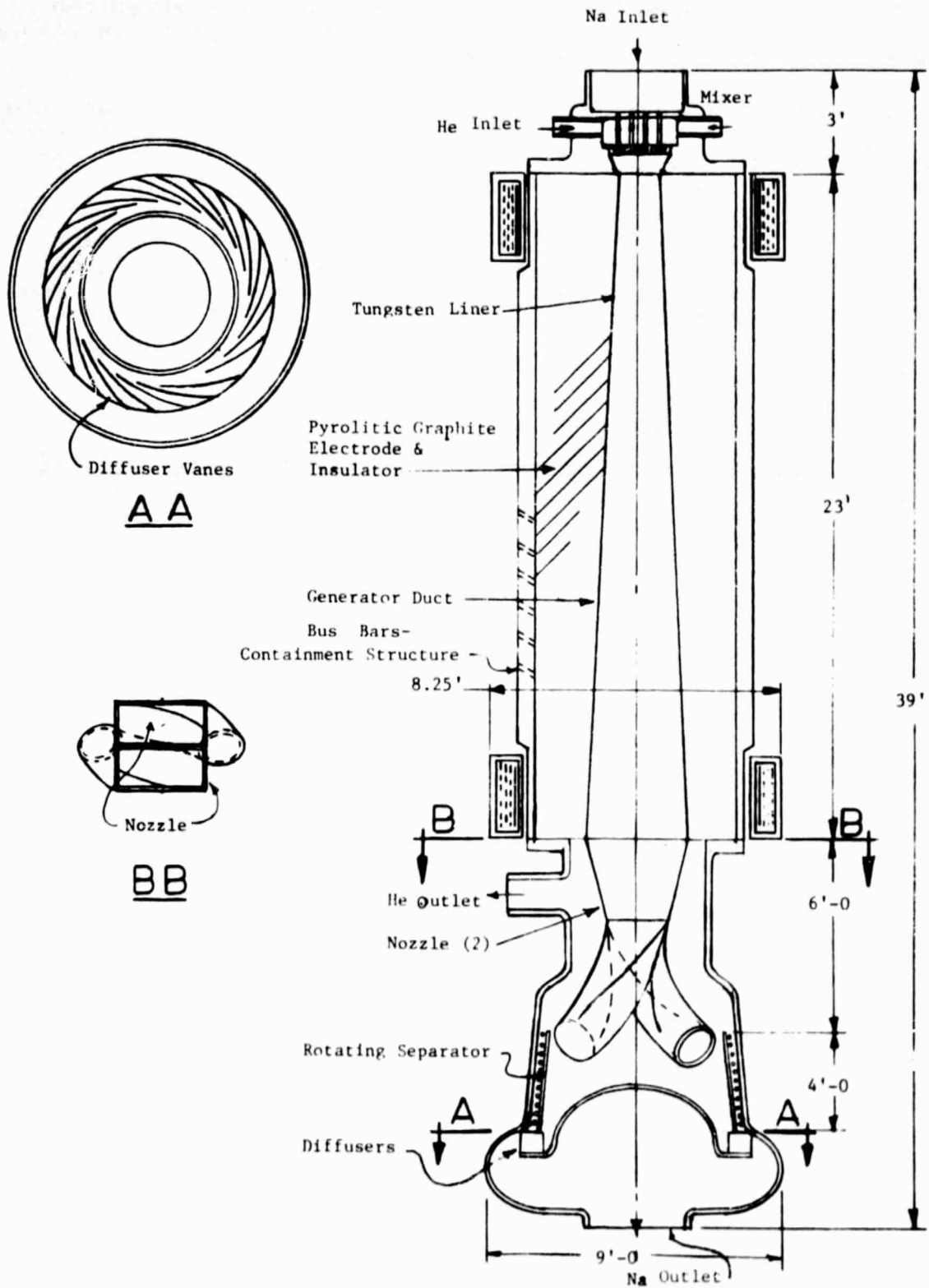


Figure 2.10-2. 47-MWe MHD Power Module with Nozzle-Separator-Diffuser

3. The gas phase is an ideal gas.
4. Heat transfer to the surroundings is negligible.
5. Viscous dissipation is neglected.
6. The mixture is homogeneous and slip is negligible.
7. The mixture conserves entropy as a two-phase mixture with no mass transfer between phases.
8. The specific heats of the gas and liquid phases and the volume expansivity of the liquid are all constant.
9. The liquid metal is a pure (simple compressible) substance.
10. Deviations from the ideal device will be accounted for by defining an isentropic efficiency.

The scheme used in this case is to analyze the ideal device and to account for deviations from the ideal through the use of an isentropic efficiency. Then using the conservation of mass, the first and second laws of thermodynamics, the ideal gas equation of state, and the appropriate thermodynamic property relationships for the homogeneous mixture of two pure substances, there result mathematical expressions relating characteristics of the flow at generator entrance and exit and the generator output.

Nozzle-Separator-Diffuser. A conceptual design of a nozzle-separator is shown in Figure 2.10-2. After exiting the MHD generator the mixture is accelerated in the nozzle and flows tangentially onto a rotating drum where the liquid and gas phases are separated. The liquid is then collected in diffuser vanes to regain a pressure sufficient to return the liquid to the mixer. The gas flows out the helium outlet at very nearly the mixer temperature to continue to the bottoming-cycle interface, compressor, etc.

In modeling this device, the nozzle and diffuser are treated as nonideal devices with deviations from the ideal (isentropic) behavior accounted for through the use of isentropic efficiencies. Isentropic efficiencies of 90 percent have been used for both devices. The separator performance and, in particular, the losses incurred in separation must also be included in the analysis. Losses for the specific device shown in Figure 2.10-2 have not been analyzed in detail, but it is expected that this new device should yield better performance than a more conventional flat plate separator. Two values of separator loss coefficient, defined as

separator loss coefficient = $1 - \frac{\text{separator outlet kinetic energy flux}}{\text{separator inlet kinetic energy flux}}$
 have been used, 0.24 for Cases 1-17 and 0.10 for Case 101.

The designs and performances of the combustor systems and the steam generators are described in Section 6. The helium compressors are conventional axial flow machines that represent a modest extrapolation from current commercial practice. The steam bottoming cycles used are conventional 3500/1000/1000 single re-heat supercritical cycles with final feedwater temperatures of 117 F (321 K) corresponding to cycle efficiencies (ratio of a-c electrical power out to the thermal power transferred to the steam) of approximately 0.375. The actual heat rates for the turbine designs selected were calculated for each case.

MHD Component Designs

Mixer. The liquid flows straight through the mixer at about constant velocity to minimize pressure drop, and the gas is injected by a series of tubes. A homogeneous two-phase flow is formed about one foot before the generator duct inlet.

The mixer is brazed directly to the generator duct housing. To minimize losses due to circulating currents, it is proposed that the mixer be flame sprayed over its entire surface with an electrical insulator such as Al_2O_3 . A thin coating of tungsten or molybdenum would then be applied over the insulator for protection and to serve as a brazing surface at the cost of a high-resistance electrical path.

Generator. The principal generator parameters are given in Table 2.10-1. The decision to use 13 generators for the base case came from the desire to have a roughly square exit channel for optimum fit into the circular containment structure, shown in Figure 2.10-3, and the need to attain a reasonable voltage level for the inverters. The terminal voltage of 390 volts for Case 1 is obtained by connecting 13 generators electrically in series.

The generator duct is rectangular in cross section, with the distance between electrodes remaining constant while the flow area increases to maintain a given two-phase velocity. Previous designs for the generator duct have been visualized as thin metal cans that are integral on two sides with the electrodes, with the remaining sides electrically insulated from the containment pressure housing. Ideally the electrodes should be separated by an electrical insulator to prevent added ohmic losses. Since at present there are no known insulators compatible with high-temperature liquid metals, thin metal walls are required to provide protection with minimum ohmic loss. The structural housing required to contain the pressure in the duct while maintaining electrical isolation of the electrodes can evolve into a rather complex design. Thus a new approach has been proposed, namely, generator duct containment by the use of pyrolitic graphite.

The use of pyrolitic graphite (PG) as electrode, insulator, and containment is without any known precedent. Theoretically

Table 2.10-1

POWER MODULE PARAMETERS

	Case 1 Na-1300 F	Case 2 Na-1300 F	Case 3 Na-1300 F	Case 11 Li-1400 F	Case 12 Li-1500 F	Case 13 Na-100 Atm	Case 17 Gas Turbine
Nominal power output (total) power/unit MWe	600 MWe 47.1	300 MWe 47.3	1200 MWe 87.46	600 MWe 43.73	600 MWe 43.7	600 MWe 47.3	600 MWe 68.03
Generator length (ft)	22.7	22.7	30.9	22.47	21.7	15.43	32.0
Electrode spacing (ft)	3.067	3.067	4.17	3.031	2.931	2.081	4.32
Electrode height (ft)	1.280-3.025	1.189-2.809	1.75-4.13	1.199-2.845	1.17-2.95	0.930-2.058	2.85-4.19
Field strength (tesla)	1.13	1.13	0.97	1.15	1.18	1.95	0.92
Voltages	30	30	35	30	30	35	35
No. of power modules	13	7	14	14	14	14	9
OD of graphite housing ID of Cu electrodes (ft)	6	6	7	5.5	5.5	5	7
Nominal refig. power kW	329	177	545	330	325	210	370
OD of cryostat (ft)	8.25	8.25	9.0	7.5	7.5	8.0	9.0

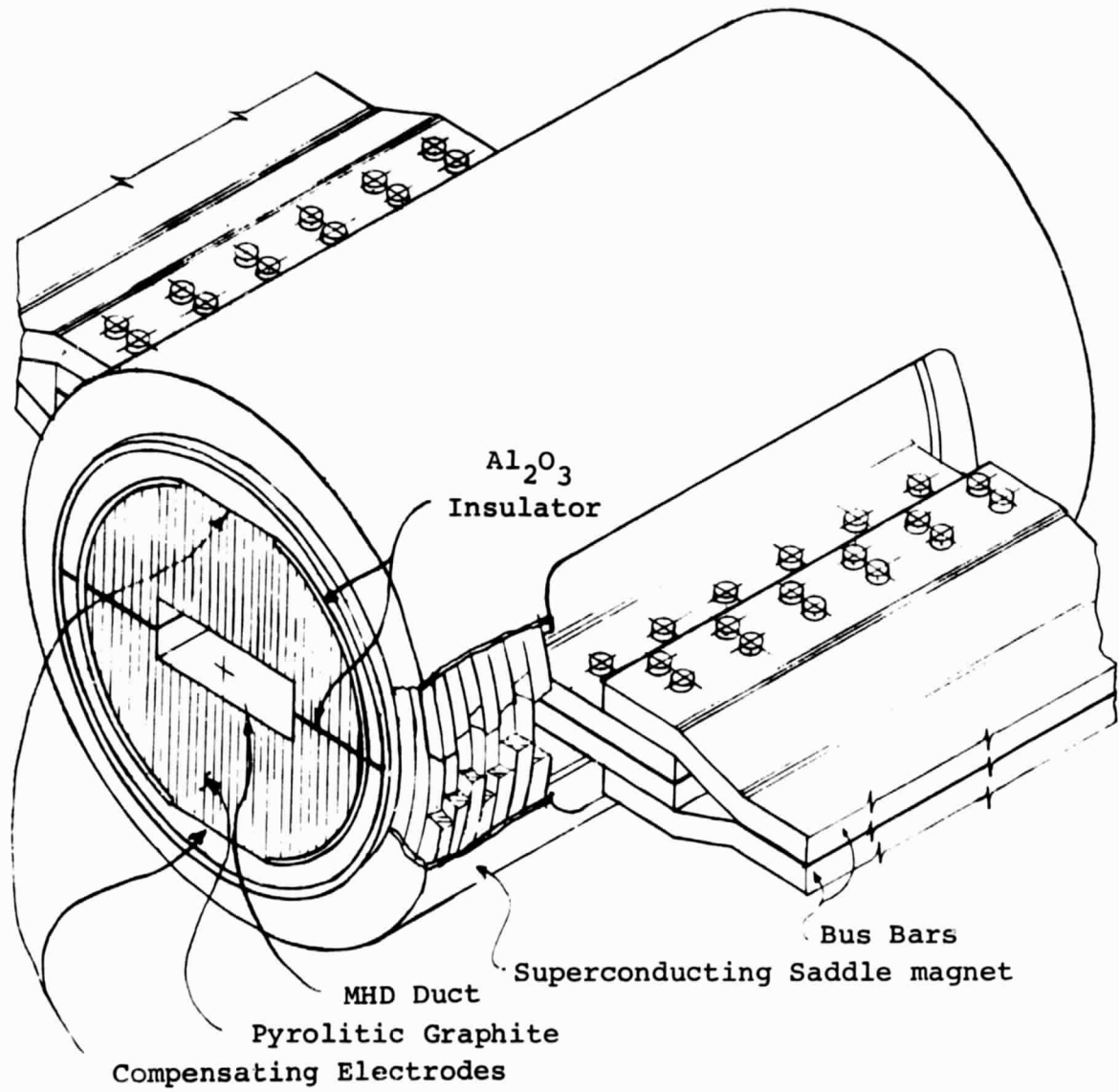


Figure 2.10-3. Schematic of Generator Assembly

the desired features are there. PG is an excellent material for high-temperature service, actually increasing in mechanical strength with increasing temperature up to 4500 F (2756 K) while also exhibiting high resistance to thermal shock. The anisotropic properties of PG permit electrical conductivity approaching that of aluminum in one plane, while acting as an electrical and thermal insulator comparable to ceramics in the normal direction. Pyrolytic graphite is especially intriguing because of its method of manufacture, i.e., being deposited in layers from a hydrocarbon gas. This process allows additional materials such as refractory metals or ceramics to be alloyed with the carbon, and also deposition temperatures can be varied (3181 to 4081 F [2023 to 2523 K]) to control the desired mechanical, thermal, and electrical properties. Although standard commercial grades of PG offer an electrical resistivity between 300 and 500 micro-ohm-cm in the conductive direction, carefully controlled PG has been produced with a resistivity of 39 micro-ohm-cm. It is noteworthy that the electrical resistivity of PG, unlike most metal conductors, remains fairly constant with temperature increase up to 3000 F (1922 K).

The geometry of the generator duct could be machined into a cylindrical block of pyrolytic graphite with the conducting plane parallel to the direction of the generated current. Normal to this plane the graphite is an insulator. The cylinder could be made in longitudinal halves separated by an electrical insulator to ensure against any generated cross currents. Graphite is not compatible with liquid metals, so a layer of tungsten or molybdenum must be flame sprayed or chemically vapor deposited on the duct surface and the ends of the housing. The mixer and nozzle-separator-diffuser units can then be brazed to the generator housing for leakproof seals. The graphite provides an integral housing and the desired electrical properties but is not strong enough to withstand the high pressures involved without structural backup. This backup is provided by the bus bars formed into flanged half rings extending the length of the generator and electrically insulated from the graphite except in the current-carrying areas, as shown in Figure 2.10-3. The two bus bars with an insulating interface are bolted together to provide the necessary structure and also act as compensation for the induced currents generated in the liquid metal.

Nozzle-Separator-Diffuser. After the MHD generator it is necessary to separate the liquid and gas components of the flow. This is accomplished by impinging the mixture tangentially onto the inner surface of a cone, as indicated in Figure 2.10-2, causing the cone to rotate. The large centrifugal force concentrates the gas in the center of the cone. This method of separation appears to have significant advantages over a conventional flat-plate separator. The slight taper of the cone forces the liquid to move toward the exit diffuser at a controlled rate. A single, approximately 90-degree large radius bend is used after each nozzle to direct the mixture tangentially to the rotor.

In principle, the nozzle-diffuser system can be used to allow the gas to "pump" the liquid back to the mixer pressure thus eliminating the need for a separate liquid pump. In the nozzle the gas-liquid mixture is accelerated so that the liquid acquires sufficient kinetic energy to overcome the separator and pipe losses and recover the mixer pressure in the diffuser.

DESIGN AND COST BASIS

A liquid-metal MHD power module is shown in Figure 2.10-2. In costing these components, definitive information is available only for the magnet system. The other major components are in a first-iteration conceptual stage with other alternatives of mechanical design and resolution of detail yet to be considered. The estimated cost of these components was determined by approximating their weights and applying appropriate rates for cost per pound for raw materials and fabrication based on a recent cost study for fusion power plants, as tabulated in Table 2.10-2.

Table 2.10-2

RAW MATERIAL AND FABRICATION COSTS USED FOR
ESTIMATING COSTS OF
MIXER/GENERATOR/SEPARATOR TRAIN

Component	Price (\$/lb)	
<u>Generator</u>		
Copper raw price	1.50	
Copper fabrication	2.50	
	Total	4.00
Graphite raw price	4.00	
Graphite fabrication	2.00	
	Total	6.00
<u>Mixer</u>		
Raw inconel	3.00	
Fabrication	9.00	
	Total	12.00
<u>Separator</u>		
Inconel + SS	3.00	
Fabrication	6.00	
	Total	9.00

Recent procurements by the Argonne National Laboratory of fully stabilized Nb-Ti superconducting saddle magnets indicate a cost of about \$1.50/k amp-ft (\$4.92/k amp-m) for conductor materials and winding. The 7-meter-long, 1.13-tesla magnet for the base case designed for a current of 5000 amps and a current density of 5000 amps/cm² requires approximately 1300 turns for a 1.83 meter bore or about 125,000 k amp-ft (38,100 k amp-m). The cost of the winding and conductor was thus rounded out to \$200,000. The weight of the windings, assuming the mean density to be that of the copper stabilizer (8.9 gm/cm³) was determined by the empirical formula for "crescent" saddle magnets:

$$\frac{M(\text{metric tons})}{L(\text{meters})} = 2.83 (10^7/J) B D + [B/6.3(f) (10^7/J)];$$

where B is in tesla, D is the bore diameter in meters, J is amperes per square meter, and f is the winding factor. The weight of the restraining structure was calculated by $M_s(\text{kg}) = 2.36 \times 10^{-5} W_B$, where W_B is the stored energy of the field in joules. The resultant weight, M_s , appears rather optimistic and was therefore utilized as the weight per meter length of the magnet instead of the total weight. The cryostat diameter, and thereby its weight, was estimated by the relationship $B = \mu_0 Jcf$, where c is the maximum winding thickness in meters and μ_0 is the permeability of free space. The cost of the cryostat and structure was conservatively assumed to be \$300,000. Summing the weights of the winding, structure, and conductors; the total cost per pound for the assembly is \$14.7 for the base case. The magnet costs for the other cases were calculated as the magnet weight times \$14.7/lb (\$32.41/kg). A single complete refrigeration unit including liquefier, purifier, 500-liter Dewar, and local transfer lines in the 25 watt heat load range for 4.2 K liquid helium service is currently priced at \$150,000. Although a central refrigeration plant consisting of several large refrigeration units run off large compressors would be more economical than individual units for each power module, the cost of a single unit was assumed for each module.

The base case was estimated as outlined and the remaining system cases scaled accordingly. The resulting power module weights and costs for all cases are given in Tables 2.10-3 and 2.10-4, respectively.

In the above costs neither indirect costs nor projected component replacement costs due to limited lifetime have been included. With the recognition of periodic component replacement requirements and with appropriate design to accommodate the necessary maintenance, an additional cost for the power plant could be the price of one set of spare components to maximize plant availability and allow repair of the worn component at nominal cost without requiring plant shutdown during the repair operation.

Table 2.10-3

POWER MODULE WEIGHTS

	Case 1/2 Na-600/300 MWe	Case 3 Na-1200 MWe	Case 11 Li-1400 F	Case 12 Li-1500 F	Case 13 Na-100 atm	Case 17 Gas Turbine
Magnet	17,000	24,700	16,800	16,700	18,200	26,700
Magnet structure	3,000	6,200	2,900	2,000	3,200	6,500
Cryostat	14,000	17,800	14,600	14,000	9,200	18,200
Generator copper	42,600	59,000	42,200	40,700	26,000	58,500
Generator graphite	54,200	115,000	56,500	54,500	36,000	104,000
Mixer	7,000	12,000	8,500	10,500	13,500	16,000
Separator-Nozzle- Diffuser	11,000	18,000	13,200	16,500	21,000	25,000
Total Weight per unit	148,800	252,700	154,700	155,700	127,100	254,900
No. of units (Power modules)	13/7	14	14	14	14	9
Total weight (m tons)	877.3/472.6	1605.2	982.7	989	807.4	1040.8

Table 2.10-4

POWER MODULE COSTS

	Case 1/2 Na-600/300 MWe	Case 3 Na-1200 MWe	Case 11 Li-1400 F	Case 12 Li-1500 F	Case 13 Na-100 atm	Case 17 Gas Turbine
Magnet & cryostat refrigeration	\$ 650,000	\$ 885,000	\$ 654,000	\$ 602,000	\$ 600,000	\$ 905,600
Generator	521,000	937,000	531,000	512,000	334,000	814,300
Mixer	85,000	146,000	204,000	252,000	163,000	194,000
Separator nozzle-diffuser	100,000	164,000	290,000	363,000	191,000	228,000
Supports, insulation assembly & instrumentation	200,000	200,000	200,000	200,000	200,000	200,000
Total cost per unit	\$1,556,000	\$2,312,000	\$1,879,000	\$1,929,000	\$1,488,000	\$2,401,900
No. of units (power modules)	13/7	14	14	14	14	9
Total cost (millions)	\$20.2/\$10.89	\$32.37	\$26.31	\$27.0	\$20.8	\$21.6

RESULTS

Table 2.10-5 summarizes the principal design parameters and results of calculations of efficiencies and overall costs for all cases studied here. Table 2.10-6 summarizes for all cases the void (helium) fractions in flows at the generator entrances (α_2) and exits (α_{3p}), the mass flow rates of helium (MG) and liquid metal (ML), the machine efficiencies of the mixer and MHD generator combinations, and the powers produced by the MHD generators or absorbed in the helium compressors and liquid metal pumps.

Table 2.10-2 gives material and fabrication costs used in estimating costs for the mixer/generator/separator train. Tables 2.10-3 and 2.10-4 give estimated weights and costs for the mixer/generator/separator power modules of all systems. (The same MHD power module is used for Cases 1, 2, 4-10, 15 and 16. Case 2 requires 7 MHD power modules; the others in this group use 13.)

Table 2.10-7 summarizes the principal design parameters and calculated outputs for the base case, Case 1.

Table 2.10-8 gives detailed breakdowns of calculated costs for all cases studied.

Discussion of Results

Table 2.10-9 details the auxiliary power losses for all cases studied.

A review of the results tabulated in the lower part of Table 2.10-5 indicates that these systems might be divided for discussion into four groups: (1) the atmospheric fluidized bed fired Cases 1-5 and 11-16; (2) the pressurized furnace and pressurized fluidized bed fired Cases 6-10; (3) Case 17; and (4) Case 101.

The first group, which includes the base case, show a total cost of electricity near 90 mills/kWh (except for Case 12 at 111), which is about 3 times that for advanced steam cycles. Of this cost, 75 to 80 mills/kWh usually is contributed by capital charges. The thermodynamic efficiencies of these systems range over 0.43 to 0.47 and the overall (coal pile to bus bar) efficiencies range over 0.34 to 0.39, with only the higher temperature lithium cycles doing much better than 0.36. Thus, despite their higher costs, these systems are little or no more efficient than more conventional steam systems.

It appears that within this group only the higher peak temperatures (and consequent shift to lithium liquid metal from sodium) of Cases 11 and 12 and the lower furnace efficiency of Case 5 (North Dakota lignite) produce significant changes in costs or efficiencies. This fact reflects the fixed system configuration and the care that has been taken to select most parameters of this configuration near optimum values.

Table 2.10-5

PARAMETRIC VARIATIONS FOR TASK I STUDY
CLOSED-CYCLE LIQUID METAL MHD

Parameters	Case 1*	2	3	4	5	6	7	8	9	10	11	12	13	14	15	16	17	101	
Power Output (MWe)	486	243	972	485	488	1148	1203	1230	571	662	485	486	489	479	486	477	509	556	
Furnace, Coal, and Conversion Process	AFB Ill. #6 Direct	→		AFB Mont Direct	AFB N. D. Direct	PF Ill. #6 Lbtu	PF Mont Lbtu	PF N. D. Lbtu	PF Ill. #6 Hbtu	(PF) _R Ill. #6 Direct	AFB Ill. #6 Direct								
Topping Cycle																			
Duct inlet temperature (°F)	1300										1400	1500	1300				1200	1300	
Liquid metal	Na										Li		Na						
Inert gas	He																		
Pressure (duct inlet) (atm)	50												100	50					
Pressure ratio	3.1												3.3	2.8	3.1		1.58	2.93	
Magnetic field (f)	1.13	→	0.97	1.13									1.15	1.18	1.95	1.13		0.92	1.13
Electric load parameter	0.9														0.45	0.92	0.9		
Input heat exchanger pressure drops																			
He (Δp/p (psi))	0.025																		
Na, Li (Δp (psi))	10																		
Compressor efficiency	0.88																		
Steam generator/precooler																			
He (Δp/p (psi))	0.025																	0.025	
Steam Bottoming Cycle																			
Turbine inlet temperature (°F)	1000/1000																	1000/1000	
Turbine inlet pressure (psi)	3500																	3500	
Maximum feedwater temperature (°F)	117																	117	
Heat Rejection (in. Hg)	WCT 1.5																DCT 1.9	WCT 1.5	WCT 1.5
PF Parameters																			
Excess air (percent)	--	--	--	--	--	15			10	--	--	--	--	--	--	--	--	--	
Pressure ratio	--	--	--	--	--	10			8	--	--	--	--	--	--	--	--	--	
Furnace gas exit temperature (°F)	--	--	--	--	--	1800			1200	--	--	--	--	--	--	--	--	--	
Regenerator effectiveness	--	--	--	--	--	Steam for gasifier			--	--	--	--	--	--	--	--	--	--	
He Bottoming Cycle																			
Regenerator effectiveness	--	--	--	--	--	--			--	--	--	--	--	--	--	--	0.85	--	
Total Δp/p (psi)	--	--	--	--	--	--			--	--	--	--	--	--	--	--	0.03	--	
Turbine inlet temperature (°F)	--	--	--	--	--	--			--	--	--	--	--	--	--	--	1180	--	
Turbine pressure ratio	--	--	--	--	--	--			--	--	--	--	--	--	--	--	2.5	--	
Actual Powerplant Output (MWe)	486	243	972	485	488	1148	1203	1230	571	662	485	486	489	479	486	477	509	556	
Thermodynamic Efficiency (percent)	43.8	43.8	43.8	43.8	43.8	43.8	43.8	43.8	43.8	43.8	45.2	46.6	43.6	43.1	43.8	43.8	34.9	44.2	
Powerplant Efficiency (percent)	36.2	36.1	36.2	35.1	33.9	33.6	33.9	33.8	34.2	36.4	37.3	38.5	35.9	35.6	36.1	37.5	28.4	36.7	
Overall Energy Efficiency (percent)	36.2	36.1	36.2	35.1	33.9	33.6	33.9	33.8	34.2	36.4	37.3	38.5	35.9	35.6	36.1	35.5	28.4	36.7	
Coal Consumption (lb/kWh)	0.87	0.88	0.87	1.09	1.46	0.94	1.13	1.47	1.83	0.87	0.85	0.82	0.88	0.89	0.88	0.89	1.11	0.86	
Plant Capital Cost (\$ million)	1180	582	2495	1182	1185	1656	1771	1824	1015	1206	1230	1477	1151	1160	1180	1187	1243	1180	
Plant Capital Cost (\$/kWe)	2429	2396	2567	2437	2426	1443	1471	1482	1777	1821	2534	3036	2353	2422	2429	2489	2444	2110	
Cost of Electricity, Capacity Factor = 0.65																			
Capital (mills/kWh)	76.8	75.8	81.2	77.0	76.7	45.6	46.5	46.9	56.2	57.6	80.1	96.1	74.4	76.6	76.8	78.7	77.3	66.7	
Fuel (mills/kWh)	8.0	8.0	8.0	8.3	8.6	8.6	8.6	8.6	25.9	8.0	7.8	7.5	8.1	8.2	8.0	8.2	10.2	7.9	
Maintenance and operating (mills/kWh)	4.2	5.6	3.8	4.2	4.2	3.7	3.7	3.4	3.1	3.5	4.8	6.7	4.1	4.1	4.2	4.3	4.1	2.8	
Total (mills/kWh)	89.0	89.4	93.0	89.5	89.4	58.0	58.8	58.9	85.2	69.0	92.7	110.1	86.5	88.9	89.0	91.2	91.6	77.5	
Sensitivity																			
Capacity factor = 0.50 (total mills/kWh)	113.3	113.8	118.5	113.9	113.7	72.8	73.9	74.0	103.0	87.4	118.2	141.1	110.1	113.1	113.3	116.1	116.0	98.3	
Capacity factor = 0.80 (total mills/kWh)	73.8	74.1	77.1	74.3	74.7	48.7	49.4	49.5	74.1	57.6	76.9	91.0	71.8	73.7	73.8	75.6	76.3	64.4	
Capital Δ = 20 percent (Δ mills/kWh)	15.4	15.2	16.2	15.4	15.3	9.7	9.3	9.4	11.2	11.5	16.0	19.2	14.9	15.3	15.4	15.7	15.5	13.3	
Fuel Δ = 20 percent (Δ mills/kWh)	1.6	1.6	1.6	1.7	1.7	1.7	1.7	1.7	5.2	1.6	1.6	1.5	1.6	1.6	1.6	1.6	2.0	1.6	
Estimated Time for Construction (years)	6	5	7	6	6	6	6	6	5	6	6	6	6	6	6	6	6	6	
Estimated Date of 1st Commercial Service (year)	1991	1991	1995	1991	1991	1991	1991	1991	1991	1991	1999	1999	1991	1991	1991	1991	1991	1991	

*Base case
 AFB - Atmospheric fluidized bed
 DCT - Dry cooling tower
 Hbtu - High Btu
 Ill. - Illinois
 Lbtu - Low Btu
 Mont - Montana
 N. D. - North Dakota
 PF - Pressurized furnace
 (PF)_R - Pressurized fluidized bed (recuperative)
 WCT - Wet cooling tower

REPRODUCIBILITY OF THE
ORIGINAL PAGE IS POOR

Table 2.10-6
SUMMARY OF RESULTS

Case Number	α_2	α_{3P}	MG (lb/s)	ML (lb/s)	MHD Gen Efficiency	MHD Power (MWe)	Compressor Power (MW)	Liquid Metal Pump Power (MWe)
1, 4-10 15, 16	0.652	0.850	527.1	88285.8	0.80	612	412.9	75.9
2	0.652		263.5	44142.9		306	206.4	37.9
3	0.652		1054.0	176571.5		1224	825.7	151.7
11	0.650		449.1	52023.5		609.2	394.9	74.4
12	0.634		439.8	51118.5		610.9	382.2	76.0
13	0.670		572.3	44237.3	0.80	609.9	403.4	70.0
14	0.652		534	89465.3	0.78	604.5	418.2	76.9
101	0.661		548.7	88320.5	0.80	612.0	428.4	--
17	0.780	0.850	1443.1	122553.7	0.80	612.3	884	64.4

Table 2.10-8 (Page 1 of 2)

CAPITAL COST DISTRIBUTIONS FOR CLOSED-CYCLE LIQUID METAL MHD

	CASE NO.	11	12	13	14	15	16	17	101
MAJOR COMPONENTS									
PRIME CYCLE									
MHD GEN-DIFFUSER	MMS	15.9	18.6	12.4	11.8	11.8	11.8	13.5	11.8
MAGNET	MMS	9.2	8.4	8.4	8.4	8.4	8.4	8.1	8.4
LIQUID METAL PUMP	MMS	18.5	18.4	16.5	28.3	28.0	28.0	35.4	0.
HELIUM RECUPERATOR	MMS	0.	0.	0.	0.	0.	0.	16.0	0.
PRECOOLER	MMS	0.4	0.2	0.7	0.5	0.5	0.5	1.8	0.5
COMPRESSOR	MMS	15.5	15.5	15.8	16.4	16.4	16.3	0.	19.2
BOTTOMING CYCLE									
STEAM BOILER	MMS	11.2	10.5	12.3	12.0	12.6	12.6	0.	14.7
HELIUM TURB-COMP	MMS	0.	0.	0.	0.	0.	0.	20.0	0.
PRIMARY HEAT INPUT AND FUEL SYSTEM									
FURNACE MODULES	MMS	87.5	212.4	50.8	46.7	55.0	55.0	59.4	62.5
HIGH TEMP AIR PREHEATER	MMS	0.	0.	0.	0.	0.	0.	0.	0.
LOW TEMP AIR PREHEATER	MMS	2.0	1.9	2.1	1.9	2.1	2.1	2.8	2.3
PRESSURIZING GAS TURBINE (COMP-GEN-HEAT EXCH)	MMS	0.	0.	0.	0.	0.	0.	0.	0.
GASIFIER (INCLUDING BOOST STEAM TURB-COMP)	MMS	0.	0.	0.	0.	0.	0.	0.	0.
SUB-TOTAL OF MAJOR COMPONENTS	MMS	160.2	285.9	118.9	126.1	134.8	134.7	156.9	119.5
BALANCE OF PLANT									
COOLING TOWER	MMS	4.3	4.3	4.3	4.3	4.3	5.6	6.9	4.3
DC TO AC INVERTERS	MMS	107.0	107.0	108.0	105.5	107.2	107.2	109.6	122.4
ALL OTHER	MMS	280.8	280.8	280.8	280.8	280.8	281.9	283.7	280.8
SITE LABOR	MMS	73.2	73.2	73.2	73.2	73.2	74.2	75.2	73.2
SUB-TOTAL OF BALANCE OF PLANT	MMS	465.3	465.3	466.3	463.8	465.5	468.9	475.4	480.7
CONTINGENCY	MMS	125.1	150.2	117.1	118.0	120.1	120.7	126.5	120.0
ESCALATION COSTS	MMS	214.6	257.8	200.8	202.4	206.0	207.1	217.0	206.0
INTEREST DURING CONSTRUCTION	MMS	264.4	317.6	247.4	249.4	253.8	255.1	267.3	253.7
TOTAL CAPITAL COST	MMS	1229.7	1476.9	1150.6	1159.6	1180.1	1186.6	1243.1	1179.9
MAJOR COMPONENTS COST									
MAJOR COMPONENTS COST	S/KWE	330.1	588.4	243.3	263.3	277.5	282.7	308.5	213.7
BALANCE OF PLANT	S/KWE	959.0	957.6	953.8	968.9	958.5	983.8	934.9	860.0
CONTINGENCY	S/KWE	257.8	309.2	239.4	246.4	247.2	253.3	248.7	214.7
ESCALATION COSTS	S/KWE	442.4	530.5	410.8	422.8	426.1	434.6	426.7	368.5
INTEREST DURING CONSTRUCTION	S/KWE	544.9	653.5	506.0	520.9	522.5	535.3	525.6	453.9
TOTAL CAPITAL COST	S/KWE	2534.2	3039.2	2353.4	2422.4	2429.7	2480.7	2444.3	2110.8

Table 2.10-8 (Page 2 of 2)

CAPITAL COST DISTRIBUTIONS FOR CLOSED-CYCLE LIQUID METAL MHD

	CASE NO.	1	2	3	4	5	6	7	8	9	10
MAJOR COMPONENTS											
PRIME CYCLE											
MHD GEN-DIFFUSER	MMS	11.8	6.3	20.3	11.8	11.8	11.8	11.8	11.8	11.8	11.8
MAGNET	MMS	8.4	4.6	12.1	8.4	8.4	8.4	8.4	8.4	8.4	8.4
LIQUID METAL PUMP	MMS	28.0	16.5	45.9	28.0	28.0	28.0	28.0	28.0	28.0	28.0
HELIUM RECUPERATOR	MMS	0.	0.	0.	0.	0.	0.	0.	0.	0.	0.
PRECOOLER	MMS	0.5	0.2	1.0	0.5	0.5	0.5	0.5	0.5	0.5	0.5
COMPRESSOR	MMS	16.4	10.1	25.4	16.4	16.4	16.4	16.4	16.4	16.4	16.4
BOTTOMING CYCLE											
STEAM BOILER	MMS	12.6	6.3	25.2	12.6	12.6	12.6	12.6	12.6	12.6	12.6
HELIUM TURB-COMP	MMS	0.	0.	0.	0.	0.	0.	0.	0.	0.	0.
PRIMARY HEAT INPUT AND FUEL SYSTEM											
FURNACE MODULES	MMS	55.0	27.5	110.0	54.6	56.3	13.1	13.1	13.3	20.2	57.4
HIGH TEMP AIR PREHEATER	MMS	0.	0.	0.	0.	0.	0.	0.	0.	0.	0.
LOW TEMP AIR PREHEATER	MMS	2.1	1.0	4.1	2.1	2.1	0.	0.	0.	0.	0.
PRESSURIZING GAS TURBINE (COMP-GEN-HEAT EXCH)	MMS	0.	0.	0.	0.	0.	61.8	65.7	67.9	7.8	26.7
GASIFIER (INCLUDING BOOST STEAM TURB-COMP)	MMS	0.	0.	0.	0.	0.	199.1	216.8	241.5	0.	0.
SUB-TOTAL OF MAJOR COMPONENTS	MMS	134.8	72.6	244.1	134.4	136.1	351.7	373.4	400.4	105.7	161.7
BALANCE OF PLANT											
COOLING TOWER	MMS	4.3	2.2	8.6	4.3	4.3	4.3	4.3	4.3	4.3	4.3
DC TO AC INVERTERS	MMS	107.2	53.6	214.5	107.2	107.2	107.2	107.2	107.2	107.2	107.2
ALL OTHER	MMS	280.8	151.4	561.7	281.8	281.8	301.3	339.8	339.8	274.0	274.0
SITE LABOR	MMS	73.2	39.7	146.4	73.6	73.4	78.1	76.1	76.1	66.2	66.2
SUB-TOTAL OF BALANCE OF PLANT	MMS	465.5	246.9	931.2	466.9	466.9	490.9	527.4	527.4	451.7	451.7
CONTINGENCY	MMS	120.1	63.9	235.0	120.3	120.6	168.5	180.2	185.6	111.5	122.7
ESCALATION COSTS	MMS	206.0	91.6	472.3	206.3	206.9	289.1	309.1	318.4	159.9	210.5
INTEREST DURING CONSTRUCTION	MMS	253.8	106.6	612.4	254.2	254.9	356.2	380.8	392.2	186.0	259.3
TOTAL CAPITAL COST	MMS	1180.1	581.6	2494.9	1182.0	1185.4	1656.3	1770.8	1823.9	1014.7	1205.9
MAJOR COMPONENTS COST											
MAJOR COMPONENTS COST	\$/KWF	277.5	299.0	251.1	277.1	278.6	306.4	310.3	325.6	185.1	244.2
BALANCE OF PLANT	\$/KWF	958.5	1017.7	958.2	962.6	955.7	427.7	438.3	428.8	791.1	682.1
CONTINGENCY	\$/KWF	247.2	263.3	241.9	248.0	246.9	146.8	149.7	150.9	195.2	185.3
ESCALATION COSTS	\$/KWE	424.1	377.6	486.0	425.4	423.6	251.9	256.9	258.9	280.0	317.9
INTEREST DURING CONSTRUCTION	\$/KWF	522.5	439.3	630.1	524.1	521.8	310.3	316.5	318.9	325.7	391.6
TOTAL CAPITAL COST	\$/KWF	2429.7	2397.0	2567.3	2437.2	2426.5	1443.3	1471.7	1483.0	1777.1	1821.1

Table 2.10-9

**POWER OUTPUT AND AUXILIARY POWER DEMAND
FOR BASE CASE AND PARAMETRIC VARIATIONS:
CLOSED-CYCLE LIQUID METAL MHD**

	CASE NO.	1	2	3	4	5	6	7	8	9	10
PRIME CYCLE POWER OUTPUT	MW	536.2	268.1	1072.3	536.2	536.2	536.2	536.2	536.2	536.2	536.2
BOTTOMING CYCLE POWER OUTPUT	MW	0.	0.	0.	0.	0.	0.	0.	0.	0.	0.
FURNACE POWER OUTPUT	MW	0.	0.	0.	0.	0.	639.1	695.1	722.0	59.5	160.4
BALANCE OF PLANT AUX. POWER REQ'D.	MW	11.1	5.7	21.8	11.2	10.1	11.1	11.2	11.3	10.9	11.1
FURNACE AUX. POWER REQ'D.	MW	26.0	13.0	51.9	26.6	24.2	0.	0.	0.	0.	9.1
TRANSFORMER LOSSES	MW	2.7	1.3	5.4	2.7	2.7	5.9	6.2	6.3	3.1	3.5
INVERTER LOSSES	MW	10.7	5.4	21.4	10.7	10.7	10.7	10.7	10.7	10.7	10.7
NET STATION OUTPUT	MW	485.7	242.6	971.8	485.0	488.5	1147.6	1203.2	1229.9	571.0	662.2

	CASE NO.	11	12	13	14	15	16	17	101
PRIME CYCLE POWER OUTPUT	MW	534.9	534.9	539.9	527.6	536.2	536.2	547.9	612.0
BOTTOMING CYCLE POWER OUTPUT	MW	0.	0.	0.	0.	0.	0.	20.3	0.
FURNACE POWER OUTPUT	MW	0.	0.	0.	0.	0.	0.	0.	0.
BALANCE OF PLANT AUX. POWER REQ'D.	MW	11.1	11.1	11.1	11.1	11.1	20.2	11.1	11.1
FURNACE AUX. POWER REQ'D.	MW	25.2	24.5	26.4	24.6	26.0	26.0	34.7	26.6
TRANSFORMER LOSSES	MW	2.7	2.7	2.7	2.6	2.7	2.7	2.9	3.1
INVERTER LOSSES	MW	10.7	10.7	10.8	10.6	10.7	10.7	11.0	12.2
NET STATION OUTPUT	MW	485.2	485.9	488.9	478.7	485.7	476.6	508.6	559.0

The second group, Cases 6-10, show generally lower overall efficiencies and lower costs in mills/kWh or \$/kWe than the first group. The lower efficiencies may be attributed largely to losses in either the integrated (Cases 6-8) or nonintegrated (Case 9) gasifiers. The lower costs occur because these systems consist effectively of gas turbine cycles operating in parallel with the MHD-steam cycles. The power generated by the furnace gas turbine is relatively inexpensive. MHD technology, however, is not likely to gain significantly from this effect, for it appears that optimization of this type of system for lowest total cost of electricity would result in little or no power production in the liquid metal MHD generator.

The results for Case 17 have been disappointing because the expected lower overall efficiency (0.28) for this case has not been accompanied by expected lower costs. The larger mass flow of helium in Case 17 relative to Case 1 (about a factor of 2.7) results in a doubling of compressor power and a helium turbocompressor that is somewhat more expensive than the steam driven compressor of Case 1. Similarly, the helium recuperator is somewhat more expensive than the steam generator of Case 1. The reduction in balance of plant costs associated with the change from steam to helium turbomachinery is significant, but not large enough to overcome those increases and other effects of lowered efficiency and lowered output energy per unit mass of helium circulated.

The results for Case 101 show that slightly improved efficiency (0.37) and significantly reduced cost of electricity (78 mills/kWh) result from improved separator efficiency and elimination of the expensive mechanical pumps for circulation of the liquid metal.

The costs of d-c to a-c inversion of the liquid metal MHD generator output deserve special attention. The estimate used here, \$200/kWe, is approximate and not well based on experience with any current conventional technology. This estimate indicates the minimum cost that might result with relatively conventional electronic inversion devices and carefully balanced circuitry in the near future. The true significance of this estimate, however, is that use of that foreseeable technology in this application would not be economically feasible. Thus liquid metal MHD shares with other technologies (e.g., batteries, thermionic energy conversion) producing d-c power at voltages under 1 kV and having output devices with high short circuit current capability a need for new inversion techniques.

The high cost of inversion of low voltage d-c power from systems having high short circuit current capacity arises in large part from the need to protect the inversion apparatus from serious damage in the infrequent cases when part or all of the apparatus fails to commutate current at an a-c current zero. Commutation failures are most often caused by current surges resulting from switching operations or lightning strikes on the

C-2
a-c lines, but they might also be caused by component failures within the inversion equipment. To prevent damage in such events, the design used here segments the inversion equipment into independent modules of about 4 kamp load current, each of which is protected by a d-c circuit breaker of about 40 kamp peak interruption current capability. Because each of these modules controls only a small power flow, near 1.5 MWe, the cost per kilowatt inverted is high.

There have been suggestions that the d-c circuit breakers are an unnecessary expense because the MHD generator would choke and the helium compressor would stall before damaging currents could develop if all or a large part of the inversion equipment failed to commutate. This argument is correct as far as it goes, but it does not apply to commutation failures affecting only a small fraction of the inverters. The many modules used here and the large number of d-c breakers are needed to protect the system against the full range of probable failure modes.

RECOMMENDED CASE

Because even the best closed-cycle liquid metal MHD systems identified thus far appear to have efficiencies no better than those of steam systems and projected total electricity costs no less than 2 to 2.5 times those of steam systems, it seems premature to go to detailed system design at this time. Work on improved systems, however, might start with a configuration like that of Case 101.

REFERENCES

1. Hsu, C., Petrick, M., and Pierson, E.S., "A Study of Factors Pertinent to the Development of an Efficient High Power Two-Phase Liquid-Metal MHD Generator System," Proceedings-Fifth International Conference on Magnetohydrodynamic Electrical Power Generation (Munich, Germany, April 19-23, 1971), Vol. 3, European Nuclear Energy Agency, Paris, France, 1971, pp. 81-84.

2.11 FUEL CELLS-LOW TEMPERATURE

DESCRIPTION OF CYCLE

Figure 2.11-1 is a schematic of the base case for low-temperature fuel cells. The base case was a solid polymer electrolyte (SPE) fuel cell. This case used high-Btu gas as the fuel entering the plant, but this fuel was converted to hydrogen before it entered the fuel cell. In the fuel conversion process, the shift reactor converts carbon monoxide to carbon dioxide (with the addition of water). The methanator converts the small remaining amount of carbon monoxide to methane because even small quantities of carbon monoxide are harmful to the performance of the SPE fuel cell.

The hydrogen fuel (containing 3 percent by volume of methane) enters the anode side of the fuel cell, where most of the hydrogen is consumed. The fuel purge, containing mostly methane (on a mass basis), is returned to the reformer to satisfy part of the thermal energy requirements of the reformer. Except for the use of fuel purge, no integration was assumed between the fuel cell and the fuel conversion system.

Air is used as the oxidizer on the cathode side of the cell. The air passes through a blower and into a humidifier-cooler, where it is preheated and saturated to the correct water vapor pressure for use in the fuel cell. The air passes through the fuel cell, where oxygen is consumed and product water is added; the air is then discharged to the atmosphere.

The coolant stream, which is water in the case of the SPE cells, is cooled by evaporation of a fraction of the water and by warming up the cooler air stream. Thus the humidifier-cooler serves to remove most of the fuel cell waste heat.

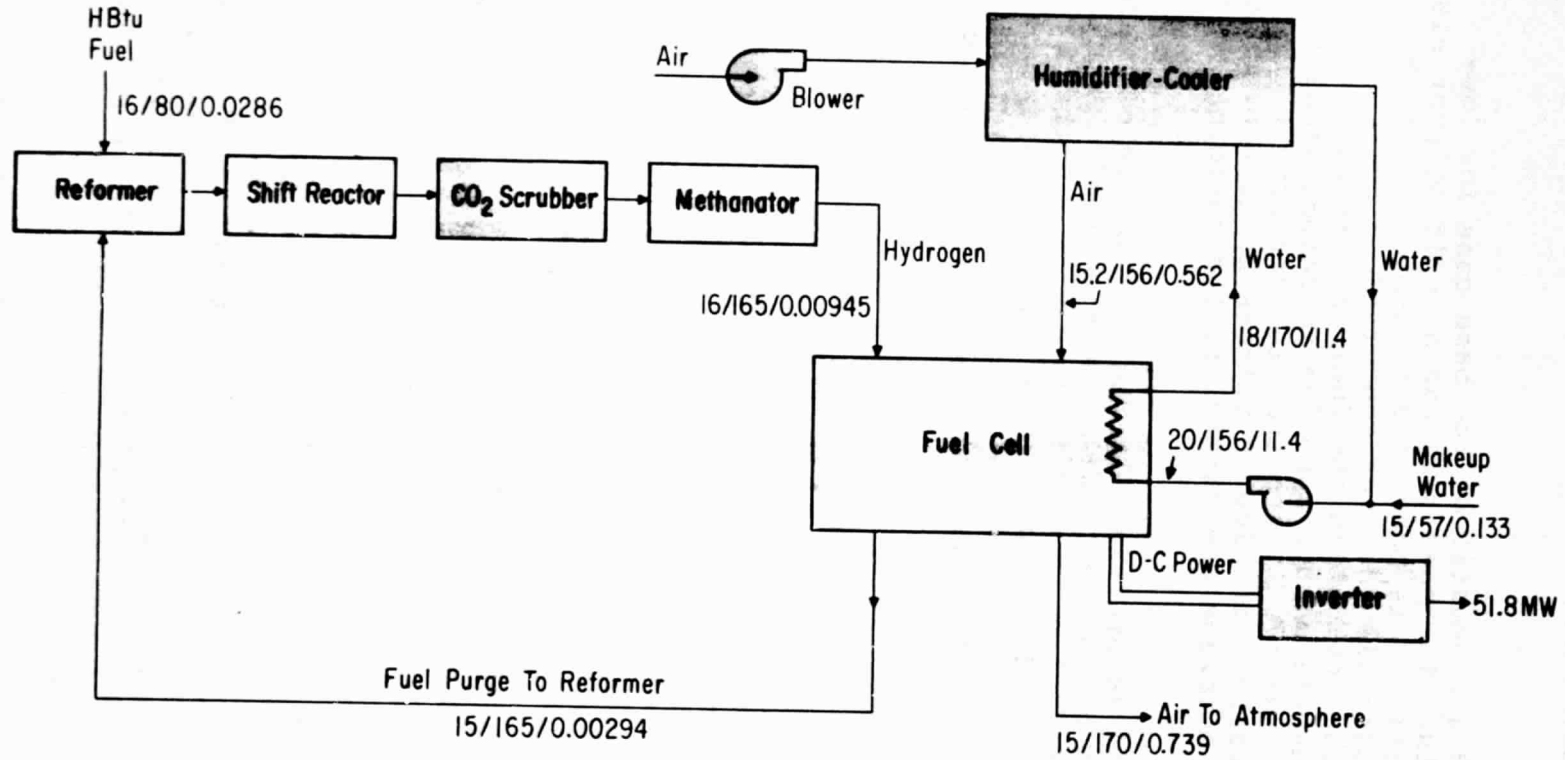
High-Btu gas was selected as the fuel for the base case, as high-Btu gas is a possible future fuel to be pipelined to fuel cell plants.

SPE Fuel Cells

The base case and most of the parametric variations from the base case were with SPE type cells.

Parametric variations included the substitution of hydrogen for the high-Btu fuel. This eliminated the need for the fuel conversion system, as hydrogen was assumed to be piped into the power plant from a remote hydrogen plant. Since the piped-in hydrogen was assumed to be dry, a humidifier had to be added to the incoming fuel stream.

Another variation for the SPE cell was the substitution of oxygen for air as the oxidizer (Case 8). Case 8 is unique in

**Note**

Pressure (Psia) / Temperature (°F) / Flow Rate ($\times 10^6$ Lb/Hr)

Figure 2.11-1. Low-Temperature Fuel Cell (base case)

that the operating pressure and temperature were increased and the mass flow of oxygen was the stoichiometric rate (there was no purge of the oxidizer stream from the cathode compartment to the atmosphere). In that case, the coolant water was cooled by flashing a portion of the cooling water stream, and all of the product water, into low pressure steam (about 59 psia (407 kN/m²) with a saturation temperature of 292 F [418 K]). This steam, which represents most of the fuel cell waste heat, is available for integration with the hydrogen plant, if it could be located at the power plant site. A potential exists for utilizing the waste heat from a low-temperature fuel cell, thereby reducing the cost of electricity. This possibility was not explored in the parametric variations.

The base case current density, temperature, and electrolyte thickness were chosen as typical of the SPE cells. Variations above and below these values were examined in the parametric variations.

Phosphoric Acid Fuel Cells

Four parametric variations were calculated for phosphoric acid cells (Cases 12 through 15). For the phosphoric acid cases, the methanator shown in Figure 2.11-1 was eliminated, as the phosphoric acid cell is less sensitive to carbon monoxide.

The phosphoric acid cell was assumed to operate at 375 F (464 K) and near atmospheric pressure. To achieve good performance levels, the acid concentration in the matrix was held at 98 percent. This requires a vapor pressure of about 6 psia (41 kN/m²) in the reactant streams; consequently, as shown in Figure 2.11-1, a humidifier was used, followed by a heater to provide the correct temperature. The coolant was changed to an organic fluid to permit operation near atmospheric pressure at 375 F (464 K). This permits thin-walled cooling passages within the fuel cell and reduces costs (compared with using water as a coolant).

ANALYTICAL PROCEDURE AND ASSUMPTIONS

Hydrogen Purity

The purity of hydrogen produced from high-Btu gas in an on-site reformer (as in the base case, Figure 2.11-1) was assumed to be 96 percent hydrogen by volume, on a dry basis, and saturated with water at 165 F (374 K). The hydrogen produced in a remote plant and piped into the power plant was assumed to be completely dry, and 98 percent hydrogen, at a temperature of 59 F (288 K).

SPE Fuel Cells

The performance data used for the SPE cell were generated using the best demonstrated cell resistance. This has the effect of optimizing cell performance within the demonstrated capabil-

ity. No allowances for diffusion losses were included; these losses could amount to as much as 0.5 percent of the required fuel flow rates. Air flow rates were established at 2.5 times the stoichiometric oxygen requirement. Above this rate no further performance improvement is noted on test. This value may be found to be in excess of optimum when the blower energy is examined more closely.

The hydrogen purge rates were set to hold the minimum hydrogen mole fraction within the cell at 48 percent on a dry basis. An examination of test data with a wide variation in mole fraction at the inlet shows that the mole fraction of hydrogen may be reduced in the cell by a factor of two without affecting measured cell performance.

The concentration of carbon monoxide in the fuel in the order of 10 ppm was assumed to have no effect on performance of the SPE cells; this has been confirmed by test data.

A primary assumption made for the SPE cell (also for the phosphoric acid cell) is that there will be no improvement in the performance over the best that has been experimentally demonstrated. The only assumption of improvement over present day practice is a decrease in platinum catalyst loading. Present-day minimum catalyst loadings (total of both anode and cathode loadings) are in the range of 1.2 to 1.5 g/ft² (13 to 16 g/m²) while some of the performance data for this study were from SPE cells with 8 g/ft² (86 g/m²). The assumed catalyst loading for this study was taken to be 0.2 g/ft² (2.2 g/m²). This assumption is based on platinum surface areas now available (about 20 m²/g), compared with the maximum surface areas that have been produced experimentally on substrates (about 150 m²/g). The reduction to 0.2 g/ft² is considered feasible, without a degradation in performance or life, assuming that further research and development in this area is carried out. The effect of changes in catalyst loading on costs is covered in the following section "Design and Cost Basis."

The efficiency of the inverter (including transformer losses) was assumed to be 98.2 percent for output power levels less than 60 MW, and 98.5 percent for greater than 60 MW, to account for increased transformer losses in smaller sizes.

Phosphoric Acid Fuel Cells

Data that were available on phosphoric acid fuel cells were from General Electric Company tests that were performed in 1968 and earlier. It is understood that more recent proprietary development by other organizations has improved both the performance and life from these earlier tests. Because precise recent data were not available, performance characteristics of the SPE cell were used, even though that performance is somewhat better than what is understood to be the performance now forecast for phosphoric acid cells.

The analytical procedures used were similar to those used for the SPE except that the reactants were humidified to a partial pressure permitting operation of the cells at 98 percent acid concentration. No provision was made for methanation as it is understood that 0.5 percent CO can be tolerated at 375 F (464 K). No performance penalty was taken for the effect of the CO. Considering the 1968 General Electric data and the very low purge rates used in this study, this is an optimistic assumption. Further development tests may well show that the CO may have to be reduced by methanation or partial oxidation.

Catalyst loading for the phosphoric acid cells was assumed to be the same as for the SPE cells.

DESIGN AND COST BASIS

Hydrogen and Oxygen Costs

For this study, the cost of hydrogen piped in from a remote plant was \$2.53/million Btu (\$2.40/billion J). For this piped-in hydrogen the composition was taken to be:

	<u>Composition, percent</u>	
	<u>By Volume</u>	<u>By Mass</u>
H ₂	98	84.27
CH ₄	1.6	10.95
N ₂	<u>0.4</u>	<u>4.78</u>
	100.0	100.00

The higher heating value of hydrogen is 61,031 Btu/lb (142 MJ/kg), and of methane is 23,890 Btu/lb (55.6 MJ/kg), giving a higher heating value of the mixture of 54,047 Btu/lb (125.7 MJ/kg). This value was used in determining the cost of piped-in hydrogen.

Rather than making a detailed analysis of how the anode purge gas could be used to satisfy part of the heat requirements of the reformer, a cost credit for the purge gas was allowed as follows. The dry-basis composition of this purge gas is

	<u>Composition, percent by mass</u>
H ₂	8.84
CH ₄	57.48
N ₂	33.67

and the higher heating value of this mixture is 19,130 Btu/lb (44.50 MJ/kg). This heating value was multiplied by a cost

credit of \$2.00/million Btu (\$1.90/billion J) and by the dry-basis purge flow rate to calculate the purge flow cost credit.

For Case 8, where oxygen was used as the oxidizer, the oxygen cost used was \$9.00/ton (\$9.92/Mg). This cost was provided by NASA.

Reformer System

The reformer system consisted of the four elements (reformer, shift reactor, CO₂ scrubber, and methanator) shown in Figure 2.11-1. Capital costs for the reformer system were determined from the data in Table 2.11-1, provided by the Foster Wheeler Energy Corporation.

Table 2.11-1

CAPITAL COSTS FOR REFORMER SYSTEM

Capacity		On-Site Investment (\$ millions)	Off-Site Investment* (\$ millions)	Total Investment (\$ millions)
Standard ft ³ /day	lb/hr			
25 x 10 ⁶	5,427	6.25	1.25	7.50
50 x 10 ⁶	10,850	9.98	2.00	11.98
100 x 10 ⁶	21,710	17.29	3.46	20.75

*Includes water treatment and waste disposal equipment, initial charge of catalyst and chemicals, etc.

A reformer system with a capacity of 100 x 10⁶ standard ft³/day (2.8 x 10⁶ standard m³/day) is about the largest plant that can be built; plants larger than that would be built in modules. For purposes of this study, interpolations were made using data from Table 2.11-1.

For the phosphoric acid cell cases, the reformer system costs were reduced by 8 percent to account for the fact that the methanator is not needed to remove carbon monoxide for the phosphoric acid cells.

The efficiency of the reformer system (ratio of Btu/hr of product out to Btu/hr of high-Btu gas in) was calculated to be 0.70.

Fuel Cell

The cost of the fuel cell stack was expressed on the basis of dollars per square foot of active cell electrolyte area. For the two types of low temperature cells studies, the overall fuel cell stack costs were:

- For the SPE cell, \$15.12/ft² (\$163/m²)
- For the phosphoric acid cell, \$14.40/ft² (\$155/m²)

These costs do not include catalyst cost but do include materials, manufacturing, and assembly labor for the following elements of the fuel cell stack:

- Electrolyte
- Anode
- Cathode
- Cooling passages
- Frame
- End plates
- All other parts that make up the fuel cell stack

Table 2.11-2 gives data on electrolyte areas, and sizes and weights of the fuel cell stack.

Table 2.11-2

DATA FOR FUEL CELL STACK

Case Number	Total Active Area of Cell Electrolyte (ft ²)	Cost per Unit Area (\$/ft ²)	Total Cost of Fuel Cell Stack* (\$ millions)	Volume of Fuel Cell Stack (ft ³)	Weight of Fuel Cell Stack (lb)
1	315,600	15.12	4.77	2362	100,000
2	157,800	15.12	2.39	1181	50,000
4	315,600	15.12	4.77	2362	100,000
5	315,600	15.12	4.77	2362	100,000
6	315,600	15.12	4.77	2362	100,000
7	252,200	15.12	3.81	2000	80,000
8	827,200	15.12	12.5	6200	300,000
9	735,200	15.12	11.1	5501	240,000
10	309,100	15.12	4.67	2350	100,000
11	324,000	15.12	4.90	2500	104,000
12	315,600	14.40	4.54	2950	145,000
13	315,600	14.40	4.54	2950	145,000
14	733,500	14.40	10.56	6900	335,000
15	252,200	14.40	3.63	2400	116,000

* Not including catalyst

Catalyst Cost

The cost of platinum catalyst was assumed to be \$5.50/g, a cost near the 1974 market value of platinum. As discussed previously, the platinum loading was taken to be 0.2 g/ft² (2.1 g/m²) of active electrolyte area (this loading is the sum of the anode and cathode loadings).

The total catalyst cost can be calculated by taking the product of the surface area from Table 2.11-2, the cost of \$5.50/g and the loading of 0.2 g/ft².

Inasmuch as the platinum loading of 0.2 g/ft² has not been demonstrated experimentally but rather is a projection from present practice, it is useful to predict the effect of changes in catalyst loadings. Figure 2.11-2 shows the effect of loading on the catalyst capital cost and on cost of electricity. Two cases are shown. Case 1 is for a relatively low power density (net output: 152 W/ft² [1640 W/m²]) and Case 8 is for a high density (243 W/ft² [2620 W/m²]). From the figure it can be determined for Case 1 that an increase in loading from 0.2 to 1.2 g/ft² will increase the cost of electricity by about 1.2 mills/kWh.

Catalyst and Electrolyte Replacement

The useful life of a low-temperature fuel cell is generally limited by degradation of the catalyst or electrolyte. After a period of some years, the electrolyte and catalyst must be replaced. The estimated costs for replacement are given below.

The replacement cost is divided into two elements. First, there is the reprocessing of the platinum. In this process there is a processing charge and a loss of platinum, which is estimated to be 2 percent of the platinum submitted for reprocessing. The estimated costs are:

Processing	= \$0.46/g
Loss (0.02 x \$5.50/gram)	= <u>\$0.11/g</u>
Total reprocessing cost	= \$0.57/g

This reprocessing cost is estimated to be the same for the SPE and the phosphoric acid cell.

The second cost element is the materials and labor charge to disassemble the cells, replace the electrolyte and other parts, and reassemble the cell. The estimated costs for the SPE cells are:

Electrolyte material	= \$2.15/ft ²
Labor	= <u>\$5.00/ft²</u>
Total	= \$7.15/ft ² (\$77.00/m ²)

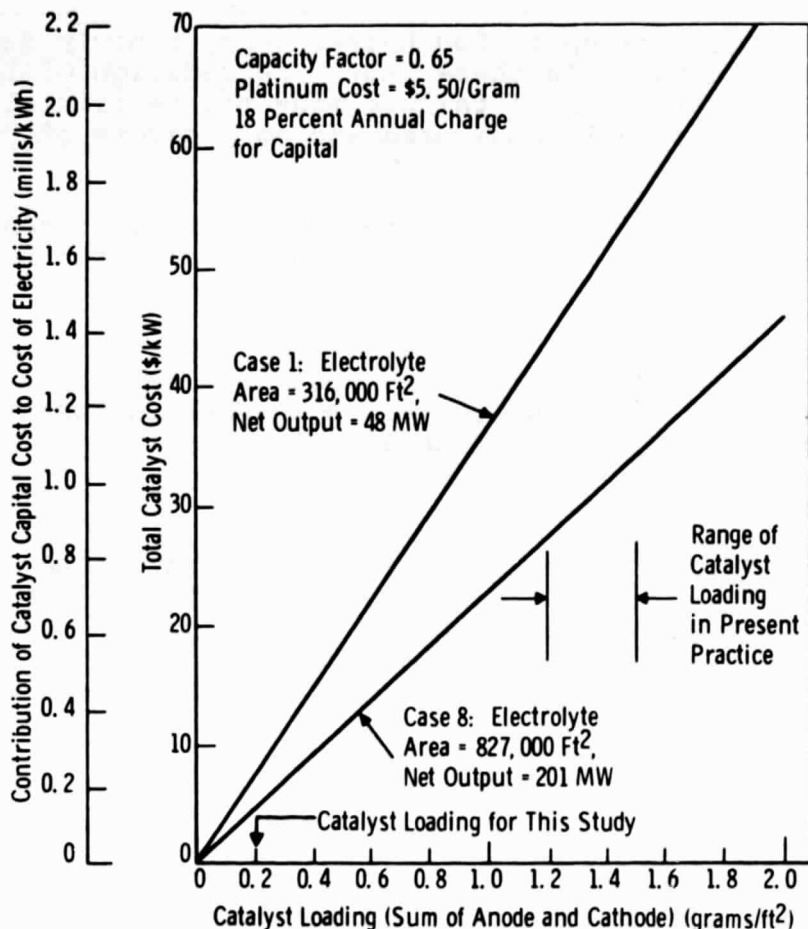


Figure 2.11-2. Effect of Change in Catalyst Loading

It was not possible to estimate accurately the labor and materials costs but a crude analysis led to about the same cost for the phosphoric acid cells as for the SPE cells.

The catalyst and electrolyte replacement costs are therefore estimated to be \$0.57/g of platinum, plus \$7.15/ft² (\$77.00/m²) of active electrolyte area, for both types of cells.

The period of time between replacements is difficult to estimate because of the lack of experimental data over long periods of time under operating conditions. For the phosphoric acid cell the period of 40,000 hours of operation was chosen, as this is believed to be the goal of present development. For the SPE cell a period of 100,000 operating hours was selected because long-term tests have been conducted at 180 F (355 K) for up to 34,000 hours, with no sign of performance deterioration. For those cases operating near 180 F, the extension of time by a factor of three should be realistic. For the higher temperature Case 8 (300 F or 472 K), there was less justification for selecting 100,000 hours. However, there have been life tests at this ele-

vated temperature for up to 800 hours, using a newly developed electrolyte material. In these tests, degradation of the electrolyte polymer (the normal failure mode for earlier electrolyte materials) was carefully monitored and no products of degradation were found.

In order to determine the effect of changes in replacement period, Figure 2.11-3 was prepared. This figure can be used to determine, for example, the cost effect of reducing the 100,000 hour period for Case 8 to some lower number, say to 30,000 hours. At a 30,000-hour replacement period, the contribution of catalyst and electrolyte replacement to the cost of electricity will rise to 1.0 mills/kWh, compared with 0.3 mills/kWh at the assumed period of 100,000 hours for Case 8.

Oxygen Case

In Case 8, oxygen was used as the oxidizer. One reason for this is that the fuel cell plant is assumed to be located near the plant that converts coal to hydrogen, and this hydrogen plant also needs an oxygen supply. Thus, one oxygen plant could supply both the hydrogen plant and the fuel cell power plant.

A unique characteristic of Case 8 is that it is the only one in which steam can be produced conveniently and in large quanti-

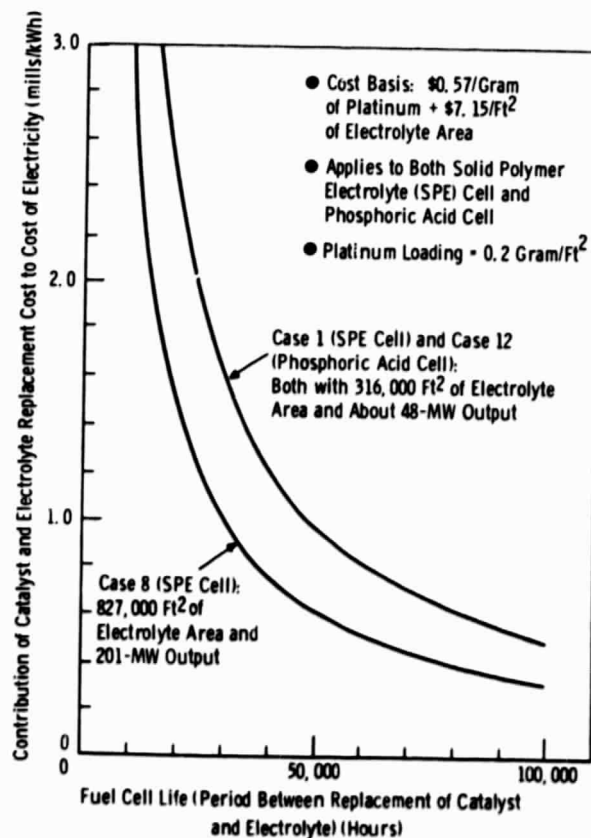


Figure 2.11-3. Effect of Fuel Cell Life

ties. In the SPE cell, there is no vapor pressure suppression (as in the phosphoric acid cells), and product water collects in the cell at the cell operating conditions of 115 psia (793 kN/m²) and 300 F (422 K). This water can be collected and flashed into steam at about 292 F (418 K) and a saturation pressure of about 59 psia (407 kN/m²). In addition, the separate stream of cooling water circulating through the cell can be partially flashed to steam to join the product water steam. The water not flashed to steam is returned to the cooling water loop. Thus, almost all of the waste heat from the fuel cell appears as the latent heat of steam, which could be used in fuel conversion or other processes.

A complete integration of the fuel cell and the hydrogen plant was beyond the scope of this contract. However, some opportunity for integration does exist, and an approximate evaluation indicated that about one-third of the steam produced could be used in the hydrogen plant. To approximate the cost savings of integration, it was assumed that a cost credit could be allowed for one-third of the steam produced by the fuel cell. The credit allowed for each 1000 pounds of steam used was 1.35 multiplied by the fuel cost in dollars per million Btu. This is a typical figure for industrial steam, saturated and at pressures under 100 psi (690 kN/m²). For a fuel cost of \$2.00/million Btu, the credit amounted to \$2.70/1000 lb of steam (\$5.95 per 1000 kg), and this is the figure that was used.

Table 2.11-3 shows the effect of allowing this steam credit. The table also shows a cost breakdown, and illustrates the effect of an increase in catalyst loading from the 0.2 g/ft² (2.2 g/m²) assumed in the study to 1.2 g/ft² (13 g/m²) that is typical of the minimum loading for present commercial units. It can be seen from the table that the steam credit is relatively large, and that integration between the fuel cell and the hydrogen plant is essential from a cost standpoint. If a use could be found for any part of the remaining two-thirds of the steam, an even further cost savings could be realized.

The steam credit was allowed only in Table 2.11-3, and not in the other cost data presented later.

Current Inverters

Costs for the d-c and a-c inverters were based upon present solid state technology that has been developed for high voltage d-c power transmission projects.

Total inversion equipment costs in 1974 dollars, including installation, are as follows for various plant ratings:

<u>Plant Rating in MW</u>	<u>Dollars per kW at High Voltage Terminal</u>
25	69
50	58
200	44

Table 2.11-3

FUEL CELL COST BREAKDOWN

(Case 8, Solid Polymer Electrolyte [SPE] Cell with Oxygen)

	Results for Case 8	Effect of Change in Platinum Loading	Effect of Cost Credit by Using 1/3 Steam Generated by Fuel Cell
Platinum Loading (g/ft ²)	0.2	1.2	0.2
Capital Charge, Catalyst (Mill/kWh)	0.14	0.86	0.14
Capital Charge, Other (Mills/kWh)	7.56	7.56	7.56
Fuel Cost (Hydrogen) (Mills/kWh)*	15.93	15.93	15.93
Oxygen Cost (Mills/kWh)	3.67	3.67	3.67
Maintenance and Operating Charge (Mills/kWh)	4.10	4.10	4.10
Credit for Steam (Mills/kWh)**	0.0	0.0	(3.58)
Totals (Mills/kWh)	31.40	32.12	27.82

*Includes credit of 0.83 mill/kWh for fuel purge flow returned
 **Steam credit of \$2.70/1000 pounds of steam supplied

This equipment cost includes arrestors, valves and control equipment, converter transformer, auxiliary power and motor control center, capacitors, smoothing reactors, etc. Voltages are assumed to be 600 V on the d-c side, and 230 kV on the a-c side (except for the nominal 25 MW system, for which the a-c side is at 69 kV).

RESULTS

Results for the study of low-temperature fuel cells are tabulated in Table 2.11-4, which includes the major cycle input parameters.

Table 2.11-4

**PARAMETRIC VARIATIONS FOR TASK I STUDY
FUEL CELLS—LOW TEMPERATURE**

Parameters	Case 1*	2	4	5	6	7	8	9	10	11	12	13	14	15
<u>Power Output (MWe)</u>	48	24	48	48	48	48	201	48	48	48	47	47	47	47
<u>Coal and Conversion Process</u>	Ill. #6 HBtu	→	Mont HBtu	N. D. HBtu	Ill. #6 H ₂	→	Ill. #6 H ₂ (on site)	Ill. #6 H ₂	→	Ill. #6 HBtu	Ill. #6 H ₂	→		
<u>Oxidizer</u>	Air	→				→	O ₂	Air	→					
<u>Fuel Cell Type</u>	SPE	→							→	Phos	→			
<u>Current Density (A/ft²)</u>	250	→				350	300	100	250	→			100	350
<u>Operating Temperature (maximum) (°F)</u>	170	→					300	170	→		375	→		
<u>Electrolyte Thickness (inches)</u>	0.005	→							0.002	0.010	0.020	→		
<u>Actual Powerplant Output (MWe)</u>	48	24	48	48	48	48	201	48	48	48	47	47	47	47
<u>Thermodynamic Efficiency (percent)</u>	0.	0.	0.	0.	0.	0.	0.	0.	0.	0.	0.	0.	0.	0.
<u>Powerplant Efficiency (percent)</u>	25.2	25.1	25.2	25.2	38.3	34.6	51.1	41.3	39.1	36.7	29.8	37.9	40.8	33.9
<u>Overall Energy Efficiency (percent)</u>	12.7	12.7	12.7	12.7	23.3	21.1	31.1	25.2	23.9	22.4	15.0	23.1	24.9	20.7
<u>Coal Consumption (lb/kWh)</u>	2.50	2.50	3.01	3.91	1.36	1.50	1.02	1.26	1.33	1.41	2.10	1.37	1.27	1.53
<u>Plant Capital Cost (\$ million)</u>	30	16	30	30	16	14	49	26	16	16	27	15	25	14
<u>Plant Capital Cost (\$/kWe)</u>	634	687	634	634	325	295	742	542	329	335	570	317	527	287
<u>Cost of Electricity, Capacity Factor = 0.65</u>														
<u>Capital (mills/kWh)</u>	20.1	21.7	20.1	20.1	10.3	9.3	7.7	17.1	10.4	10.6	18.0	10.0	16.7	9.1
<u>Fuel (mills/kWh)</u>	32.9	33.0	32.9	32.9	21.2	23.4	19.6	19.6	20.7	22.1	28.6	21.4	19.9	23.9
<u>Maintenance and operating (mills/kWh)</u>	4.7	5.1	4.7	4.7	4.7	4.7	4.1	5.4	4.7	4.8	5.5	5.5	7.1	5.3
<u>Total (mills/kWh)</u>	57.7	59.9	57.7	57.7	36.2	37.4	31.3	42.1	35.9	37.5	52.1	36.9	43.7	38.3
<u>Sensitivity</u>														
<u>Capacity factor = 0.50 (total mills/kWh)</u>	65.0	67.8	65.0	65.0	40.6	41.5	34.8	48.6	40.3	41.9	58.8	41.2	50.0	42.3
<u>Capacity factor = 0.80 (total mills/kWh)</u>	53.2	54.9	53.2	53.2	33.5	34.9	27.2	38.1	33.1	34.7	48.0	34.2	39.7	35.8
<u>Capital Δ = 20 percent (Δmills/kWh)</u>	4.0	4.3	4.0	4.0	2.1	1.9	1.5	3.4	2.1	2.1	3.6	2.0	3.3	1.8
<u>Fuel Δ = 20 percent (Δmills/kWh)</u>	6.6	6.6	6.6	6.6	4.2	4.7	3.2	3.9	4.1	4.4	5.7	4.3	4.0	4.8
<u>Estimated Time for Construction (years)</u>	2	2	2	2	2	2	3	2	2	2	2	2	2	2
<u>Estimated Date of 1st Commercial Service (year)</u>	1986	1986	1986	1986	1986	1986	1992	1985	1985	1985	1982	1982	1982	1982

*Base case HBtu = High Btu N. D. = North Dakota
 Ill. = Illinois Phos = Phosphoric acid
 Mont = Montana SPE = Solid polymer electrolyte

Capital cost distributions are given in Table 2.11-5.

A summary giving major cycle characteristics for the low temperature fuel cell base case is given in Table 2.11-6.

Auxiliary losses and power outputs are shown in Table 2.11-7.

DISCUSSION OF RESULTS

A number of observations can be made from the results shown in Table 2.11-4.

When high-Btu gas is used as the fuel, the overall energy efficiency is extremely low (12.7 percent for the base case), because of the double penalty of converting coal to high-Btu gas, followed by converting high-Btu gas to hydrogen. Further, the cost of fuel is very high (32.9 mills/kWh for the base case) because of the high cost of high-Btu gas.

When hydrogen is used as the fuel, the overall energy efficiency rises, and the fuel cost drops (see Cases 6 and 13, for example).

The highest overall energy efficiency (31.1 percent) and the lowest cost of fuel (19.6 mills/kWh) were obtained with hydrogen and oxygen (Case 8). (Note that the energy efficiency does not include the energy required to produce the oxygen, but the fuel cost does include the cost of oxygen; this is consistent with the approach taken in the open-cycle MHD system.) If the steam produced in the hydrogen-oxygen cell can be utilized in the hydrogen plant, the cost of electricity could be reduced to 27.8 mills/kWh, as shown in Table 2.11-3.

The fuel cell costs of electricity, for those cases where hydrogen was the fuel, were characterized by very low capital costs and very high fuel costs. This would normally place the fuel cell in a peaking plant category from an economic standpoint. However, it should be pointed out that these economics are a consequence of assuming the hydrogen to be purchased "over the fence" at a certain cost per Btu. Therefore, the capital charges associated with the equipment that converts coal to hydrogen are included in the fuel costs, and consequently appear to be a variable cost. If the capital cost of the hydrogen plant were included with the capital cost of the power plant, and if the fuel cost were only the cost of coal to the hydrogen plant, then the cost of electricity would not change, but the cost distribution between capital and fuel would be more characteristic of a base load plant.

There was very little cost difference between the SPE and the phosphoric acid cells; for example, the costs of electricity of comparable Cases 6 and 13 were 36.2 and 36.9 mills/kWh, respectively.

Table 2.11-5 (Page 1 of 2)

CAPITAL COST DISTRIBUTIONS FOR LOW-TEMPERATURE FUEL CELL

	CASE NO.	1	2	4	5	6	7	8	9	10	11
MAJOR COMPONENTS											
PRIME CYCLE											
FUEL CELL STACK	MMS	4.8	2.4	4.8	4.8	4.8	3.8	12.5	11.1	4.8	4.9
HUMIDIFIER-COOLFR	MMS	0.1	0.0	0.1	0.1	0.1	0.1	0.	0.0	0.0	0.1
CATALYST	MMS	0.3	0.2	0.3	0.3	0.3	0.3	0.9	0.8	0.3	0.4
(LOADING GRAM/SQ.FT.)		(0.2)	(0.2)	(0.2)	(0.2)	(0.2)	(0.2)	(0.2)	(0.2)	(0.2)	(0.2)
FURNACE AND FUEL PROCESSING											
FUEL PROCESSING	MMS	10.5	5.8	10.5	10.5	0.	0.	0.	0.	0.	0.
FUEL PREHEATER-HUMIDIFIER		0.	0.	0.	0.	0.3	0.3	0.	0.3	0.3	0.3
SUB-TOTAL OF MAJOR COMPONENTS	MMS	15.7	8.4	15.7	15.7	5.5	4.4	13.4	12.2	5.5	5.6
BALANCE OF PLANT											
COOLING TOWER	MMS	0.	0.	0.	0.	0.	0.	0.	0.	0.	0.
DC TO AC INVERTERS	MMS	3.0	1.8	3.0	3.0	3.0	3.0	9.0	3.0	3.0	3.0
ALL OTHER	MMS	1.9	1.0	1.9	1.9	1.9	1.9	7.3	2.3	2.0	2.0
SITE LABOR	MMS	0.4	0.2	0.4	0.4	0.4	0.4	1.4	0.5	0.4	0.4
SUB-TOTAL OF BALANCE OF PLANT	MMS	5.3	2.9	5.3	5.3	5.3	5.3	17.7	5.8	5.5	5.5
CONTINGENCY	MMS	4.2	2.3	4.2	4.2	2.2	1.9	6.2	3.6	2.2	2.2
ESCALATION COSTS	MMS	2.8	1.5	2.8	2.8	1.4	1.3	5.7	2.4	1.5	1.5
INTEREST DURING CONSTRUCTION	MMS	2.3	1.3	2.3	2.3	1.2	1.1	5.6	2.0	1.2	1.2
TOTAL CAPITAL COST	MMS	30.3	16.4	30.3	30.3	15.6	14.1	48.6	26.0	15.8	16.0
MAJOR COMPONENTS COST	\$/KWF	328.6	352.4	328.6	328.6	114.8	93.4	66.9	254.6	114.0	117.8
BALANCE OF PLANT	\$/KWF	110.9	123.7	110.9	110.9	110.9	111.4	88.5	121.0	114.0	114.7
CONTINGENCY	\$/KWF	87.9	95.2	87.9	87.9	45.1	40.9	31.1	75.1	45.6	46.5
ESCALATION COSTS	\$/KWF	58.9	63.9	58.9	58.9	30.3	27.5	28.2	50.4	30.6	31.2
INTEREST DURING CONSTRUCTION	\$/KWF	48.5	52.5	48.5	48.5	24.9	22.6	27.9	41.4	25.1	25.6
TOTAL CAPITAL COST	\$/KWF	634.8	687.7	634.8	634.8	325.9	295.7	242.5	542.5	329.3	335.7

REPRODUCIBILITY OF THE
ORIGINAL PAGE IS POOR

Table 2.11-5 (Page 2 of 2)

CAPITAL COST DISTRIBUTIONS FOR LOW-TEMPERATURE FUEL CELL

	CASE NO.	12	13	14	15
MAJOR COMPONENTS					
PRIME CYCLE					
FUEL CELL STACK	MMS	4.5	4.5	10.6	3.6
HUMIDIFIER-COOLER	MMS	0.1	0.1	0.0	0.1
CATALYST	MMS	0.3	0.3	0.8	0.3
(LOADING GRAM/SQ.FT.)		(0.2)	(0.2)	(0.2)	(0.2)
FURNACE AND FUEL PROCESSING					
FUEL PROCESSING	MMS	8.3	0.	0.	0.
FUEL PRE-HEATER-HUMIDIFIER		0.	0.	0.	0.
SUB-TOTAL OF MAJOR COMPONENTS	MMS	13.2	4.9	11.5	3.9
BALANCE OF PLANT					
COOLING TOWER	MMS	0.	0.	0.	0.
DC TO AC INVERTERS	MMS	3.0	3.0	3.0	3.0
ALL OTHER	MMS	2.0	2.0	2.3	2.0
SITE LABOR	MMS	0.5	0.5	0.5	0.5
SUB-TOTAL OF BALANCE OF PLANT	MMS	5.5	5.5	5.9	5.5
CONTINGENCY	MMS	3.7	2.1	3.5	1.9
ESCALATION COSTS	MMS	2.5	1.4	2.3	1.3
INTEREST DURING CONSTRUCTION	MMS	2.1	1.1	1.9	1.0
TOTAL CAPITAL COST	MMS	27.0	15.0	25.0	13.6
MAJOR COMPONENTS COST					
	\$/KW	278.7	103.5	241.7	83.1
BALANCE OF PLANT					
	\$/KW	116.2	116.2	123.4	116.2
CONTINGENCY					
	\$/KW	79.0	44.0	73.0	39.9
ESCALATION COSTS					
	\$/KW	53.0	29.5	49.0	26.7
INTEREST DURING CONSTRUCTION					
	\$/KW	43.5	24.2	40.3	22.0
TOTAL CAPITAL COST	\$/KW	570.4	317.4	527.4	287.9

Table 2.11-6

SUMMARY SHEET
FUEL CELLS—LOW-TEMPERATURE BASE CASE

<u>CYCLE PARAMETER</u>		<u>PERFORMANCE AND COST</u>	
<u>Net Power Output (MWe)</u>	48	Thermodynamic efficiency (percent)	
<u>Coal Type</u>	Illinois No. 6	Powerplant efficiency (percent)	25.2
<u>Prime Cycle</u>		Overall energy efficiency (percent)	12.7
Oxidizer	Air	Plant capital cost (\$ x 10 ⁶)	30
Fuel cell type	Solid polymer electrolyte	Plant capital cost (\$/kWe)	634
Current density (A/ft ²)	250	Cost of electricity (mills/kWh)	57.7
Operating temperature (°F)	170		
Electrolyte thickness (inch)	0.005		

<u>NATURAL RESOURCES</u>	
<u>Coal (lb/kWh)</u>	2.50
<u>Water (gal/kWh)</u>	
Total	
Cooling (H ₂ plant cooling tower)	0.05
Processing (H ₂ plant)	0.31
Fuel cell cooling and air humidification	0.33
<u>Land (acres/100 MWe)</u>	8.3

ENVIRONMENTAL INTRUSION

	<u>Lb/10⁶-Btu Input</u>	<u>Lb/kWh Output</u>
SO ₂	0	0
NO _x (from H ₂ process)	0.1	5.7 x 10 ⁻⁴
HC	0	0
CO	0	0
Particulates	0	0
		<u>Btu/kWh</u>
Heat to water		0
Heat, total rejected		10,128
Wastes		None

MAJOR COMPONENT CHARACTERISTICS

<u>Major Component</u>	<u>Unit or Module</u>			<u>Units Required</u>	<u>Total Cost (\$ x 10⁶)</u>	<u>\$/kW Output</u>
	<u>Size (ft) (W x L (or D) x H)</u>	<u>Weight (lb) (x 10⁶)</u>	<u>Cost (\$ x 10⁶)</u>			
Fuel cell stack	10 x 40 x 6	0.10	4.8	1	4.8	100
Humidifier-cooler	10 x 40 x 10	0.02	0.1	1	0.1	2.1

Table 2.11-7

POWER OUTPUT AND AUXILIARY POWER DEMAND
FOR BASE CASE AND PARAMETRIC VARIATIONS:
FUEL CELLS—LOW TEMPERATURE

	CASE NO.	1	2	4	5	6	7	8	9	10	11
PRIME CYCLE POWER OUTPUT	MW	52.1	26.0	52.1	52.1	52.1	52.1	708.3	52.1	52.1	52.1
BOTTOMING CYCLE POWER OUTPUT	MW	0.	0.	0.	0.	0.	0.	0.	0.	0.	0.
FURNACE POWER OUTPUT	MW	0.	0.	0.	0.	0.	0.	0.	0.	0.	0.
BALANCE OF PLANT AUX. POWER REQ'D.	MW	3.4	1.7	3.4	3.4	3.4	3.6	4.6	3.2	3.3	3.6
FURNACE AUX. POWER REQ'D.	MW	0.	0.	0.	0.	0.	0.	0.	0.	0.	0.
TRANSFORMER LOSSES	MW	0.4	0.2	0.4	0.4	0.4	0.4	1.0	0.4	0.4	0.4
INVERTER LOSSES	MW	0.5	0.3	0.5	0.5	0.5	0.5	2.1	0.5	0.5	0.5
NET STATION OUTPUT	MW	47.8	23.8	47.8	47.8	47.8	47.6	700.5	48.0	47.9	47.6

	CASE NO.	12	13	14	15
PRIME CYCLE POWER OUTPUT	MW	52.1	52.1	52.1	52.1
BOTTOMING CYCLE POWER OUTPUT	MW	0.	0.	0.	0.
FURNACE POWER OUTPUT	MW	0.	0.	0.	0.
BALANCE OF PLANT AUX. POWER REQ'D.	MW	3.8	3.8	3.8	3.8
FURNACE AUX. POWER REQ'D.	MW	0.	0.	0.	0.
TRANSFORMER LOSSES	MW	0.4	0.4	0.4	0.4
INVERTER LOSSES	MW	0.5	0.5	0.5	0.5
NET STATION OUTPUT	MW	47.4	47.4	47.4	47.4

REPRODUCIBILITY OF THE
ORIGINAL PAGE IS POOR

RECOMMENDED CASE

Because of a sizable advantage in cost of electricity, the hydrogen-oxygen case with an SPE cell (Case 8) is recommended for further study.

2.12 FUEL CELLS-HIGH TEMPERATURE

DESCRIPTION OF CYCLE

While most of the fuel cell effort was devoted to low-temperature cells, a brief investigation was made of high-temperature, solid electrolyte fuel cells.

Figure 2.12-1 shows a schematic of the high-temperature fuel cell base case. In this system, the low-Btu gas fuel is preheated before it enters the cell. After passing through the anode side of the cell, the gas passes on to a combustor that provides hot gas to the boiler and reheater for the bottoming cycle.

The cathode side of the cell is supplied with air from a blower and air preheater. Hot air leaving the fuel cell is cooled in the fuel preheater and then joins the anode stream in the combustor.

The bottoming cycle uses conventional temperatures of 1000 F (811 K) for superheating and reheating, and a pressure at the turbine inlet of 3515 psia (24.2 MN/m²).

Three variations of this base case were studied (the parametric variations are listed later in the "Results" section). The first variation was a change in the type of coal supplied to the gasifier. The next two variations were made to determine the effect of changes in the current density and the electrolyte thickness.

ANALYTICAL PROCEDURE AND ASSUMPTIONS

The solid electrolyte for the high-temperature fuel cell was zirconia (ZrO₂). Cell operating temperature was 1832 F (1273 K). In order to maintain a temperature near this level throughout the cell, a large amount of air was circulated through the air side of the cell (see Figure 2.12-1). At this temperature, no catalyst is needed.

The low-Btu gasifier providing fuel to the cell is basically the same as the other gasifiers in this study. One difference is that the gasifier was free standing; that is, there was no integration between the fuel cell system, or its bottoming cycle, and the gasifier.

The high-temperature fuel cell requires low-pressure gas. Because the gasifier operates at elevated pressures, the low-Btu gas was expanded through a turbine at the end of the gasification process. This expansion cooled the gas, and moisture had to be removed before the gas left the gasifier.

As shown in Figure 2.12-1, the fuel was preheated by high-temperature air leaving the fuel cell. Because of the high tem-

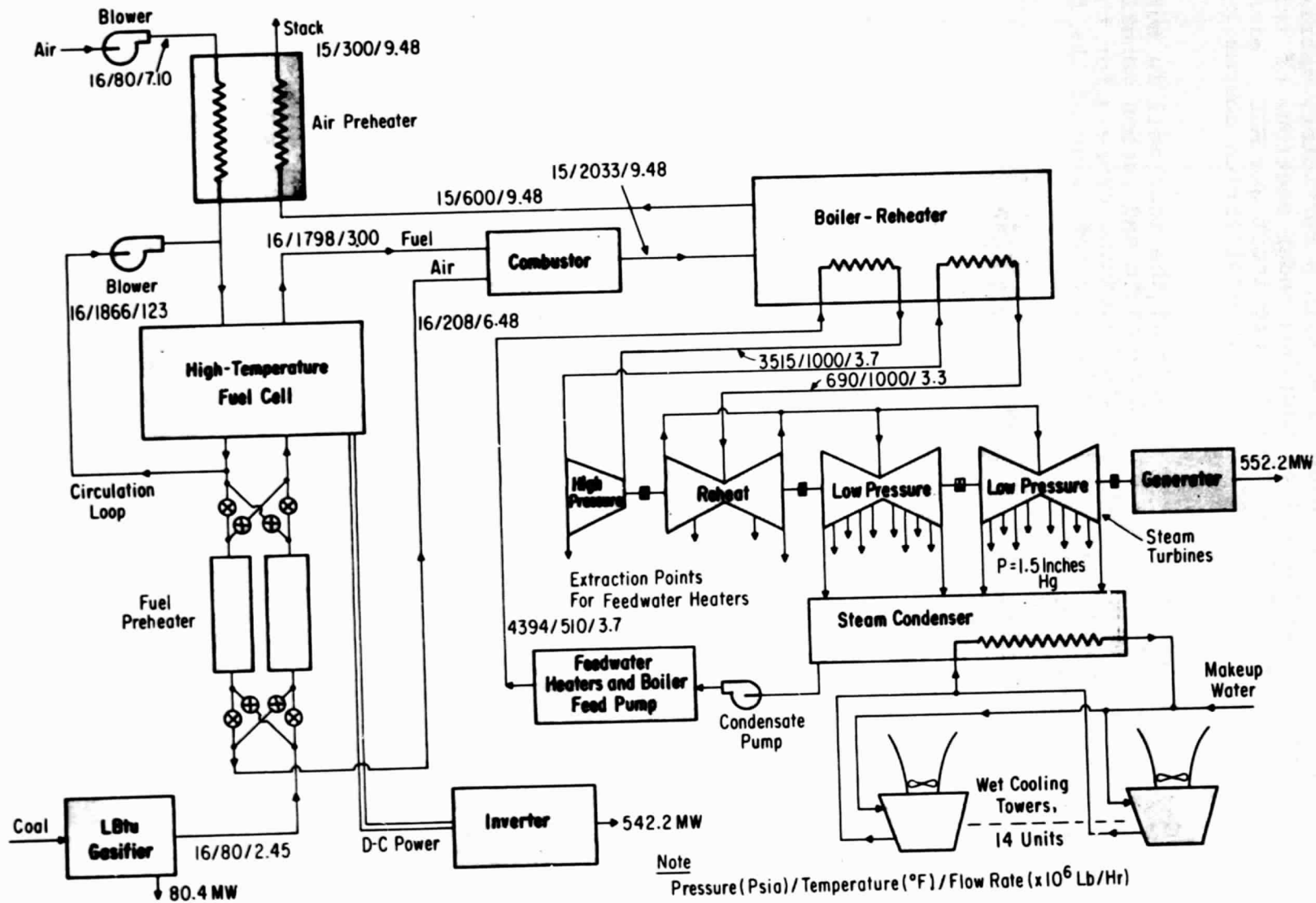


Figure 2.12-1. High-Temperature Fuel Cell Base Case

peratures, a heat storage regenerator with a refractory matrix was used, similar to the units described under sections of this report on open-cycle MHD and closed-cycle inert gas MHD. Within the preheater, the fuel changed to a new equilibrium composition at the high-temperature discharge.

The stream leaving the anode side of the fuel cell is not completely depleted of fuel; enough hydrogen and carbon monoxide remain to burn in a combustor for the bottoming cycle. For the cases studied, the constituents leaving the fuel side of the fuel cell and entering the combustor were:

<u>Constituent</u>	<u>Percent by mass</u>
H ₂	0.9
N ₂	39.1
H ₂ O	16.2
CO	15.2
CO ₂	<u>28.6</u>
	100.0

Performance data for the high-temperature fuel cell were obtained primarily from General Electric tests. Reference 1 describes the work on which the test data were based and gives a number of references to literature used in this study.

DESIGN AND COST BASIS

The following materials were assumed for the cost estimates:

Porous tube support	ZrO ₂
Fuel electrode	Ni and zirconia
Interconnections	Cobalt chromite
Electrolyte	Calcium-stabilized zirconia
Air electrode	Indium oxide doped with tin

Cost data were taken from Reference 2. This document gave a "most probable" cost of \$13.42/ft², which was estimated to escalate to \$15.83/ft² (\$170/m²) by mid-1974.

The performance estimates of Reference 2 showed much higher performance than was estimated from the General Electric tests (Reference 1). For example, the power density used in Cases 1 and 2 was 117 W/ft² (1260 W/m²) (based on the General Electric data), while the Reference 1 data projected a power density of 688 W/ft² (7410 W/m²). If this higher density could be achieved, a sizable reduction in fuel cell capital cost could be realized.

RESULTS

Results for the study of high-temperature fuel cells are tabulated in Table 2.12-1, which includes the major cycle input parameters.

A breakdown of capital costs is given in Table 2.12-2.

A summary giving major cycle characteristics for the high-temperature fuel cell base case is given in Table 2.12-3.

Auxiliary losses and power outputs are shown in Table 2.12-4.

DISCUSSION OF RESULTS

Several observations can be made from the results shown in Table 2.12-1.

The overall energy efficiency was moderate (a maximum of 34.3 percent). Increasing the current density to 700 amp/ft² (7500 W/m²) caused a large drop in efficiency.

The principal drawback appeared to be the very high capital cost (\$974/kW for the base case). Largely because of this high cost, the cost of electricity was also relatively high (45 mills/kWh for the base case).

The largest contributions to the capital cost were made by the gasifier (\$202 million for the base case) and the balance of plant (\$226 million). The balance of plant was costly principally because of the large amount of high-temperature piping.

RECOMMENDED CASE

The high-temperature fuel cell case that is recommended for further study is Case 1. A variation on that case that should be considered is the integration of the high-temperature fuel cell system with the low-Btu gasifier.

REFERENCES

1. White, D.W., Progress in High-Temperature, Zirconia-Electrolyte Cell Technology at General Electric, Report 68-C-254, Corporate Research and Development, General Electric Company, Schenectady, New York, July 1968.
2. Project Fuel Cell Final Report, R&D Report 47, Office of Coal Research, Department of the Interior, Contract 14-01-0001-303, Westinghouse Electric Corporation, Pittsburgh, Pa., 1970.

Table 2.12-1

PARAMETRIC VARIATIONS FOR TASK I STUDY
(Fuel Cells-High Temperature)**

Parameters	Case 1*	2	3	4
<u>Power Output (MWe)</u>	1112	1111	632	824
<u>Coal and Conversion Process</u>	Ill. #6 LBtu	Mont LBtu	Ill. #6 LBtu	→
<u>Oxidizer</u>	Air			→
<u>Current Density (A/ft²)</u>	200	→	700	→
<u>Electrolyte Thickness (inches)</u>	0.020	→	→	0.005
<u>Steam Bottoming Cycle</u>				
Turbine inlet temperature (°F)	1000	→	→	→
Turbine inlet pressure (psig)	3500	→	→	→
Reheat temperature (°F)	1000	→	→	→
Maximum feedwater temperature (°F)	510	→	→	→
Heat rejection (in. Hg)	WCT	→	→	→
	1.5			
<u>Actual Powerplant Output (MWe)</u>	1112	1111	632	824
<u>Thermodynamic Efficiency (percent)</u>	0.	0.	0.	0.
<u>Powerplant Efficiency (percent)</u>	31.5	34.3	24.5	27.9
<u>Overall Energy Efficiency (percent)</u>	31.5	34.3	24.5	27.9
<u>Coal Consumption (lb/kWh)</u>	1.00	1.11	1.29	1.14
<u>Plant Capital Cost (\$ million)</u>	1083	1087	575	710
<u>Plant Capital Cost (\$/kWe)</u>	974	978	910	861
<u>Cost of Electricity, Capacity Factor = 0.65</u>				
Capital (mills/kWh)	30.8	30.9	28.8	27.2
Fuel (mills/kWh)	9.2	8.5	11.8	10.4
Maintenance and operating (mills/kWh)	5.7	5.0	4.8	4.7
Total (mills/kWh)	45.7	44.4	45.4	42.3
<u>Sensitivity</u>				
Capacity factor = 0.50 (total mills/kWh)	44.7	55.2	55.5	51.9
Capacity factor = 0.80 (total mills/kWh)	38.3	37.7	39.1	36.4
Capital Δ = 20 percent (Δ mills/kWh)	6.2	6.2	5.8	5.4
Fuel Δ = 20 percent (Δ mills/kWh)	0.8	1.7	2.4	2.1
<u>Estimated Time for Construction (years)</u>	6	6	5	5
<u>Estimated Date of 1st Commercial Service (year)</u>	1998	1998	2005	2005

*Base case
**Zirconia, 1832 F operating temperature

Ill. = Illinois
LBtu = Low Btu
Mont = Montana
WCT = Wet cooling tower

Table 2.12-2

CAPITAL COST DISTRIBUTIONS FOR HIGH-TEMPERATURE FUEL CELLS

	CASE NO.	1	2	3	4
MAJOR COMPONENTS					
PRIME CYCLE					
FUEL CELL STACK	MMS	74.1	74.1	10.2	14.6
AIR PREHEATER	MMS	2.2	2.2	1.6	1.9
BOTTOMING CYCLE					
STEAM BOILER	MMS	16.5	16.5	10.9	13.0
STEAM TURB-GEN	MMS	20.3	20.3	20.3	20.3
FUEL PROCESSING					
GASIFIER (INCLUDING BOOST STEAM TURB-COMP)	MMS	202.0	204.0	157.0	175.0
FUEL PREHEATER	MMS	9.6	9.6	6.9	8.0
SUB-TOTAL OF MAJOR COMPONENTS	MMS	324.7	326.7	206.9	232.8
BALANCE OF PLANT					
COOLING TOWER	MMS	3.5	3.5	3.5	3.5
DC TO AC INVERTERS	MMS	19.6	19.6	4.2	11.5
ALL OTHER	MMS	154.3	154.3	75.6	107.1
SITE LABOR	MMS	48.9	48.9	25.9	35.2
SUB-TOTAL OF BALANCE OF PLANT	MMS	226.3	226.3	109.2	157.3
CONTINGENCY	MMS	110.2	110.6	63.2	78.0
ESCALATION COSTS	MMS	189.1	189.8	90.6	111.9
INTEREST DURING CONSTRUCTION	MMS	232.9	233.8	105.5	130.2
TOTAL CAPITAL COST	MMS	1093.2	1087.1	575.4	710.2
MAJOR COMPONENTS COST					
	\$/kWh	292.1	294.0	327.4	282.4
BALANCE OF PLANT					
	\$/kWh	203.5	203.6	172.8	190.9
CONTINGENCY					
	\$/kWh	99.1	99.5	100.0	94.7
ESCALATION COSTS					
	\$/kWh	170.1	170.7	143.4	135.7
INTEREST DURING CONSTRUCTION					
	\$/kWh	209.5	210.3	166.9	157.9
TOTAL CAPITAL COST	\$/kWh	974.5	978.1	910.5	861.6

REPRODUCIBILITY OF THE
ORIGINAL PAGE IS POOR

Table 2.12-3

SUMMARY SHEET
FUEL CELLS-HIGH-TEMPERATURE BASE CASE

<u>CYCLE PARAMETER</u>		<u>PERFORMANCE AND COST</u>	
<u>Net Power Output (MWe)</u>	1112	<u>Thermodynamic efficiency (percent)</u>	--
<u>Coal Type</u>	Illinois No. 6	<u>Powerplant efficiency (percent)</u>	--
<u>Prime Cycle</u>		<u>Overall energy efficiency (percent)</u>	31.5
Oxidizer	Air	<u>Plant capital cost (\$ x 10⁶)</u>	1083
Current density (A/ft ²)	200	<u>Plant capital cost (\$/kWe)</u>	974
Electrolyte thickness	0.020	<u>Cost of electricity (mills/kWh)</u>	45.0
<u>Bottoming Cycle (Steam)</u>		<u>NATURAL RESOURCES</u>	
Turbine inlet temperature (°F)	1000	<u>Coal (lb/kWh)</u>	1.00
Turbine inlet pressure (psig)	3500	<u>Water (gal/kWh)</u>	
Reheat temperature (°F)	1000	Total	0.277
Heat rejection	Wet cooling tower	Cooling	0.187
		Processing	0.090
		Makeup	0
		NO _x suppression	0
		Stack gas cleanup	0
		<u>Land (acres/100 MWe)</u>	0.36
		<u>ENVIRONMENTAL INTRUSION</u>	
		<u>SO₂</u>	0.2
		<u>NO_x</u>	0
		<u>HC</u>	0
		<u>CO</u>	0
		<u>Particulates</u>	--
		<u>Heat to water</u>	2080
		<u>Heat, total rejected</u>	7420
		<u>Wastes</u>	
		Ash	0.113
		Sulfur	0.033

<u>Major Component</u>	<u>MAJOR COMPONENT CHARACTERISTICS</u>				<u>Units Required</u>	<u>Total Cost (\$ x 10⁶)</u>	<u>\$/kW Output</u>
	<u>Unit or Module</u>	<u>Size (ft) (W x L for D) x H)</u>	<u>Weight (lb) (x 10⁶)</u>	<u>Cost (\$ x 10⁶)</u>			
<u>Prime Cycle</u>							
Fuel cell stack	8 x 293 x 30	1.58	7.41	10	74.1		
Air preheater		2.42	2.2	1	2.2		
Fuel preheater			9.6	1	9.6		
<u>Bottoming Cycle</u>							
Furnace-boiler	80 x 77 x 82	6.43	16.5	1	16.5		
Steam turbine-generator	30 x 174 x 25	4.60	20.3	1	20.3		

Table 2.12-4

POWER OUTPUT AND AUXILIARY POWER DEMAND
FOR BASE CASE AND PARAMETRIC VARIATIONS:
FUEL CELLS—HIGH TEMPERATURE

	CASE NO.	1	2	3	4
PRIME CYCLE POWER OUTPUT	MW	550.5	550.5	80.6	269.0
BOTTOMING CYCLE POWER OUTPUT	MW	555.0	555.0	550.0	552.0
FURNACE POWER OUTPUT	MW	80.8	80.8	59.0	67.7
BALANCE OF PLANT AUX. POWER REQ'D.	MW	63.3	63.4	53.3	57.3
FURNACE AUX. POWER REQ'D.	MW	0.	0.	0.	0.
TRANSFORMER LOSSES	MW	5.9	5.9	3.6	4.4
INVERTER LOSSES	MW	5.5	5.5	0.8	2.7
NET STATION OUTPUT	MW	1111.6	1111.5	631.9	824.3

REPRODUCIBILITY OF THE
ORIGINAL PAGE IS POOR

Section 3

SUMMARY OF RESULTS-CONVERSION SYSTEMS

The objective of the Task I Study of Advanced Energy Conversion Systems for coal or coal-derived fuel was to develop a technical-economic information base on the ten conversion systems under investigation. A large number of parametric variations were studied in an attempt to identify system and cycle conditions which demonstrated the potential of the energy conversion concept. This information base provided a foundation to aid selection of the energy conversion system which will be subjected to the more in-depth investigation in the Task II, conceptual design portion of this study. A General Electric Company recommendation is given as to which systems appear, from the results of the Task I Study, to have a potential of competing against the conventional utility system. This recommendation is presented for perspective. The ultimate selection of cycles for continuing study in Tasks II and III, however, was the responsibility of the ECAS Interagency Steering Committee.

Since the objective of the Task I Study was to generate a data base and not to "rank order" the conversion systems, the results will be presented in a summary basis in the order of investigation. The technical approach and assumptions are given in Section 1 and Appendix A of Part 1 of Volume II. Different scenarios or assumptions could be proposed for comparison of the conversion systems, e.g., economics of changes during construction, fuel costs, and method of calculating cost of electricity; however, these variations were not within the scope of the study. The technical-economic data are presented in a format that will permit these variations to be made.

ENERGY CONVERSION SYSTEMS

The parametric evaluation of the ten energy conversion systems under investigation in the Task I effort involved changes in the heat input technique, fuel, cycle conditions, bottoming cycles, and heat rejection technique. For each parametric point variation, technical-economic information was generated. For the "base" case configurations, additional information on environmental intrusion, natural resource requirements, size and weight of major components, etc., was generated.

The characterizing parameter most often presented for advanced conversion techniques is the thermodynamic efficiency. This is only a portion of the total story since fuel conversion losses and auxiliary power demands must be extracted to achieve an overall coal pile to electrical bus bar efficiency. The efficiency of the ten energy conversion systems along with important parametric variations is shown in Figure 3-1. The power plant (not including off-site fuel processing inefficiency), overall coal pile to bus bar efficiency, and the specific coal

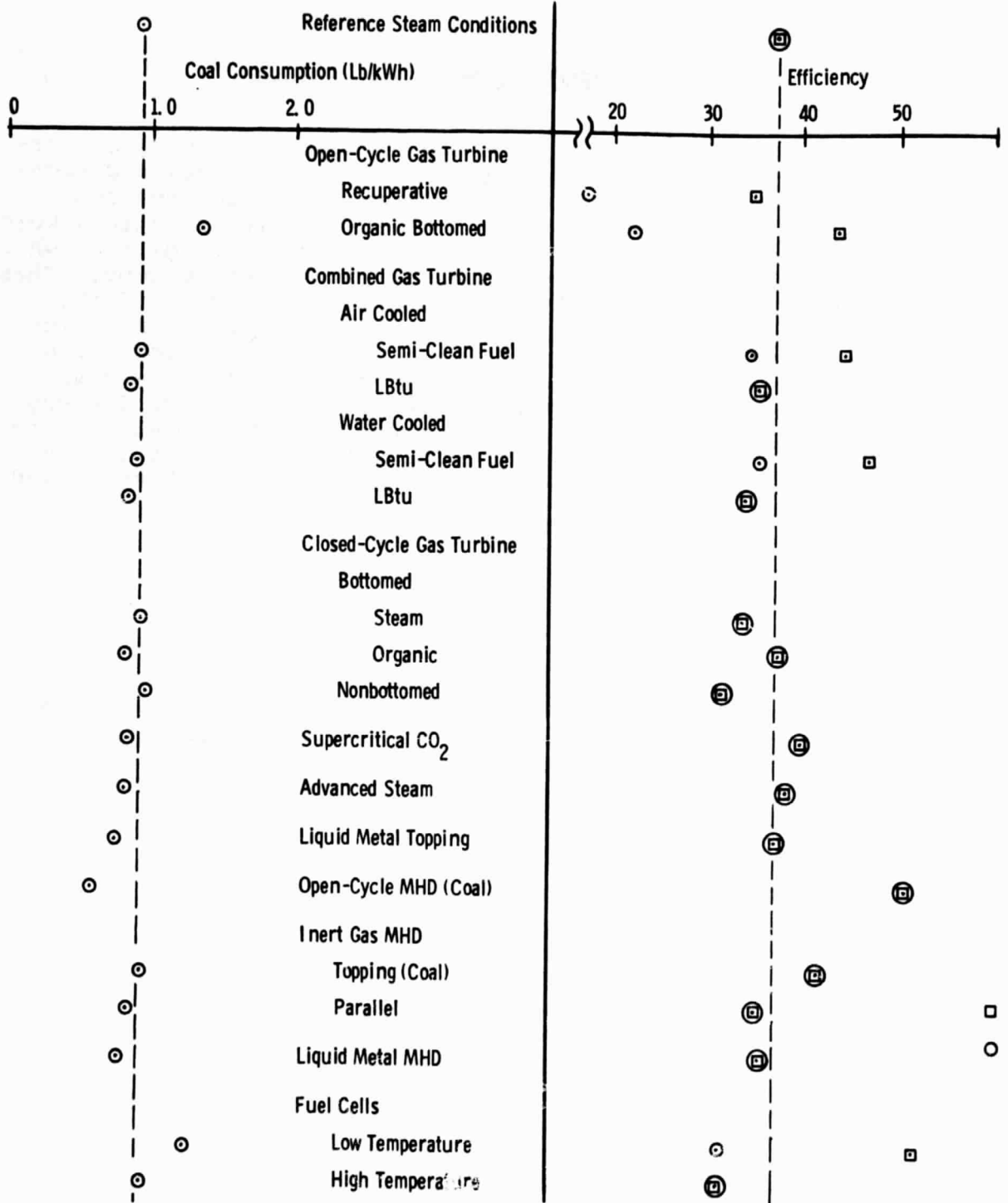


Figure 3-1. Summary Comparison of Cycles (efficiency)

consumption are given on this figure. A comparison is also presented which demonstrates the standard steam conditions (3500 psi/1000 F/1000 F [2.41×10^7 N/m²/811 K/811 K]), conventional furnace with stack gas cleanup and mechanical draft wet cooling towers. This is the system presently employed in a steam power plant. The values which are plotted are representative of a specific system and do not necessarily represent the highest efficiency or lowest cost.

The open-cycle MHD system burning coal directly is the only system which resulted in efficiencies approaching 50 percent. A group of cycles fit in the 40 percent to 45 percent efficiency range category: advanced steam, supercritical CO₂, liquid metal topping, and inert gas MHD (topping). In the same range with the standard steam plant, the mid thirties, are the open-cycle gas turbine-combined cycle, closed gas turbine with organic bottoming, liquid metal MHD and inert gas MHD (parallel). The remaining conversion systems are less efficient than would be expected from a standard steam plant of current design. It should be noted that both the low-temperature fuel cycle and the open-cycle gas turbine recuperative with organic bottoming had power plant efficiencies in the 40 percent range. Both these cycles have a clean fuel requirement, however, and the reduction from power plant to overall efficiency resulted from the processing efficiency in the production of high-Btu gas as consumed by the conversion cycle.

The capital cost estimates for the energy conversion concepts are shown in Figure 3-2 representative points. The total capital cost is divided into specific elements: major components, balance of plant, contingency and interest, and escalation during construction. The capital costs for the standard steam plant are projected to be approximately 700/kW. The cycles which were lower than the standard steam plant in capital costs were the plants with short construction times and simple construction. These are the gas turbine cycles, both open and closed, and low-temperature fuel cells. The more complex systems featured significant balance-of-plant costs and long construction times (resulting in high interest and escalation charges during construction). The supercritical CO₂ cycle employs a combination of high temperature and high pressure in the major components and had the largest cost for that item. The closed-cycle MHD systems, inert gas and liquid metal, had the highest balance-of-plant costs.

Neither the efficiency nor the capital cost projects the total picture for technical-economic evaluation. The combination of the two values along with the fuel cost gives a more realistic evaluation of the attractiveness of the various concepts for representative points. This value is the cost of electricity and is shown in Figure 3-3 for the various conversion systems. The cost of electricity is subdivided into contributions of capital charges, fuel cost, and operating and maintenance charges. Once again, the as-analyzed standard steam plant is supplied as a reference: cost of electricity = ~30 mills/kWh. In plants with very high capital costs—MHD, supercritical CO₂, liquid metal topping, etc.—the

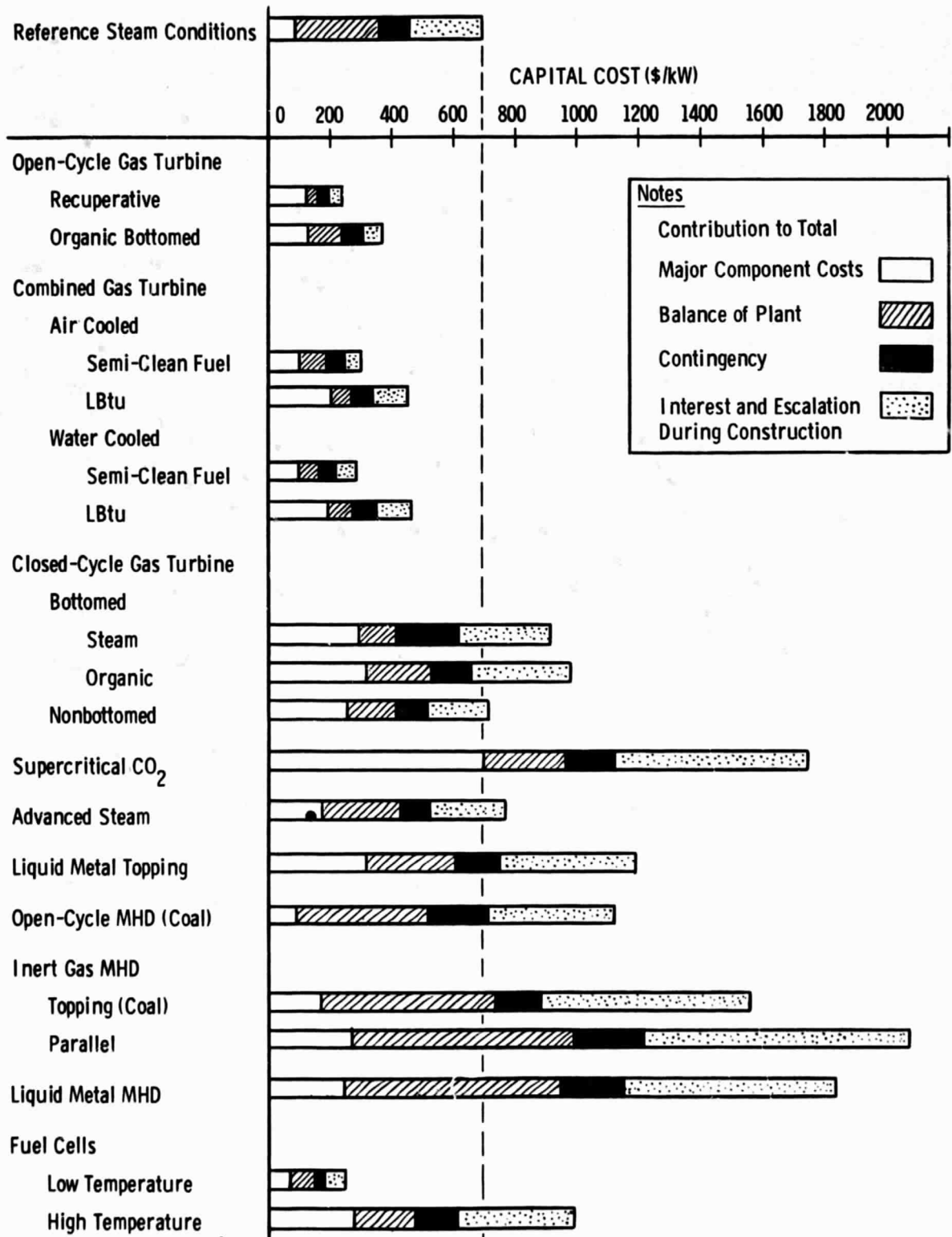


Figure 3-2. Summary Comparison of Cycles (Capital Cost)

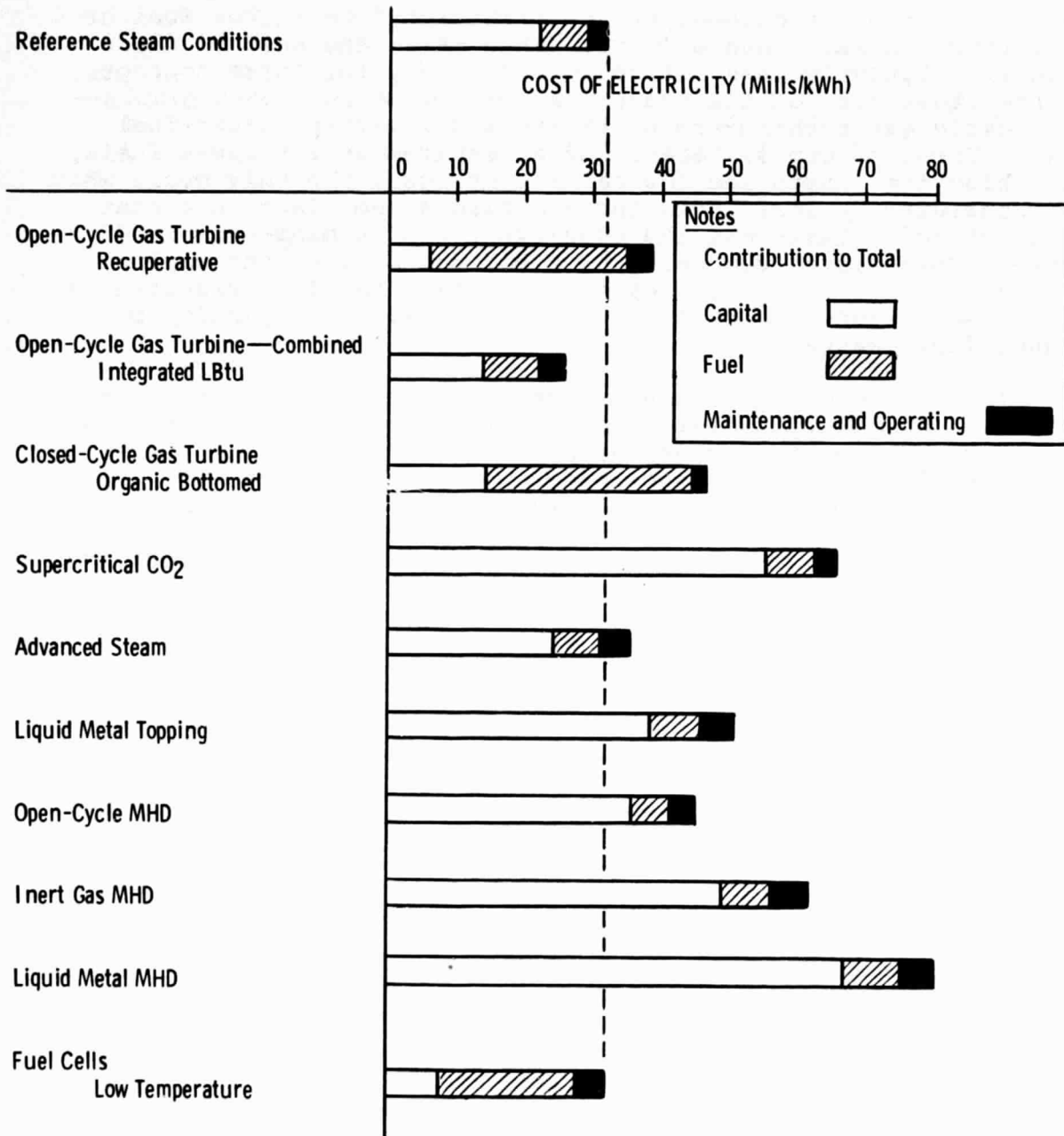


Figure 3-3. Summary Comparison of Cycles (Cost of Electricity)

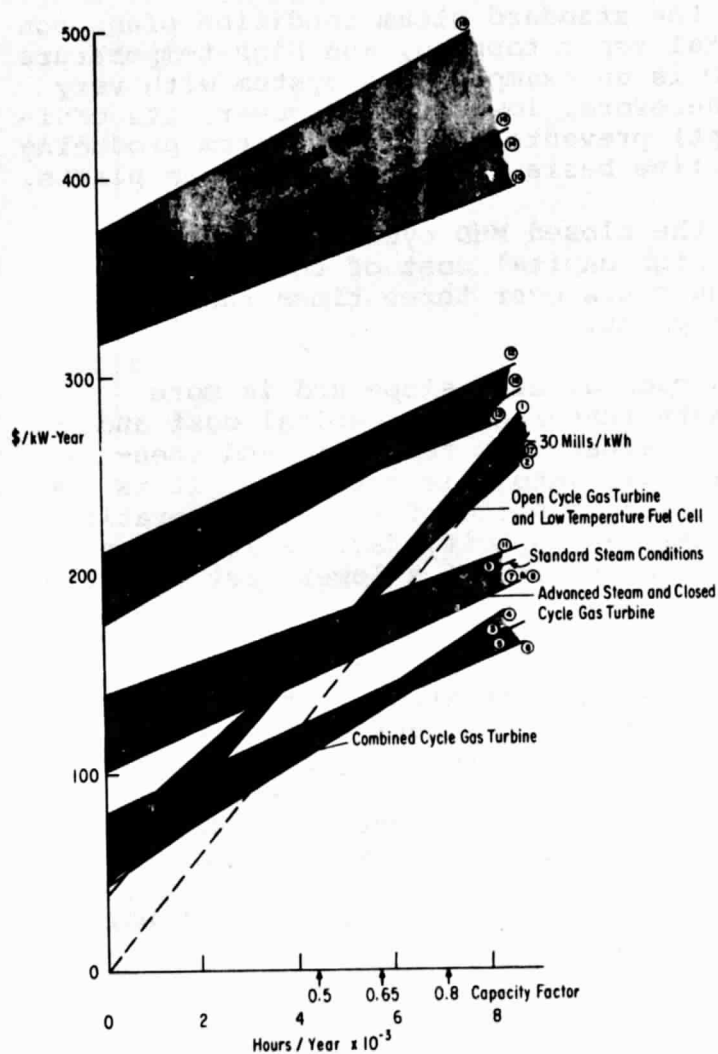
capital charge far exceeds the contribution from either fuel or Operating and Maintenance (O&M). This makes the cost of electricity relatively insensitive to efficiency for these concepts. On the other side of the scale are the low capital cost plants—open-cycle gas turbine—recuperative and low-temperature fuel cells. These concepts, because of a requirement for clean fuels, have high fuel costs and low capital charges. The only cycle which was consistently lower than the standard steam plant on a cost of electricity basis was the open-cycle gas turbine—combined cycle. This system demonstrated a balance between the capital and fuel charges. The employment of semi-clean fuel resulted in a less expensive on-site capital cost but with the penalty of higher fuel charges.

The economic comparison presented in Figure 3-3 was for a 65 percent capacity factor. Another approach to presentation of this information is through use of a "screening curve." This curve is presented as a function of hours of plant operation per year. A screening curve representation is shown in Figure 3-4 for the conversion systems. These curves show the cost of operation of the plant on a \$/kW-year basis vs the hours of operation. The "y" axis intercept, at zero hours, shows the capital charge which is incurred if the plant is not operated. The slope is representative of the operating charges including both O&M and fuel. The plants with high efficiency generally have small slopes and are characteristic of baseloaded plants. These screening curves demonstrate the economic data for a plant operating with a range of capacity factors. However, no evaluation was made of the energy conversion system's technical ability to operate in an "other-than-baseload" mode. The capital costs for control equipment necessary to operate in the peaking or mid-range mode was not included in the evaluations.

Five specific bands have been placed on this curve to represent classes of economic attractiveness. Two dashed lines also appear. The dashed line through the origin represents a 30 mill/kWh electrical charge. The second dashed line represents the standard steam plant. The intercept of the dashed first line (which passes through the origin) and the characteristic line for a specific conversion system indicates the number of hours per year the plant must operate in order to produce 30 mill/kWh power. The intercept with the standard steam line occurs at approximately a 65 percent capacity factor.

The band around the standard steam condition line contains the advanced steam cycle and the closed gas turbine cycles. All of the concepts could generate approximately 30 mill/kWh power for a capacity factor of approximately 65 percent.

The only band which is significantly better than the standard steam plant band over the whole range of capacity factors is the combined gas turbine cycles. These cycles have the lowest yearly operating costs in the study.



KEY

1. Open Cycle Gas Turbine -- Recuperative
2. Open Cycle Gas Turbine -- Recuperative, Organic Bottomed
3. Combined Cycle Gas Turbine -- Air Cooled Integrated LBitu
4. Open Cycle Gas Turbine Combined Cycle -- Air Cooled, Solvent Refined Coal
5. Open Cycle Gas Turbine Combined Cycle -- Water Cooled, Solvent Refined Coal
6. Open Cycle Gas Turbine Combined Cycle -- Water Cooled, Integrated Gasifier
7. Closed Cycle Gas Turbine -- Nonbottomed
8. Closed Cycle Gas Turbine -- Organic Bottomed
9. Closed Cycle Gas Turbine -- Steam Bottomed
10. Supercritical CO₂ Cycle
11. Advanced Steam Cycle
12. Liquid Metal Topping Cycle
13. Open Cycle MHD -- Direct Coal
14. Closed Cycle Inert Gas MHD -- Topping
15. Closed Cycle Inert Gas MHD -- Parallel
16. Closed Cycle Liquid Metal MHD
17. Fuel Cells -- Low Temperature
18. Fuel Cells -- High Temperature

Figure 3-4. Screening Curves for Advanced Energy Conversion Cycles

REPRODUCIBILITY OF THE ORIGINAL PAGE IS POOR

The band directly above the standard steam condition plant contains the open-cycle MHD, metal vapor topping, and high-temperature fuel cell. The open-cycle MHD is an example of a system with very good operating efficiency, therefore, low slope. However, its capital charge ("Y" axis intercept) prevents this system from producing electricity on a cost competitive basis with standard steam plants.

The upper band features the closed MHD cycles and super-critical CO₂. The extremely high capital cost of these systems makes their projected operating costs over three times those expected for the standard steam plant.

The remaining band has a much greater slope and is more characteristic of peaking plants featuring low capital cost and high operation costs. The low-temperature fuel cell and open-cycle gas turbine recuperative fall into this category. It is interesting to note, however, that in spite of the high operating charges for this class of cycles, at capacity factors less than 50 percent, they will produce electricity at a lower cost than the standard steam plant.

These screening curves represent the concepts evaluated under the ground rules established in this study. If these ground rules change, the comparison is no longer valid. For example, higher fuel costs would be reflected in greater curve slopes. This effect would of course be less pronounced on the more efficient cycles. The fact remains, however, that no matter how efficient a cycle is, the effect of high, fixed capital charges cannot be neglected. Within the economic constraints, a limit is therefore placed on the initial capital investment which can be justified to achieve an efficiency increase.

RECOMMENDATIONS FOR TASK II STUDY

As previously stated, the objective of the Task I study was to develop a data base which could be utilized by the Interagency Steering Committee for selecting the advanced energy conversion systems to be evaluated in more detail in Task II. However, the General Electric Company was requested to provide recommendations for systems to be evaluated in Task II. The recommendations presented herein are based upon the Task I results.

The criteria employed for the selection process were:

- Performance
 - High power plant efficiency
 - Low specific coal consumption
- Economics
 - Low capital cost

Low cost of electricity

- Established basis for high plant availability
- Potential adaptability for base load operation

Of equal significance are some criteria which were not employed. They included:

- Technical barrier problems
- Likelihood of developmental success
- R&D plans and resources required
- Expected year of first commercial service

In some cases, the criteria not employed are at least as important as those employed. However, the information basis required to evaluate the conversion concepts with respect to this latter group of criteria will not be generated until Task II and III of the program. They will be employed in the final evaluation of systems in Task III.

The General Electric recommendations of advanced energy conversion systems for Task II study are given in two parts: a positive group and an optional group.

Positive Recommendation

- Advanced Steam

Direct combustion of coal in an atmospheric fluidized bed. This cycle is the present standard of industry for baseload power and with the inclusion of a new furnace system (atmospheric fluidized bed [AFB]) represents a firm, reliable, advanced cycle base.

- Open-Cycle Gas Turbine Combined Cycle-Water Cooled

With semi-clean fuel. This system had the lowest cost of electricity and a good power plant efficiency. The semi-clean fuel offers an alternative to gasification for gas turbine cycles.

- Open-Cycle Gas Turbine Combined Cycle-Air Cooled

With integrated low-BTU gasifier. This system had the second lowest cost of electricity and offers the potential for good overall efficiency. The integrated gasifier permits utilization of coal in a gas turbine with on-site fuel processing control.

- Open-Cycle MHD

Direct coal fired. This system offers the highest efficiency of any concept in the study and the possibility of direct combustion of coal in an open cycle machine.

Optional Recommendation

If additional systems are to be studied in Task II, a recommendation is made that these systems be selected out of the following three groups.

- Closed-Cycle Gas Turbine

This system offers low cost of electricity because of low capital costs. The specific coal consumption was not as good as a standard steam power plant.

- { Supercritical CO₂
Inert Gas MHD
Metal Vapor Topping

Each of these systems offers potential efficiencies in excess of 40 percent. However, their high capital costs resulted in their not being competitive on a cost-of-electricity basis. Of these three concepts, the metal vapor topping cycle had the lowest capital cost.

- { Fuel Cell—Low Temperature
Open-Cycle Gas Turbine Recuperative

Each of these two systems had a competitive cost of electricity compared to the steam reference cases. However, the systems required clean fuel, thus making them more suitable for peaking duty in terms of overall energy utilization.

Appendix A

POWER CONDITIONING SYSTEMS FOR MHD AND FUEL CELL APPLICATIONS

INTRODUCTION

Power sources employing MHD or fuel cells generate direct currents at relatively low voltages where transmission is not practical. Power conditioning systems are required which convert the d-c to a-c and raise the voltage to subtransmission or transmission voltages. These systems must be compatible with electric utility practice in both operation and reliability. This Appendix describes such a system that is derived from high-voltage d-c (HVDC) power transmission technology.

HVDC TECHNOLOGY

Early devices for conversion employed the mercury arc valves and approximately 6300 MW of such capacity are presently in operation. With the commissioning of the Eel River Converter Station in 1972 (refs. 1 and 2), the solid-state era in HVDC was initiated. Today a total of 6800 MW of solid-state transmission capacity are installed or are committed and under way.

The HVDC technology is sufficiently mature that it is accepted by the electric utility industry. Development continues in the United States by General Electric and in Europe; Russia is developing its own system and much academic work proceeds from Japan.

A sound basis exists for expansion of solid-state HVDC technology into the power conditioning field for such systems as MHD, fuel cells, photovoltaic systems or storage battery energy storage. Commercial activity in the solid-state HVDC transmission field will continue to advance the technology.

In HVDC transmission systems, current and voltage levels are selected for most efficient use of available semi-conductors with due respect to construction and operating costs of connected d-c lines. For instance, the Eel River 320 MW system, a back-to-back asynchronous tie, utilized two circuits at 80 kV and 2000 amperes each. The Square Butte Project, now under construction from North Dakota to Minnesota, spans a distance of approximately 450 miles and will operate at ± 250 kV and 1000 amperes. Systems are under consideration for ratings up to 600 kV and 2000 amperes. In the past, as many as four thyristor cells have been used in parallel, as in Eel River, but the present trend is toward larger cells.

Another branch of the technology has evolved using silicon diode rectifiers for low voltage and high current. Systems

supplying 25,000 A at 1,100 V are not unusual for electrochemical application. Power conditioning systems might utilize technology from this field as well as the HVDC field.

HVDC control systems are the culmination of extensive development aimed at high reliability and maximum performance. Extensive use has been made of military and space program experience. Redundant functions are provided with indication of loss of redundancy and on-line replacement of suspected circuit modules. These systems have an excellent record of reliability in the commercial power system environment and are immediately adaptable for power conditioning systems.

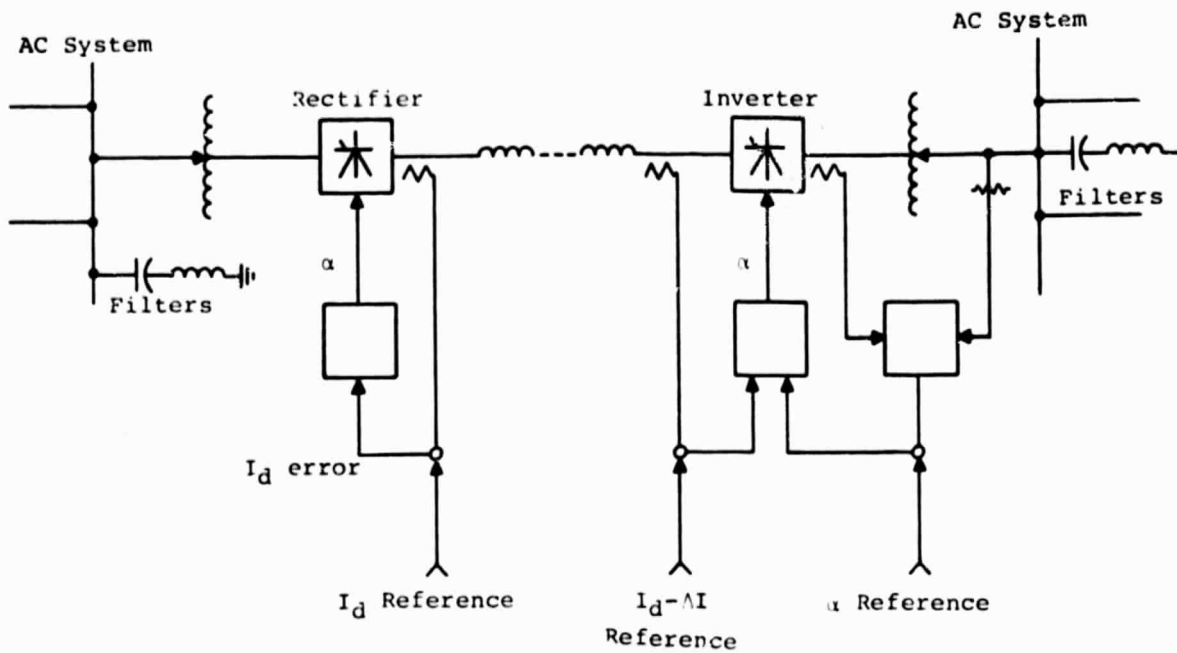
HVDC System Operation

The elements of a typical HVDC transmission system are shown in Figure A-1 and the current/voltage characteristics are shown in Figure A-2. The rectifier (a-c to d-c converter) is operated as a feedback control system to maintain constant d-c output within the limitations of the supply voltage. The constant current exists from zero voltage up to a maximum determined by system a-c voltage, converter transformer design and transformer tap position (ref. 4) and the converter firing angle limitation (ref. 4) built into the control system. The inverter normally operates in the constant extinction angle mode, where d-c voltage and power factor are maximized consistent with reliable operation. In addition, a current control mode is provided for the case when rectifier a-c system voltage is too low to allow the rectifier to control current.

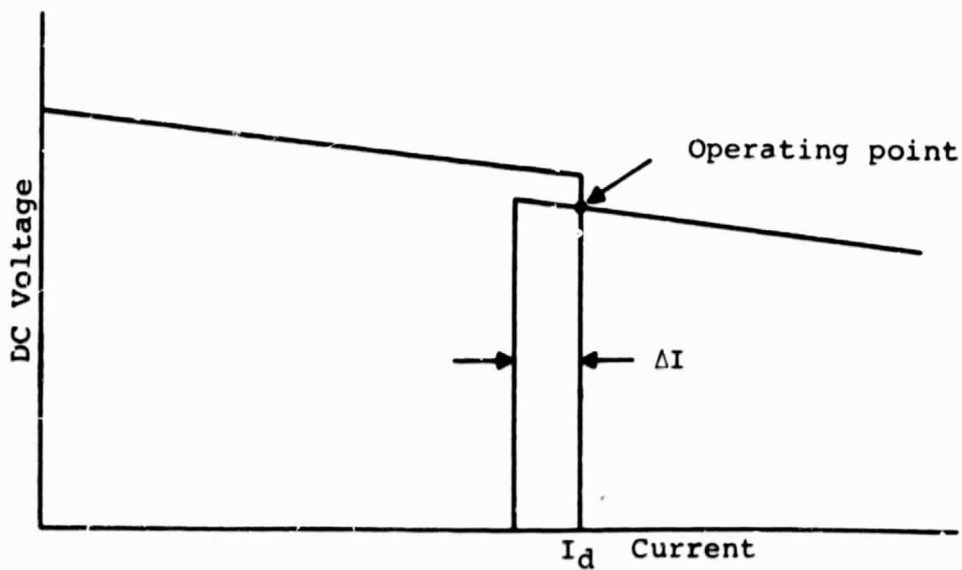
Figure A-1b shows the rectifier and inverter characteristics and the operation point where these characteristics intersect. Power is varied by changing set point of the rectifier current controller. Because of the shape of the curves, there is little disturbance to either d-c voltage or firing angles when current is changed. Transformer load tap changers are used in automatic circuits (not shown) which hold firing angles and d-c voltage within optimum ranges.

A d-c system requires an inductance in the circuit to minimize ripple current-control rate of rise during faults, and to isolate the converter waveform from the remainder of the circuit. D-C circuit breakers are not needed since the control function is accomplished electronically in the control system of the rectifier.

HVDC systems are based on line commutated inverters (refs. 3 and 4). Because of the substantial technical and cost data base available from work on these systems, the power conditioning systems for MHD and Fuel Cell applications used in this study assumed line commutated inverters.



(a) Simplified circuit diagram



(b) Idealized operating characteristics

Figure A-1. HVDC Transmission System

Converters for Power Conditioning

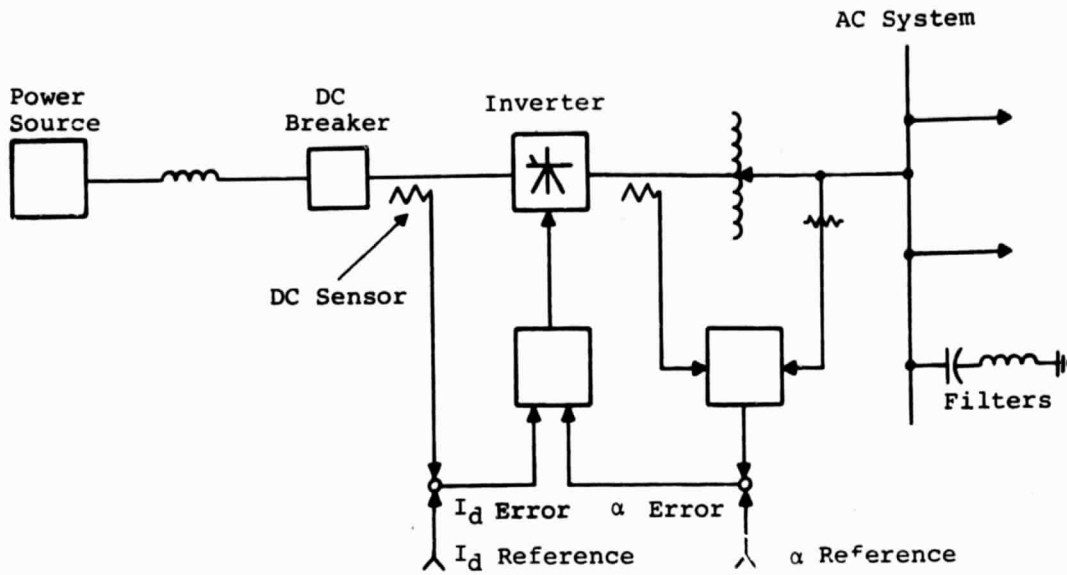
In the power conditioning system, the MHD or fuel cell equipment replaces the rectifier. There is no practical way in which these sources can control current or voltage. It is therefore necessary that a d-c circuit breaker or equivalent control be interposed between the power source and the inverter. As in the HVDC transmission system, an inductance is also required.

Figure A-2a is a one-line and block diagram of a power conditioning system, and Figure A-2b is a representative volt/ampere characteristic. A small range of voltage adjustment is available electronically in the inverter. The range of current control is determined to a large extent by the current/voltage characteristic of the power source and is rather limited. For a given source characteristic, the range can be extended by increasing transformer load tap changer range or by increasing the firing angle. The latter deteriorates the power factor and both are costly.

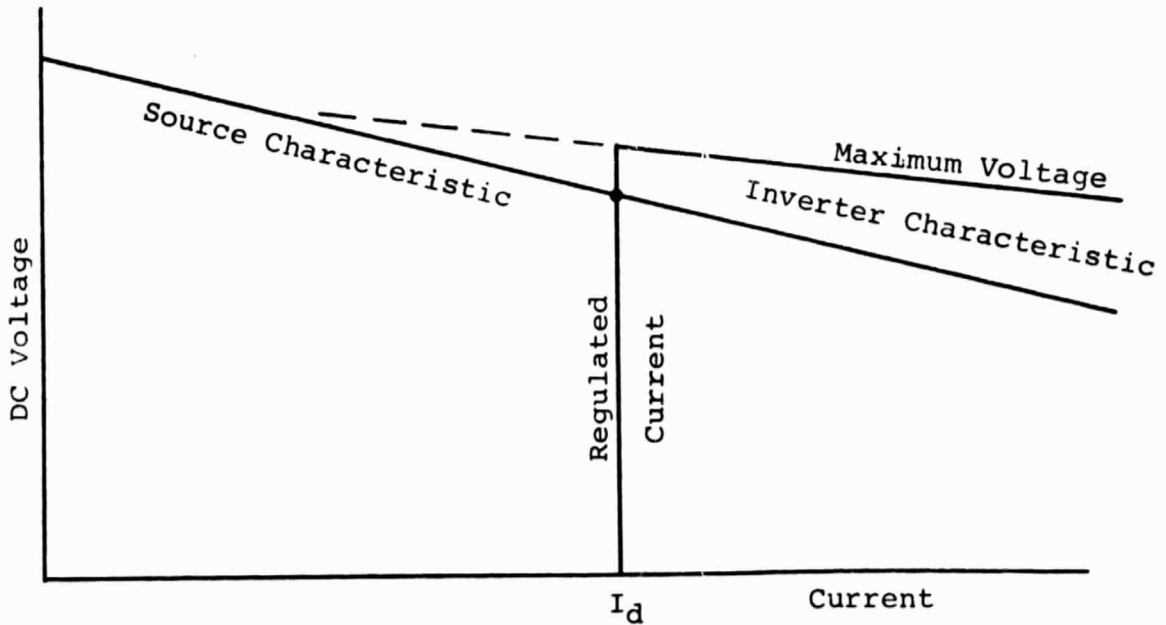
Disturbances in the connected a-c system can cause inverter malfunctions commonly known as commutation failures. The result is a collapse of the inverter voltage and, under some circumstances, a direct connection of the power source to the a-c voltage of the associated converter transformer. In HVDC systems, the direct current is controlled by the rectifier and can be reduced or cut off automatically to allow recovery of the inverter. In the MHD or fuel cell system, such control is not available and current will increase to such a level that recovery is impossible. A d-c circuit breaker is required which can interrupt the fault current from the MHD generator, to allow recovery. Stress on the circuit breaker is severe because of large, short-circuit currents and the requirement for an inductance in series with the power source.

D-C breakers are not currently available as a commercial product. However, several development projects are under way. These are directed at HVDC but will be similar to those required for MHD.

High power converters such as those used in HVDC power transmission and proposed for power conditioning systems must be connected to a-c systems having short circuit capacity in MVA at least three times the MW capacity of the converter. The converter generates current harmonics on the a-c side which are detrimental to a-c system operation. Filter circuits connected to the line side of the converter transformers are employed to absorb these harmonic currents. Another aspect of HVDC systems is that converters absorb reactive power equal to approximately 60 percent of the real power level. The harmonic filters provide some of the reactive power and the remainder must be supplied from the a-c network.



(a) Simplified circuit diagram



(b) Idealized operating characteristics
Figure A-2. Power Conditioning System

Sample Systems

Figure A-3 describes a representative power conditioning system. There are 1000 electrode pairs, each capable of producing 200 A at 7000 V. These electrode pairs must be electrically isolated from each other. It is therefore proposed that each electrode pair be provided with its own breaker, inductance and converter bridge. Four bridges would share a control system.

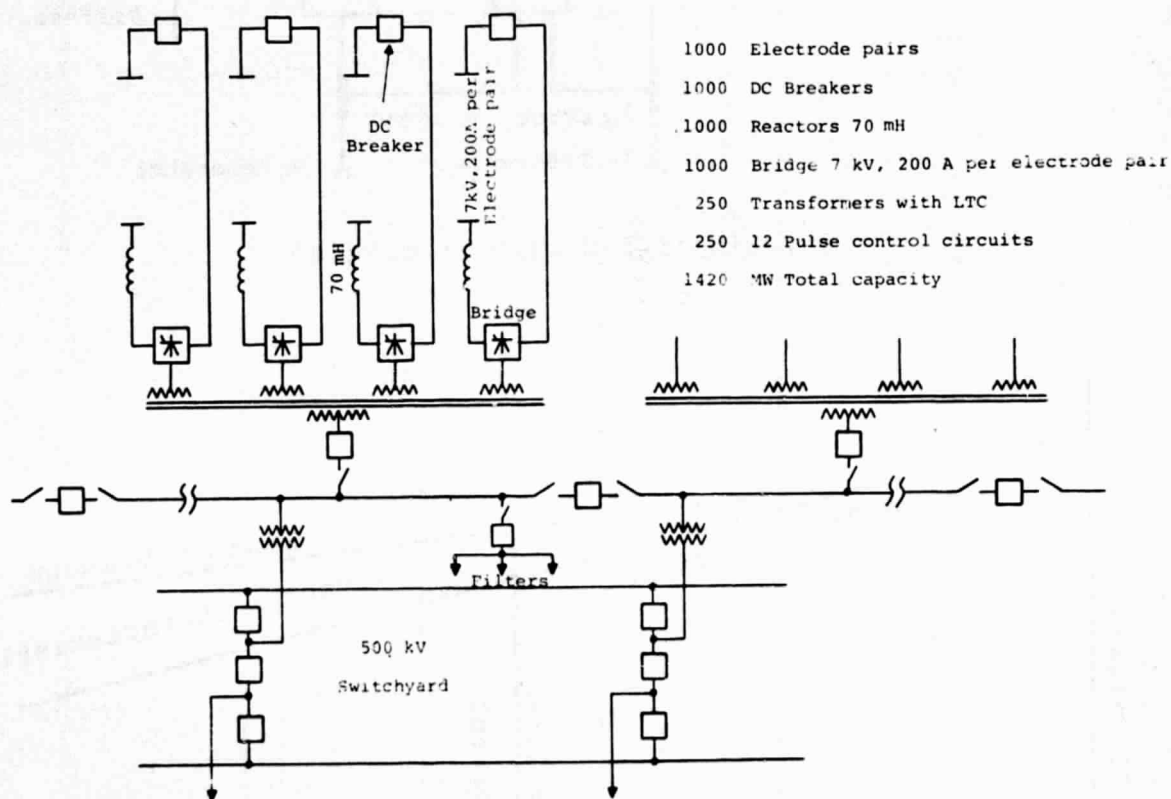


Figure A-3. MHD Converter System 1.4 MW Module

If groups of 20 electrode pairs are connected directly in parallel the system consists of 50 converters of 28 MW capacity and requires 50 transformers instead of 250. The mode of operation is the same as that described for the 1.4 MW module. A circuit diagram, being slightly different, is described by Figure A-4.

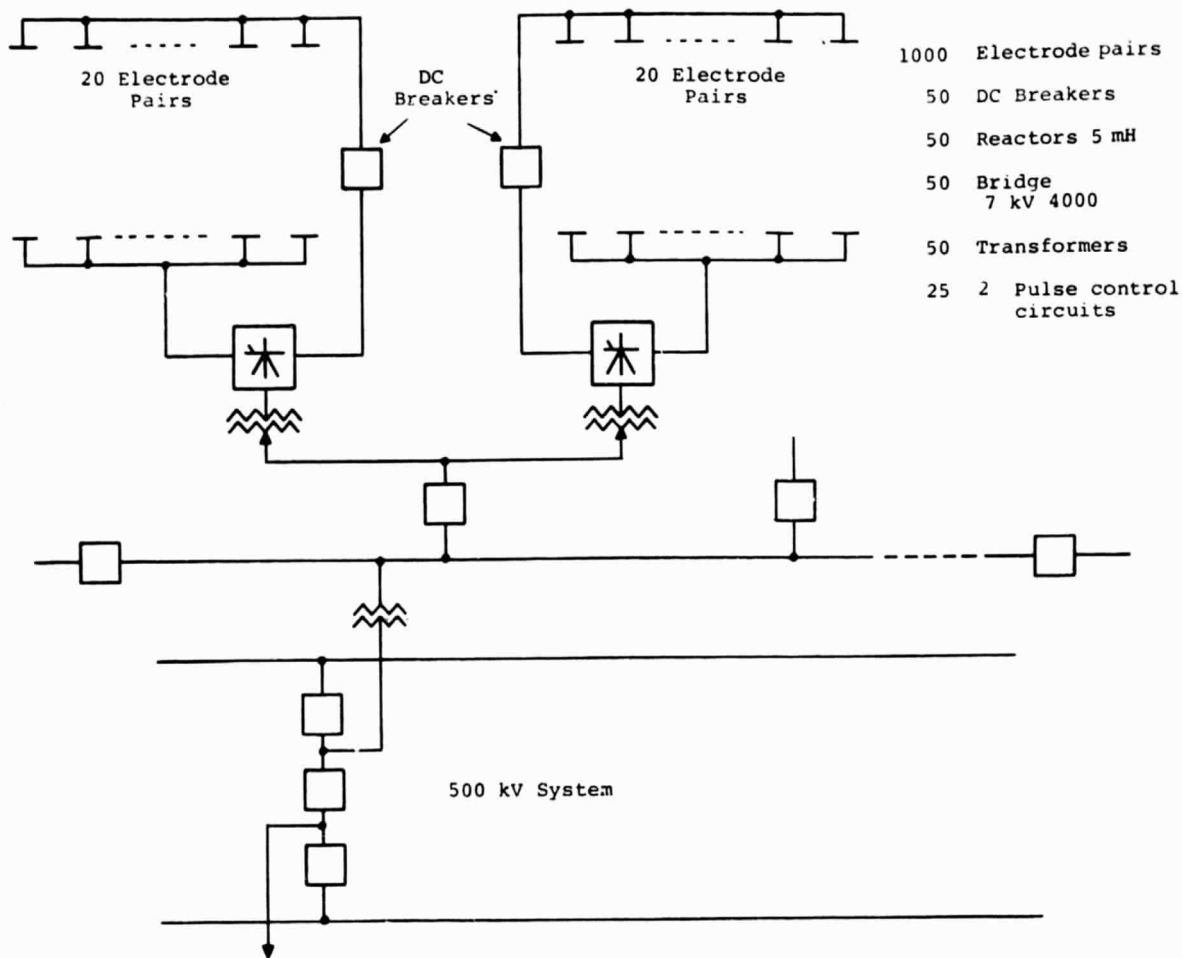


Figure A-4. MHD Power Conditioning System 28 MW Module

Efficiency for the 28 MW module system is estimated at 98.5 percent, while the 1.4 MW module is estimated to be slightly less.

Pricing

The following background applies to the price estimates:

1. The price is for terminal equipment only and does not include installation or civil work.
2. Control system price and performance are based on equipment currently in production for use in HVDC systems. Prices for transformers, valves and switchgear are based on HVDC current commercial equipment. DC breaker price estimates are based on estimated costs of equipment presently being developed.

- Thyristor prices are based on costs of forced, recirculated, air-cooled, air-insulated units similar to HVDC equipment now in the installation phase.

A "module" consists of an electrode pair or group of pairs, transformer bank, inductor, d-c breaker, thyristor valves and a control system which operates the module as a unit. Estimated costs for three equipment ratings and two different module sizes are given in Table A-1.

Table A-1

ESTIMATED COSTS (\$ PER KW RATING) FOR INVERSION EQUIPMENT

	Equipment Rating		
	50 MW	300 MW	1400 MW
1.4 MW/Module	335	305	300
28 MW/Module	125	75	65

REFERENCES

- Breuer, G.D., Fink, J.L., Ryder, F.H., Stairs, C.M., "The New Brunswick Electric Power Commission Solid-State HVDC Asynchronous Tie Installation," presented at the American Power Conference, Chicago, Ill., April 21, 1970.
- Fink, J.L., Pohl, R.V., Ryder, F.H., Stairs, C.M., "System Design Considerations of the Eel River HVDC Converter Station," CIGRE International Conference on Large High Tension Electric Systems, Paper No. 14-05, August-September 1972.
- Bedford, B.D., Hoft, R.G., Principles of Inverter Circuits, John Wiley & Sons, 1964.
- Kimbark, E.W., Direct Current Transmission, Vol. 1, Wiley Interscience, New York, N.Y., 1971.